

For Reference

NOT TO BE TAKEN FROM THIS ROOM

Ex libris
UNIVERSITATIS
ALBERTAENSIS



THE UNIVERSITY OF ALBERTA

RELEASE FORM

NAME OF AUTHOR Anthony B. Schryvers

TITLE OF THESIS The Aerobic and the Anaerobic
 Glycerol-3-phosphate Dehydrogenases of
 Escherichia coli

DEGREE FOR WHICH THESIS WAS PRESENTED Doctor of Philosophy

YEAR THIS DEGREE GRANTED August, 1981

Permission is hereby granted to THE UNIVERSITY OF ALBERTA LIBRARY to reproduce single copies of this thesis and to lend or sell such copies for private, scholarly or scientific research purposes only.

The author reserves other publication rights, and neither the thesis nor extensive extracts from it may be printed or otherwise reproduced without the author's written permission.

THE UNIVERSITY OF ALBERTA

The Aerobic and the Anaerobic Glycerol-3-phosphate
Dehydrogenases of *Escherichia coli*

by



Anthony B. Schryvers

A THESIS

SUBMITTED TO THE FACULTY OF GRADUATE STUDIES AND RESEARCH
IN PARTIAL FULFILMENT OF THE REQUIREMENTS FOR THE DEGREE
OF Doctor of Philosophy

Biochemistry

University of Alberta

FALL , 1981

91F-652

THE UNIVERSITY OF ALBERTA
FACULTY OF GRADUATE STUDIES AND RESEARCH

The undersigned certify that they have read, and recommend to the Faculty of Graduate Studies and Research, for acceptance, a thesis entitled The Aerobic and the Anaerobic Glycerol-3-phosphate Dehydrogenases of *Escherichia coli* submitted by Anthony B. Schryvers in partial fulfilment of the requirements for the degree of Doctor of Philosophy.

ABSTRACT

The aerobic and anaerobic glycerol-3-phosphate dehydrogenases, two of the primary dehydrogenases of membrane associated electron transport in *Escherichia coli*, have been purified to homogeneity and characterized. To facilitate purification of the anaerobic dehydrogenase, a group of recombinant ColE1:*E. coli* plasmids carrying the *glpA* gene (anaerobic glycerol-3-phosphate dehydrogenase) and the closely-linked *glpT* gene (glycerol-3-phosphate transport) were used. One of these plasmids in an *E. coli* strain resulted in a 3-10 fold amplification of glycerol-3-phosphate transport and, under anaerobic growth conditions, a 12-fold amplification of anaerobic dehydrogenase. Utilizing a minicell system to identify plasmid-coded proteins, a 40,000 molecular weight periplasmic polypeptide and a 26,000 molecular weight membrane polypeptide were identified as products of the *glpT* gene. Anaerobically grown cells carrying these plasmids had elevated levels of two polypeptides of 62,000 and 43,000 molecular weight, whose presence correlated with anaerobic dehydrogenase activity.

Analysis of five of the recombinant plasmids by digestion with restriction endonucleases determined of the *glpA* and the *glpT* loci on the DNA map. Since one of these plasmids did not produce a functional anaerobic dehydrogenase, but produced a 58,000 dalton polypeptide from the *glpA* locus, defined the *glpA* locus and predicted the

direction of transcription.

The purified aerobic and anaerobic glycerol-3-phosphate dehydrogenases of *E. coli* were shown to be two distinct enzymes. The aerobic dehydrogenase is an α_2 dimer of two 58,000 molecular weight subunits whereas the anaerobic dehydrogenase is an $\alpha\beta$ dimer of polypeptides of 62,000 and 43,000 molecular weight. The aerobic dehydrogenase requires detergent or phospholipid for efficient electron transfer activity to PMS whereas the anaerobic enzyme shows only a slight stimulation in the presence of detergent.

Only the activity of the anaerobic enzyme is stimulated by exogenous flavins, particularly FMN. Both enzymes are inhibited by treatment with sulfhydryl reagents but the exogenous flavin-dependent activity of the anaerobic enzyme is much more susceptible to sulfhydryl inhibition than the flavin-independent activity. Both dehydrogenases contain an FAD cofactor that is reduced by substrate. However, the reduced FAD in the anaerobic enzyme is readily reoxidized by air. The anaerobic enzyme also contains 2 non-heme irons/dimer.

The pH and temperature profile of enzymatic activity of the purified aerobic dehydrogenase is similar to that of the membrane-bound enzyme. The purified, detergent-depleted enzyme can be reconstituted with *E. coli* membrane vesicles to support glycerol-3-phosphate-dependent active transport of L-proline. The purified enzyme is competitively inhibited by a number of substrate analogs and is regulated by ATP and

GTP in a complex manner.

Ethylene glycol stabilizes the anaerobic dehydrogenase by preventing subunit dissociation and is protective during limited proteolysis, which results in conversion of the 62,000 molecular weight subunit to a 50,000 molecular weight polypeptide. Stimulation by exogenous flavin is lost concurrently with the proteolytic cleavage event.

ACKNOWLEDGEMENTS

I would like to express my appreciation to my supervisor, Dr. Joel H. Weiner, for his assistance during the course of these studies. The guidance that he provided during the early part of my graduate training was very helpful and his ability to judge when I was capable of becoming progressively more independent in my research endeavors was of immense value. The cooperation and fruitful interactions with other members of this laboratory are gratefully acknowledged. This includes the graduate students: John Robinson, Peter Dickie, Scott Hagen, Bernie Lemire and Heather Dettman; the technicians: Elke Lohmeier, Mark Ehrman and Kelly Dabbs; and the various undergraduate students who were involved in research projects in Dr. Weiner's laboratory. I would especially like to thank Miss Elke Lohmeier for the many hours of collaborative research endeavors that she shared with me.

I would like to extend my thanks to the many members of the Department of Biochemistry who provided assistance during the course of my graduate studies. Their willingness to provide their time for discussions and to generously provide their facilities for research endeavors is greatly appreciated. I would specifically like to thank Dr. L. Smillie and M. Nattriss for assistance in amino acid analyses and Dr. C. Kay, V. Ledsham and K. Oikawa for assistance in sedimentation and circular dichroism studies.

The patience and understanding that my wife Elma demonstrated and the encouragement that she provided was essential for completion of my graduate training. I would also like to thank my parents for their constant encouragement during the course of my studies.

Financial support provided by the Medical Research Council and by the Alberta Heritage Fund for Medical Research in the form of studentships is gratefully acknowledged. The research allowance provided by the Alberta Heritage Fund for Medical Research was also of great assistance.

Table of Contents

Chapter	Page
I. Introduction	1
A. Background	1
1. Chemiosmotic Hypothesis	1
2. Electron Transport Systems of <i>E. coli</i>	7
a. Aerobic Electron Transport	7
Primary Dehydrogenases	7
Terminal Oxidases	13
Sequence and Organization	14
b. Electron Transport to Nitrate	19
Primary Dehydrogenases	19
Nitrate Reductase	21
Organization of the Electron	
Transport Chain to Nitrate	21
c. Electron Transport to Fumarate	24
Primary Dehydrogenases	24
Fumarate Reductase	24
Organization of the Electron	
Transport Chain to Fumarate	25
3. Proteins Involved in the Catabolism of	
Glycerol and Glycerol-3-phosphate	26
a. Metabolic Pathway for Glycerol and	
Glycerol-3 phosphate	26
b. Expression of the Genes Involved in	
Glycerol Catabolism	30
c. Characterization of the Proteins	
Involved in Glycerol and	
Glycerol-3-phosphate Catabolism	33
Glycerol-3-phosphate Transport	
Proteins	33
Aerobic Glycerol-3-phosphate	
Dehydrogenase	34
Anaerobic Glycerol-3-phosphate	
Dehydrogenase	35
B. The Thesis Problem	36
II. Materials and Methods	39
A. Materials	39
1. Chemicals	39
2. Enzymes	40
3. Bacterial Strains and Plasmids	40
B. Microbiological Methods	43
1. Storage of Strains and Growth Conditions	43
2. Screening the Clarke and Carbon Strain	
Collection	44
3. Transfer of Recombinant Plasmids to	

Recipient Strains	45
C. Isolation Procedures and Preparation of Cellular Extracts	46
1. Preparation of Membrane Vesicles	46
2. Isolation of Minicells	46
3. Labelling Plasmid-coded Proteins	46
4. Preparation of Membranes from Minicells	46
5. Preparation of Crude Shock Fluid from Minicells	47
6. Purification of the Aerobic Glycerol-3-phosphate Dehydrogenase	47
7. Preparation of Cell Fractions for Anaerobic Dehydrogenase Identification	49
8. Isolation of Plasmid DNA	50
9. Isolation of the Subunits of the Anaerobic Dehydrogenase	51
D. Physical Methods	51
1. SDS-Polyacrylamide Gel Electrophoresis	51
2. Slicing and Counting Radioactive SDS-PAGE Gels	52
3. Electrophoresis of DNA	53
4. Electron Microscopy	54
5. Sedimentation Studies	54
6. Circular Dichroism	54
7. Determination of Endogenous Flavin	54
E. Chemical Methods	55
1. Determination of Protein Concentration	55
2. Amino Acid Analysis	55
3. Chemical Crosslinking of the Anaerobic Dehydrogenase	56
4. Iron Analysis	57
5. Acid-Labile Sulfide Analysis	57
6. Inactivation of the Anaerobic Dehydrogenase	57
7. Preparation of Dideazaflavin Analogs	57
F. Enzymatic Methods and Transport Assays	58
1. Transport Assays with Whole Cells	58
2. Transport Assays with Membrane Vesicles	59
3. Assay of Enzyme Activity	59
4. Restriction Endonuclease Digestions	60
5. Proteolysis of the Anaerobic Dehydrogenase	61
6. Determination of K_m and V_{max}	62
III. Recombinant ColE1: <i>E. coli</i> Plasmids	63
A. Introduction	63
B. Results	65
1. Selection of Recombinant Plasmids	65
2. Identification of Recombinant Plasmid-Coded Polypeptides	68

a. Glycerol-3-phosphate Transport Proteins ..	68
b. Anaerobic Dehydrogenase Polypeptides	73
3. Physical Characterization of the Recombinant Plasmids	79
C. Discussion	89
IV. Characterization of the Aerobic Dehydrogenase	94
A. Introduction	94
B. Results	94
1. Molecular Weight	94
2. Optical Properties	95
3. Amino Acid Composition	95
4. Comparison of Purified and Membrane-bound Enzyme	98
5. Electron Acceptors for the Aerobic Dehydrogenase	98
6. Inhibition by Structural Analogs	104
7. Inhibition of Activity by Purine Nucleotides	104
8. Inactivation of Aerobic Dehydrogenase	107
9. Effect of Phospholipids	110
10. Reconstitution of Aerobic Dehydrogenase with Membrane Vesicles	111
C. Discussion	113
V. Purification and Characterization of the Anaerobic Dehydrogenase	116
A. Introduction	116
B. Results	117
1. Purification of the Anaerobic Dehydrogenase	117
2. Evidence for Purity	124
3. Stability	124
4. Quaternary Structure and Hydrodynamic Properties	125
5. Circular Dichroism	129
6. Effect of Ethylene Glycol	131
7. Cofactor Identification	136
8. Optical Properties	137
9. Amino Acid Analysis	142
10. Kinetic Properties	142
11. Electron Acceptors for the Anaerobic Dehydrogenase	149
12. Effect of Detergent on Enzymatic Activity ..	151
13. Effect of Dideazaflavins on Enzymatic Activity	151
14. Inactivation Studies	153
12. Proteolytic Studies	156

C. Discussion	163
VI. Conclusions and Discussions	167
References	174

List of Tables

TABLE 1 <i>E. coli</i> Strains Utilized	41
TABLE 2 Recombinant Plasmids Utilized	42
TABLE 3 Glycerol-3-phosphate Dehydrogenase Levels in Strains Carrying Recombinant Plasmids	67
TABLE 4 Active Transport in MV12/pLC Isolates	69
TABLE 5 Expression of Anaerobic Dehydrogenase and Glycerol-3-phosphate Transport Activity	76
TABLE 6 Fragment Sizes Obtained from Restriction Endonuclease Digestion of pLC14-12	84
TABLE 7 Fragment Sizes Obtained from Restriction Endonuclease Digestion of pLC12-17	86
TABLE 8 Amino Acid Composition of the Aerobic Glycerol-3-phosphate Dehydrogenase	97
TABLE 9 Electron Acceptors for the Aerobic Dehydrogenase	103
TABLE 10 Effect of Substrate Analogues on the Aerobic Glycerol-3-phosphate Dehydrogenase	105
TABLE 11 Inhibition by Purine Nucleotides	106
TABLE 12 Inhibition of Aerobic Dehydrogenase Activity by Divalent Cations	108
TABLE 13 Inactivation of the Aerobic Dehydrogenase	109
TABLE 14 Purification of the Anaerobic Glycerol-3-Phosphate Dehydrogenase from <i>E. coli</i>	119

TABLE 15 Physical Properties of the Anaerobic Glycerol-3-Phosphate Dehydrogenase	127
TABLE 16 Amino Acid Composition of Anaerobic Glycerol-3-Phosphate Dehydrogenase	143
TABLE 17 Electron Acceptors for the Anaerobic Dehydrogenase	150
TABLE 18 Effect of Detergent on Anaerobic Dehydrogenase Activity	152
TABLE 19 Effect of Deazaflavin Analogs on Anaerobic Dehydrogenase Activity	154
TABLE 20 Inactivation of the Anaerobic Glycerol-3-Phosphate Dehydrogenase	155

List of Figures

Figure 1. Energy Transduction in Membrane Systems.	2
Figure 2. Functional Organization of Aerobic Electron Transport Carriers in <i>E. coli</i>	16
Figure 3. Functional Organization of Aerobic Electron Transport Chain in <i>E. coli</i>	18
Figure 4. Proposed Sequence of the Formate-Nitrate Electron Transfer Pathway in <i>E. coli</i>	23
Figure 5. Metabolism of Glycerol and Glycerol-3-phosphate in <i>E. coli</i>	29
Figure 6. The Location of the <i>glp</i> Genes on the <i>E. coli</i> Chromosome.	31
Figure 7. SDS-Polyacrylamide Gel Electrophoresis of Plasmid-coded Proteins from Minicells.	72
Figure 8. SDS-PAGE Analysis of Crude Cytoplasmic Fractions from Control and pLC14-12 Carrying Cells Grown Under Aerobic and Anaerobic Conditions.	77
Figure 9. Restriction Endonuclease Cleavage Map of pLC14-12.	82
Figure 10. Restriction Endonuclease Cleavage Maps of the Inserts in pLC3-46, pLC8-24, pLC14-12, pLC19-24 and pLC42-17.	83
Figure 11. SDS-PAGE Analysis of Crude Cytoplasmic Extracts from pLC14-12, pLC19-24, and pLC42-17.	87
Figure 12. Absorption Spectrum of the Aerobic Dehydrogenase.	96
Figure 13. pH Profile of Aerobic Dehydrogenase Activity. .	99

Figure 14. Temperature Profile of Aerobic Dehydrogenase Activity.	101
Figure 15. Reconstitution of Glycerol-3-phosphate-dependent Proline Transport.	112
Figure 16. Phenyl Sepharose CL-4B Chromatography of Ammonium Sulfate Pellet Fraction from Cytoplasmic Fraction of MV12/pLC14-12.	121
Figure 17. Hydroxylapatite Chromatography of Fraction Pool from Phenyl Sepharose CL-4B Column.	123
Figure 18. SDS-PAGE of Crosslinked Anaerobic Glycerol-3-phosphate Dehydrogenase.	126
Figure 19. Circular Dichroism Spectra of the Anaerobic Glycerol-3-phosphate Dehydrogenase.	130
Figure 20. Sedimentation Velocity Profile of Anaerobic Glycerol-3-phosphate Dehydrogenase.	133
Figure 21. Sedimentation Equilibrium of Anaerobic Glycerol-3-phosphate Dehydrogenase.	135
Figure 22. Absorption Spectrum of the Anaerobic Glycerol-3-phosphate Dehydrogenase.	138
Figure 23. The Visible Absorption Spectrum of the Anaerobic Glycerol-3-phosphate Dehydrogenase.	139
Figure 24. Effect of Substrate on Absorption Spectrum of Anaerobic Glycerol-3-phosphate Dehydrogenase.	141
Figure 25. Effect of Exogenous Flavins on Anaerobic Glycerol-3-phosphate Dehydrogenase Activity.	145
Figure 26. The Effect of Combinations of FAD and FMN on Enzymatic Activity.	147

Figure 27. Lineweaver-Burk Plot of Initial Velocity of Anaerobic Glycerol-3-phosphate Dehydrogenase as a Function of Substrate Concentration.	148
Figure 28. Time Course of DTNB Modification of Anaerobic Dehydrogenase.	157
Figure 29. Correlation of Sulfhydryl Modification with Inactivation of Anaerobic Dehydrogenase.	158
Figure 30. Products of Proteolysis of the Anaerobic Dehydrogenase.	160
Figure 31. Effect of Proteolysis on Anaerobic Glycerol-3-phosphate Dehydrogenase.	162

List of Abbreviations

ADP	adenosine-5'-diphosphate
AMP	adenosine-5'-monophosphate
ATP	adenosine-5'-triphosphate
DCPIP	dichlorophenolindophenol
DTNB	5,5'-dithio-(bis)-nitrobenzoic acid
DTT	dithiothreitol
EDTA	ethylenediamine tetraacetic acid
FAD	flavin adenine dinucleotide
FCCP	carbonyl cyanide trifluoromethoxyphenylhydrazone
FMN	flavin mononucleotide
G3P	glycerol-3-phosphate
G3PDH	glycerol-3-phosphate dehydrogenase
GTP	guanosine-5'-triphosphate
HEPES	N-2-Hydroxyethyl-piperazine-N'-2-ethanesulfonic acid
HOQNO	2-n-heptyl-4-hydroxyquinoline-N-oxide
MTT	3-(4,5-dimethylthiazolyl-2-yl)-2,5-diphenyl tetrazolium bromide

NAD ⁺	nicotinamide adenine dinucleotide, oxidized form
NADH	nicotinamide adenine dinucleotide, reduced form
PCMB	<i>p</i> -chloromercuribenzoic acid
PCMS	<i>p</i> -chloromercuriphenylsulfonic acid
PMS	phenazine methosulfate
SDS	sodium dodecyl sulfate
SDS-PAGE	sodium dodecyl sulfate polyacrylamide gel electrophoresis

I. Introduction

A. Background

1. Chemiosmotic Hypothesis

A number of fundamental biological processes such as oxidative phosphorylation, photophosphorylation, active transport and bacterial motility involve an input or output of energy and are intimately associated with biological membranes. Furthermore, these membrane-associated processes share a common energy pool or energy intermediate (Figure 1) and require an intact, sealed membrane. Thus, oxidation of a substrate by an electron transport chain can provide energy for synthesis of ATP or for active accumulation of metabolites by the cell. The nature of the energy intermediate and of its formation and utilization has been the subject of intensive investigation for over thirty years.

Historically, oxidative phosphorylation was the focus of investigation by workers in bioenergetics and many of the original hypotheses were developed to describe this process. One of the earlier proposals suggested the formation of a high-energy covalent bond to conserve the energy from oxidation and subsequent electron transport (1, 2). Failure to isolate the predicted chemical intermediate and the inability to explain the requirement for an intact membrane gave little support to this proposal. The proposal that an energized conformational state could store the energy from

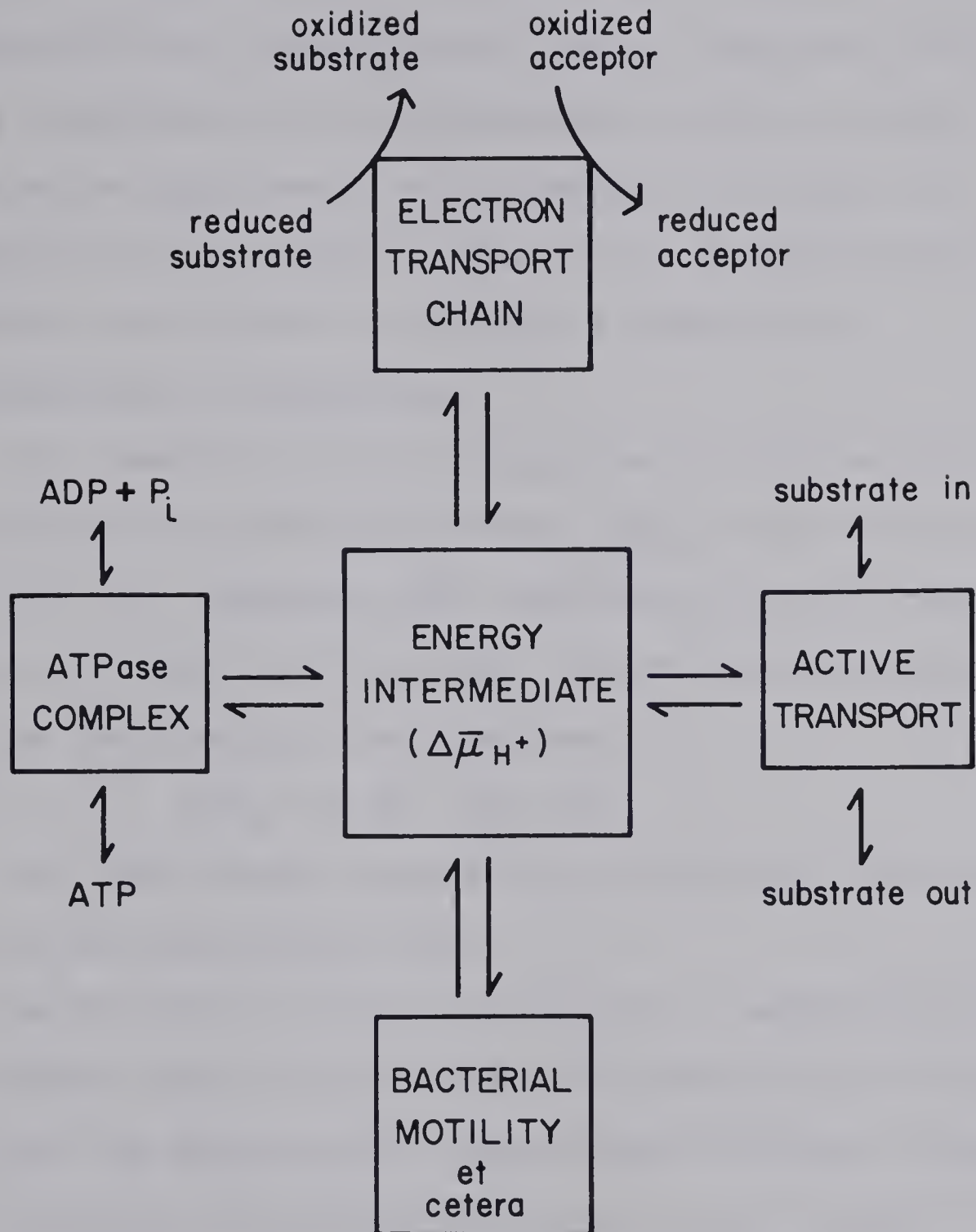


Figure 1. Energy Transduction in Membrane Systems. The above figure is a schematic representation of a general energy transduction scheme which was adapted from (13).

oxidative electron transport (3) required direct physical contact between the energy-producing and the energy-utilizing complexes but had no inherent requirement for a topologically closed membrane system. A unique alternative hypothesis was proposed by Mitchell (4). He suggested that an osmotic gradient of protons across the membrane was utilized in lieu of a chemical or conformational intermediate.

The osmotic gradient of protons across the membrane constitutes a protonmotive force, $\Delta \bar{\mu}_{H^+}$, which is composed of an electrical component, $\Delta \Psi$, and a chemical component which is proportional to ΔpH . The protonmotive force can thus be described by the equation:

$$\Delta \bar{\mu}_{H^+} = \Delta \Psi - \frac{RT}{F} \Delta \text{pH}$$

The chemiosmotic hypothesis of Mitchell (4) was founded on four main postulates (5):

1. The ATP synthetase is a reversible, membrane-associated complex that can synthesize or hydrolyze ATP dependent upon the protonmotive force present across the membrane.
2. Oxidative and photosynthetic electron transport chains are chemiosmotic, membrane-bound systems that generate a protonmotive force of the same polarity as that produced by ATP hydrolysis by the ATP synthetase complex.
3. Solute transport systems that function in accumulation of metabolites or in osmotic stabilization are coupled to fluxes of protons or hydroxyl ions.
4. The three systems discussed above are linked by their

presence in the same topologically closed membrane that has a low permeability to hydrogen ions and hydroxyl ions.

In addition to introducing the basic concept of the osmotic gradient of protons as an intermediate in bioenergetic processes, Mitchell also attempted to describe the mechanism by which this gradient was formed. He proposed that electron transport chains generate a proton gradient by the alternating asymmetric arrangement of hydrogen and electron carriers (6) as illustrated in Figures 2 and 3. The net result is translocation of hydrogen ions in one direction and the stoichiometry of the reaction is such that 2 protons are translocated per electron pair that is transferred through one "coupling site".

Mitchell's chemiosmotic hypothesis predicted a number of experimentally testable properties that have by and large been borne out. The relatively low effective proton conductance, essential for maintenance of the protonmotive force, has been demonstrated in a number of different energy-transducing membrane systems (7-10). The generation of a proton gradient by the various energy-transducing membrane systems, by ATP hydrolysis by the ATP synthetase complex, and by reconstituted respiratory complexes has been experimentally demonstrated (8,9,11-15). Artificially imposed pH or electrical gradients in a variety of different energy-transducing membrane systems resulted in the synthesis of ATP, demonstrating the reversibility of the ATP

synthetase complex and the role of the proton gradient in ATP production (16-19). The active accumulation of substrate by artificially imposed electrical gradients observed in reconstituted bacterial carrier systems (20,21) lends support to Mitchell's third postulate.

The effect of uncouplers on bioenergetic processes is consistent with the chemiosmotic hypothesis. Uncouplers comprise a wide variety of compounds that block ATP production or active accumulation of metabolites without affecting oxidation of substrate or the resulting electron transport reactions (22,23). Uncouplers increase the rate of proton conductance across biological membranes and artificial lipid bilayers (24,25) and this is the effect one would predict for chemiosmotic inhibitors. To explain the effect of uncouplers in terms of the chemical or conformational hypotheses, one has to assume there is some other common property shared by structures as different as dinitrophenol, gramicidin, and FCCP, and which allows them to interact in a similar fashion with components of energy-transducing membranes.

The demonstration of light-dependent ATP synthesis in synthetic lipid vesicles containing the mitochondrial ATP synthetase complex and the light-dependent proton pump, bacteriorhodopsin (26), lends further support to the chemiosmotic hypothesis. The fact that uncouplers inhibit this reaction (26), as well as the artificially induced, reconstituted active transport systems (20,21), is not

readily rationalized by the chemical or conformational hypotheses.

In the twenty years since its formal introduction the central thesis of the chemiosmotic hypothesis appears to have become widely accepted (5,13,14,27-29). Mitchell's proposal for the mechanism by which the protonmotive force is generated (Figures 2 and 3), however, is much more controversial. His redox-loop mechanism predicts a H^+/e^- ratio of 1, which is equivalent to a H^+/site ratio of 2. Extensive studies with mitochondrial preparations (30-32) have experimentally demonstrated that the H^+/site ratio is close to 4. These stoichiometries are not compatible with the redox loop mechanism, and indicate that there must be an alternative mechanism, at least in mitochondria. The experimental evidence, however, does not preclude the existence of a redox-loop mechanism since in some systems, such as the respiratory nitrate reductase complex of *E. coli* (33), a loop mechanism appears to be in operation. In mitochondria, conformationally-coupled H^+ pumps (34-36) or a combination of H^+ pumps and redox loops (36) may be responsible for establishment of the protonmotive force.

The current state of our knowledge and understanding of bioenergetic processes can be best described in the words of Lars Ernster: "...the chemiosmotic model...represents mainly a physical framework. The chemical mechanisms...remain to be elucidated. Progress towards this goal depends upon the success of continued efforts to understand the structure and

reaction mechanism of the individual energy-transducing catalysts as well as their relationship to, and interactions within, the membranes in which they reside. Only when this is accomplished can the problem of electron transport-linked phosphorylation -- and of membrane-associated energy transduction in general -- be regarded as solved in a satisfactory fashion."

2. Electron Transport Systems of *E. coli*

Escherichia coli is a facultative anaerobe able to derive its energy for growth either by glycolysis or by membrane-associated redox reactions utilizing either oxygen, fumarate, or nitrate as the terminal electron acceptor. The terminal electron acceptor present in the growth medium not only determines which terminal redox component will be predominant but also affects the composition of the remaining portions of the electron transport chain. Thus, studies on electron transport in *E. coli* have usually been classified relative to the terminal electron acceptor: oxygen, nitrate or fumarate.

a. Aerobic Electron Transport

Primary Dehydrogenases

A number of substrates can result in membrane energization in whole cells by utilizing cytoplasmic enzymes for the production of NADH (37). The NADH in turn is oxidized by a membrane-associated NADH dehydrogenase (37). The substrates succinate, malate, D- and L-lactate,

'Ernster, L. 1977. *Ann. Rev. Biochem.* 46: 981-995.

α -hydroxybutyrate, L-glycerol-3-phosphate, formate, dihydroorotate and pyruvate can directly feed reducing equivalents into the membrane-bound electron transport chain by utilizing specific dehydrogenases (37).

Preparations containing NADH dehydrogenase activity have been studied in a number of laboratories (38-40) and there have been two reports on the purification of this enzyme to near homogeneity (41,42). The enzyme purified on the basis of NADH-DCPIP oxidoreductase activity contained predominantly one band on SDS-PAGE gels of 38,000 molecular weight (41), whereas preparations isolated on the basis of NADH-quinone oxidoreductase activity contained a 46,000 molecular weight polypeptide with a minor amount of a 38,000 molecular weight band (42). The latter polypeptide was not believed to be responsible for the NADH-quinone oxidoreductase activity because only variable and small amounts (5-30%) were present in different preparations.

To demonstrate that the 38,000 molecular weight polypeptide was the primary dehydrogenase of the aerobic electron transport chain, Dancey and Shapiro (43) used antisera against the NADH-DCPIP oxidoreductase to inhibit NADH-oxidase and NADH-DCPIP oxidoreductase activities in membrane preparations. Although the two activities were inhibited in parallel, the role of the 38,000 molecular weight polypeptide was questioned by the subsequent finding that this antiserum also precipitated the 46,000 molecular weight polypeptide from the NADH-quinone oxidoreductase

preparations (42). Evidence implicating the 46,000 molecular weight polypeptide as the primary dehydrogenase of the aerobic electron transport chain comes from studies with a recombinant plasmid that complements a mutation in the respiratory NADH dehydrogenase (45). The presence of the recombinant plasmid resulted in increased levels of a 45,000 molecular weight membrane polypeptide. In fact, the nucleotide sequence of the gene coding for the respiratory NADH dehydrogenase has recently been published (46) and characterization of the purified protein is forthcoming in a subsequent publication.

Although the purified NADH-DCPIP oxidoreductase did not contain flavin, it had an absolute requirement for exogenous FAD (43), suggesting that FAD is the physiological cofactor (37). The NADH-quinone oxidoreductase contained 1 iron per 46,000 molecular weight polypeptide and did not have an absolute requirement for exogenous FAD although it was stimulated two-fold by its presence. The most recent preparation of NADH dehydrogenase had 1 FAD present per 45,000 polypeptide (46).

E. coli possesses both a D-lactate and an L-lactate dehydrogenase coupled to the aerobic electron transport chain (37). The membrane-bound D-lactate dehydrogenase has been purified in three different laboratories (47-49) and the effect of detergents and lipids on enzymatic activity has been the subject of two independent studies (50,51). The purified enzyme has a native molecular weight of 75,000 and

is composed of a single subunit of that molecular weight (47-49). The purified enzyme was shown to contain 1 FAD/75,000 molecular weight subunit and the flavin absorption was quenched upon addition of substrate (47,48), indicating reduction of the flavin cofactor. Enzymatic activity was not affected by treatment with sulfhydryl reagents (47,48). The effect of phospholipids on detergent-depleted enzyme was to increase both the K_m for D-lactate and the V_{max} (50,51). The phospholipid stimulation of activity was accompanied by a conversion of the enzyme from an aggregated to a monomeric form (50).

The L-lactate dehydrogenase of *E. coli* has also been purified to homogeneity (52) and the effect of amphipaths on enzymatic activity was similarly studied (53). The purified enzyme contained a single type of subunit of 43,000 molecular weight which was present as a high molecular weight species of 320,000 to 360,000 molecular weight in the presence of 1% Tween 80 or 1% cholate (56). The purified enzyme contained 1 mole FMN per mole of 43,000 molecular weight subunit. As observed with D-lactate dehydrogenase, detergent-depletion resulted in a loss in activity and addition of phospholipid stimulated the detergent-depleted enzyme with a concomittant increase in the K_m for substrate (53). In addition, it was observed that the estimated α -helical content determined from circular dichroism spectra increased 1.7 fold upon addition of phospholipid (53).

The membrane peripheral pyruvate dehydrogenase is the most thoroughly studied primary dehydrogenase from *E. coli*. This enzyme, commonly referred to as pyruvate oxidase, was purified and crystallized by Hager and coworkers (54,55) and was shown to be a tetramer of four 60,000 molecular weight subunits. The enzyme contained four moles FAD per tetramer (55,56) and required thiamin pyrophosphate for activity, binding up to 4 moles of thiamin pyrophosphate per tetramer (57,58). The *in vivo* location of pyruvate dehydrogenase was inferred from the inaccessability of enzymatic activity to antibody and to impermeable thiamin pyrophosphate analogues in membrane vesicles (59). Since the enzyme was capable of transferring reducing equivalents to the aerobic electron transport chain, it was concluded that the enzyme was associated with the inner surface of the cytoplasmic membrane.

The specific activity of the purified enzyme was stimulated 20- to 50-fold by detergents or phospholipids and this stimulation was extensively studied by Blake *et al* (60). They demonstrated that either the monomeric or micellar forms of detergents or phospholipids were effective. The quaternary structure of the enzyme was not affected by amphipaths (61), in contrast to that of D-lactate dehydrogenase (50). Similarly, limited proteolysis in the presence of thiamine pyrophosphate and pyruvate increased the specific activity about 25-fold and this form of enzyme was insensitive to detergents or phospholipids

(62). Chemical reduction of the flavin cofactor could replace the requirement for pyruvate during proteolytic activation, indicating that the redox state of the flavin was critical (62). During proteolytic activation the subunit molecular weight was reduced from 60,000 to 56,000 (62) but the enzyme remained in a tetrameric form (56). Further studies indicated that proteolytic activation and stimulation by detergents or phospholipids involved the same site on the enzyme (63).

There have been no reports of the successful purification of the succinate dehydrogenase from *E. coli*, probably due to the lability of the enzyme upon solubilization (64,65). Kim and Bragg (64) extracted the enzyme from an acetone powder of whole cells and removed contaminating cytochrome by hydroxylapatite chromatography but only achieved a doubling of the specific activity. The estimated molecular weight of the extracted enzyme was 100,000 as determined by analytical gel filtration (64). Identification of the large subunit of succinate dehydrogenase from *E. coli* (66) indicates that it is similar in molecular weight to succinate dehydrogenase from beef heart (67), *Rhodospirillum rubrum* (68), *Neurospora crassa* (69), and *Bacillus subtilis* (70) and to fumarate reductase from *Vibrio succinogenes* (71) and *E. coli* (72). Membrane-bound succinate dehydrogenase from *E. coli* is activated by pre-incubation with succinate (64,65), which is a property also observed in mitochondrial succinate

dehydrogenase (73).

The aerobic L-glycerol-3-phosphate dehydrogenase, which is distinct from the anaerobic enzyme (74,75), was initially purified and characterized by Weiner and Heppel (76). In their communication they indicated the native molecular weight was estimated at 80,000 and the subunit molecular weight was 35,000. They demonstrated that the cofactor was FAD and that it was reduced by substrate. Subsequent characterization of this enzyme in our laboratory will be discussed in Chapter 4.

Terminal Oxidases

Spectral studies have demonstrated that *Escherichia coli* has three cytochrome oxidases; cytochrome a₁, cytochrome o and cytochrome d. The reoxidation of reduced cytochrome a₁ was relatively slow (77), indicating that it probably is not the primary functional terminal oxidase in aerobically-grown *E. coli*. Cytochromes o and d have not been purified from the membrane and thus studies on these components have been restricted to membrane preparations. The relative proportions of these two cytochromes varies with the stage of growth. Cytochrome o is present at higher levels during exponential growth while cytochrome d is the predominant species during stationary phase of growth (37). The precise roles of these two components in the *in vivo* situation cannot be conclusively determined from the available information.

Sequence and Organization

In addition to the primary dehydrogenases, the aerobic electron transport chain of *E. coli* contains non-heme iron, ubiquinones, and cytochromes that are involved in the electron transport reaction. The precise role of these various components is still very much a matter of debate. However, there have been several different proposals for the sequence of the components in the aerobic electron transport chain (78-80) based on the experimental evidence available.

Measurements of the H^+/O ratio with intact *E. coli* (81,82) or spheroplasts (83,84) yielded values of nearly 4 for NADH and approximately 2 for lactate, succinate or glycerol-3-phosphate, which is equivalent to a H^+/site ratio of 2. These results suggested that a Mitchell redox loop mechanism could be responsible for generation of a protonmotive force in *E. coli*. Several models of the structural organization of the aerobic electron transport chain have been proposed which incorporate a Mitchell redox loop mechanism (78,80). Two such proposals are illustrated in Figures 2 and 3. The two schemes differ in two basic points:

1. Figure 2 implies that the NADH dehydrogenase is effectively translocating H atoms across the membrane whereas in Figure 3 this role is performed by ubiquinone.
2. Figure 2 suggests that the D-lactate (succinate or glycerol-3-phosphate) dehydrogenase transfers its

Figure 2. Functional Organization of Aerobic Electron Transport Carriers in *E. coli*. The above figure has been adapted from Haddock and Jones(78). The pathway for hydrogen atoms or electrons is indicated by the arrows and the entity being translocated is indicated above the arrows. The carriers responsible for the proposed movements are indicated between the arrows. The abbreviations utilized are: FP, flavoprotein or primary dehydrogenase; Fe/S, iron-sulfur protein; Q₈, ubiquinone-8; and cyt, cytochrome.

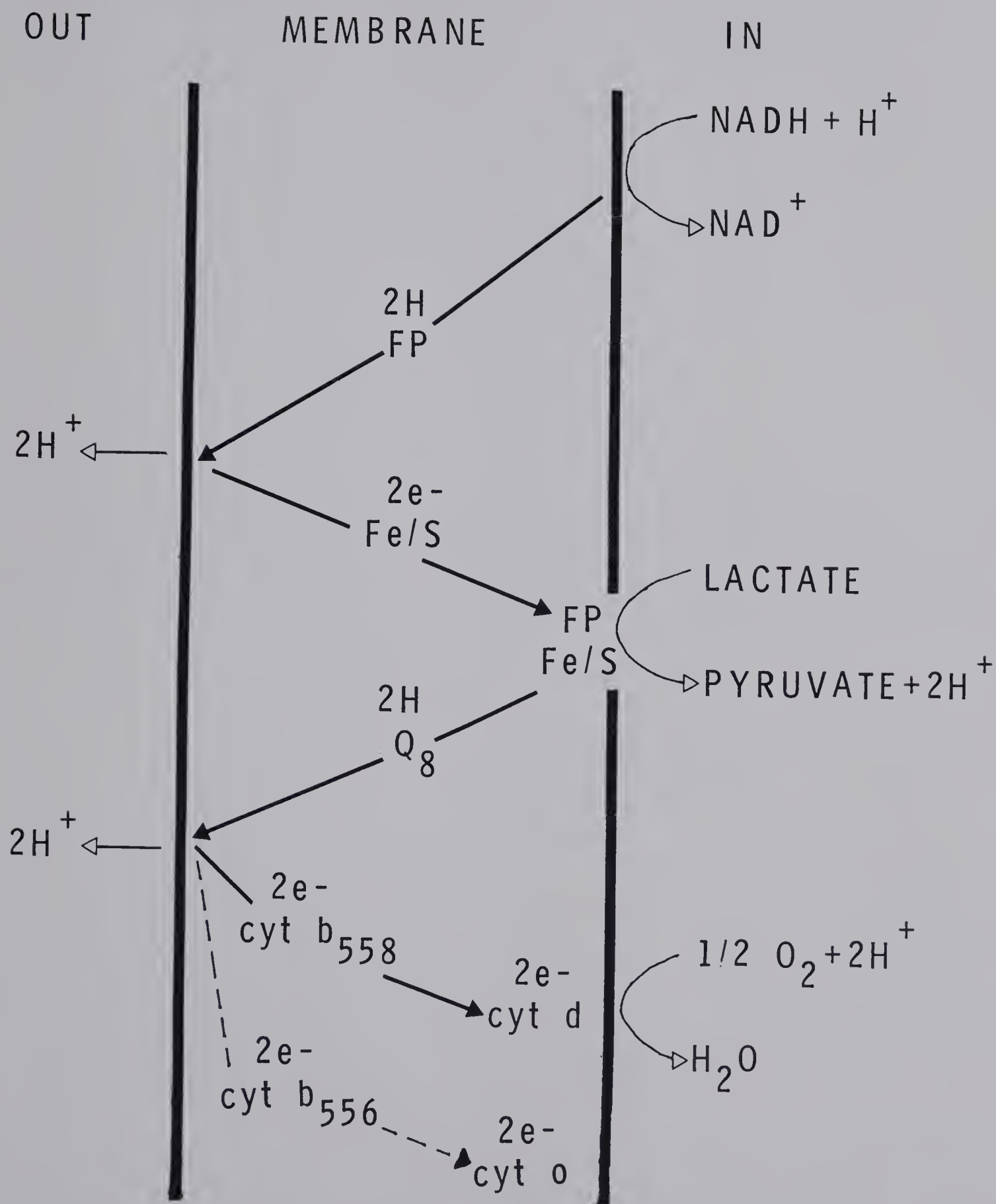
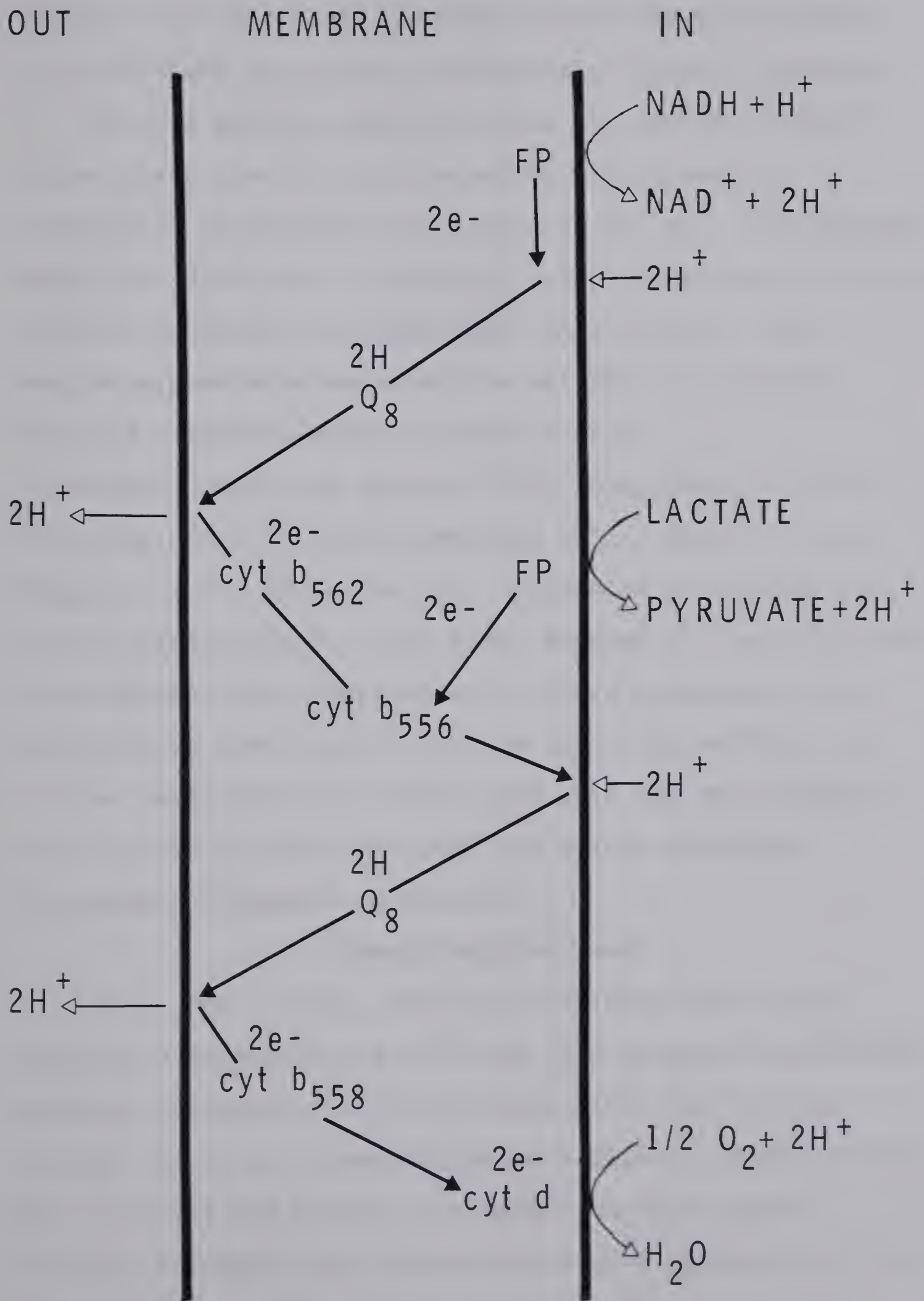


Figure 3. Functional Organization of Aerobic Electron Transport Chain in *E. coli*. The above figure has been adapted from Downie and Cox(80). Abbreviations and symbols are the same as in Figure 2.



reducing equivalents to ubiquinone, perhaps via an iron-sulfur protein, whereas Figure 3 suggests that cytochrome b_{556} is an intermediate in this transfer.

The two models, however, share the assumption that proton translocation is effected by an asymmetric orientation of hydrogen and electron carriers. The proposed models are difficult to reconcile with experimental evidence obtained by Singh and Bragg (85). They observed that ascorbate-phenazine methosulfate was able to energize inverted membrane vesicles prepared from cytochrome-containing cells or from ubiquinone deficient cells but not from cytochrome-less cells. Observation of Figures 2 and 3 indicates that ubiquinone is responsible for proton translocation in the final segment of the respiratory chain whereas the experimental evidence presented above demonstrates that this is not the case. Furthermore, the H^+ /site ratio may be 3 (86,87) and this may be too high to be accounted for by a Mitchell redox-loop mechanism.

b. Electron Transport to Nitrate

Primary Dehydrogenases

In *E. coli*, NADH, succinate, lactate, formate and glycerol-3-phosphate are oxidized by a membrane-associated electron transport chain that terminates with nitrate (78,88). It is not clear whether the primary dehydrogenases for succinate and lactate are common to both aerobic electron transport and electron transport terminating with nitrate. The coordinate increase in NADH-oxidase and

NADH-nitrate reductase levels that was observed by growth on nitrate (89) suggests that the primary dehydrogenase for these two activities may be the same. Genetic studies with *E.coli* have demonstrated that both the aerobic and the anaerobic L-glycerol-3-phosphate dehydrogenases can transfer reducing equivalents via the electron transfer pathway to nitrate (90). Growth on nitrate induces the synthesis of a b-type cytochrome, nitrate reductase, and also formate dehydrogenase. The coordinate induction of formate dehydrogenase and nitrate reductase activities and the coordinate loss of these activities in a number of mutants (91) suggests that the formate-nitrate reductase pathway may exist as a specific complex. In fact, early attempts at purifying formate dehydrogenase resulted in coordinate purification of cytochrome b and nitrate reductase (92).

Anaerobic conditions were required for purification of formate dehydrogenase from *E. coli* (93). The purified enzyme had polypeptide components of 110,000, 32,000 and 20,000 molecular weight and an apparent native molecular weight of 590,000 (93). The 110,000 and 32,000 subunits were present in a 1:1 ratio but the level of the 20,000 molecular weight component was variable. The authors suggested the structure was an α, β, γ_2 complex but this has not been directly demonstrated. The purified enzyme contained heme, molybdenum, selenium, non-heme iron and acid-labile sulfide in the molar ratio 1:1:1:13-14:13-14 but did not contain any flavin. Although the b-type cytochrome associated with

formate dehydrogenase had identical spectral characteristics to that associated with nitrate reductase the lack of a common subunit in the two preparations suggests that two distinct b-cytochromes are involved (93).

Nitrate Reductase

There have been a number of reports on the purification of nitrate reductase from *E. coli* and the properties of these different preparations have been compared in several reviews (37,78). The enzyme is composed of three polypeptides of 155,000, 63,000 and 19,000 molecular weight. The 19,000 polypeptide is not present in all preparations and is associated with the presence of a b-type cytochrome. Experimental evidence suggests that the presence of the b-type cytochrome is required for incorporation of nitrate reductase into the membrane (94). At low protein concentrations the native molecular weight of the enzyme is about 210,000 and at higher protein concentrations it is about 880,000 (95), suggesting a monomer-to-tetramer association (37). The purified enzyme contains molybdenum, nonheme iron and acid labile sulfur in a 1:12-13:12-13 ratio (37,96,97) but no flavin.

Organization of the Electron Transport Chain to Nitrate

The involvement of b-type cytochromes in the formate-nitrate oxidoreductase pathway was established from the following observations:

1. Growth anaerobically on nitrate induces the production of a distinct species of b-type cytochrome that can be

distinguished by its spectral properties and the control of its expression (98).

2. The reduction of this species of b-type cytochrome by formate and reoxidation by nitrate can be observed in whole cells (98), in the purified formate dehydrogenase and nitrate reductase components (99) and in a reconstituted system from the purified components (99).
3. Both purified preparations of nitrate reductase and formate dehydrogenase contain a b-type cytochrome and successful reconstitution of formate-nitrate oxidoreductase activity requires at least the b-type cytochrome from nitrate reductase. The involvement of two b-type cytochromes is deduced from spectral studies with the inhibitor HOQNO in which only half of the b-type cytochrome is reduced by formate or oxidized by nitrate (98). The lack of a common subunit in the formate dehydrogenase and the nitrate reductase preparations (93,99), although they both contain a b-type cytochrome, also supports this proposal.

The above considerations led to the proposed sequence of the formate-nitrate pathway which is illustrated in Figure 4. The requirement for quinone in this pathway has been demonstrated (33,99) and the inability of nitrate reductase lacking the b-type cytochrome to oxidize reduced ubiquinone (33) suggests that ubiquinone is involved before the second b-type cytochrome. However, neither the precise location of involvement of the quinone component nor whether

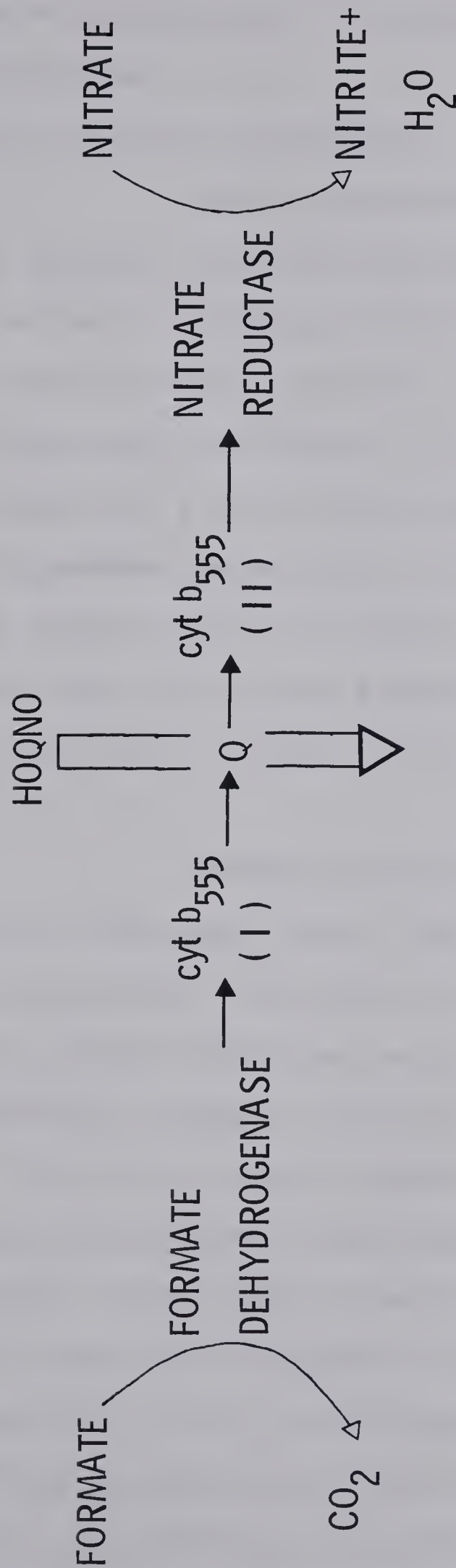


Figure 4. Proposed Sequence of the Formate-Nitrate Electron Transfer Pathway in *E. coli*. The above illustration is a modification of that presented by Bragg(37) which is based on the original proposal of Ruiz-Herrera and DeMoss(98). Linear arrows represent the direction of transfer of reducing equivalents.

ubiquinone or menaquinone is involved *in vivo* has been firmly established.

c. Electron Transport to Fumarate

Primary Dehydrogenases

NADH, lactate, glycerol-3-phosphate, formate and hydrogen can be oxidized by a membrane-associated electron transport chain terminating with fumarate reduction (78,88). Growth on glycerol and fumarate requires the presence of a distinct anaerobic glycerol-3-phosphate dehydrogenase (90). The dehydrogenases responsible for oxidation of other substrates terminating with fumarate reduction have not been well established. They could presumably be the same enzymes that are required for growth in the presence of nitrate or oxygen.

Fumarate Reductase

Fumarate reductase from *E. coli* has been purified in this laboratory (100). The purified enzyme is composed of a 69,000 and a 25,000 molecular weight subunit and has a native molecular weight of 100,000, indicating that it is an $\alpha\beta$ dimer (100). This subunit composition is similar to that of succinate dehydrogenase from mammalian mitochondria (101), from *R. rubrum* (68), from *N. crassa* mitochondria (69) and from *B. subtilis* (70) and to fumarate reductase from *V. succinogenes* (71). The *E. coli* fumarate reductase has an FAD cofactor that is covalently linked via the 8 α position of riboflavin to the N(3) of a histidine residue in the 69,000 dalton polypeptide (102). Covalent attachment of flavin to

the large subunit is also observed in succinate dehydrogenase from mammalian mitochondria, *R. rubrum* and *B. subtilis* (68,70,101) and in fumarate reductase from *V. succinogenes* (71). Furthermore, the same type of covalent linkage is observed in those systems in which it was determined (71,101). Even more striking similarities are observed when one compares the amino acid sequence of fumarate reductase, which was obtained by analysis of the nucleotide sequence from a cloned fumarate reductase gene (103), to the amino acid sequence of the flavin containing peptide of beef heart mitochondrial succinate dehydrogenase (101). There is a homologous sequence of at least nine amino acids (104).

Amino acid analysis of *E. coli* fumarate reductase subunits also revealed that there is a striking similarity to the amino acid composition of the large and small subunits of *R. rubrum* and beef heart mitochondrial succinate dehydrogenase (104). The content of nonheme iron and acid labile sulfide in *E. coli* fumarate reductase is 4 moles/mole dimer (104) which is in contrast to the 8 moles/mole dimer determined in mammalian mitochondrial (101) and *R. rubrum* (68) succinate dehydrogenase.

Organization of the Electron Transport Chain to Fumarate

Electron transport from NADH or glycerol-3-phosphate to fumarate has been shown to require quinone and b-type cytochrome in several species of bacteria (37,88). The involvement of menaquinone in the reaction in *E. coli* has

been demonstrated by Newton *et al* (105) and by Singh and Bragg (106). However, the observation that cytochrome-deficient cells could grow on glycerol (or G3P) plus fumarate but not on glycerol plus nitrate, suggested a cytochrome-independent redox reaction (106). It was further demonstrated that G3P-fumarate oxidoreductase activity, involving menaquinone, was present in membranes from cytochrome-less cells although generation of a pH gradient, as determined by quenching of atebrin fluorescence, was not observed (106). The subsequent observation that electron transport from G3P to fumarate could energize active transport of proline and glutamine in cytochrome-containing but not cytochrome-deficient cells (107) indicated that cytochromes were required for membrane energization. Energization of active transport (108-110) and of ATP synthesis (111) by G3P to fumarate electron transport was also observed in membranes prepared from cytochrome-containing cells. Thus, although the normal electron transfer pathway between G3P and fumarate involves a primary dehydrogenase, menaquinone, cytochrome, and a terminal reductase, the sites of involvement of the menaquinone and cytochrome components have not been established.

3. Proteins Involved in the Catabolism of Glycerol and Glycerol-3-phosphate

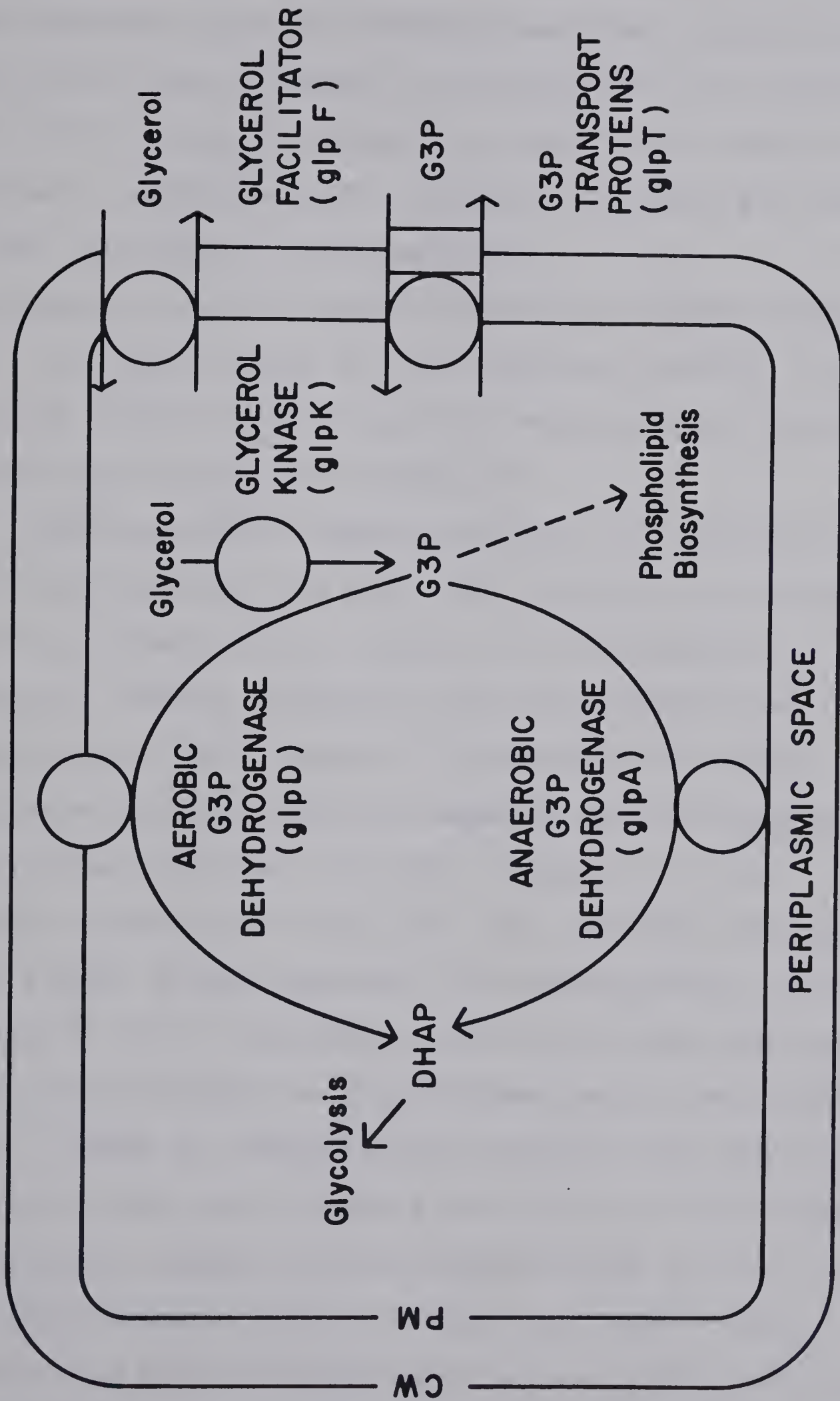
a. Metabolic Pathway for Glycerol and Glycerol-3-Phosphate

Escherichia coli is a facultative anaerobe that can grow aerobically on glycerol or G3P as the sole carbon and energy source or anaerobically on these substrates in the presence of the alternate electron acceptors, nitrate or fumarate (112). The pathway for utilization of external glycerol or G3P is depicted in Figure 5. A glycerol facilitator, coded by the *glpF* gene, enhances the rate of uptake of external glycerol into the cell (113). Glycerol is then converted to G3P by glycerol kinase, the product of the *glpK* gene (114,115). When extracellular G3P is present, it is actively accumulated by the cell by an active transport system composed of a functional periplasmic protein and a membrane component, both specified by the *glpT* gene (116,117).

The pool of internal glycerol-3-phosphate that is produced by these two alternate routes can subsequently be oxidized by either of two distinct G3P dehydrogenases (112). The aerobic dehydrogenase, product of the *glpD* gene, can function under aerobic conditions or under anaerobic conditions in the presence of nitrate (76,90). The anaerobic dehydrogenase, product of the *glpA* gene, functions under anaerobic conditions in the presence of nitrate or fumarate (90,118). The product of G3P oxidation by these enzymes (76,118), dihydroxyacetone phosphate, can be catabolized by the enzymes of the glycolytic pathway.

Prolonged selection for growth, in a glycerol medium, of a mutant strain that is deficient in both glycerol kinase

Figure 5. Metabolism of Glycerol and Glycerol-3-phosphate in *E. coli*. Abbreviations used: CW, cell wall; PM, plasma membrane.



and aerobic G3PDH results in the induction of an NAD-dependent glycerol dehydrogenase that can be utilized as the first step in glycerol catabolism (119,120). However, it is unlikely that this enzyme is normally utilized in glycerol catabolism and, although it has been purified (120), its role is still uncertain.

b. Expression of the Genes Involved in Glycerol Catabolism

The genes coding for the proteins involved in glycerol and G3P catabolism are found at three separate regions of the *E. coli* chromosome (Figure 6).

Earlier studies demonstrated that the *glpA* (anaerobic G3P dehydrogenase) and *glpT* (G3P transport) genes were closely linked (90) and appeared to be expressed in a parallel fashion suggesting they were probably part of the same operon (121). However, two recent studies have indicated that at least two separate operator-promoter regions are involved (122,123). Insertion of the bacteriophage Mu into the *glpT* gene abolished G3P transport but did not affect anaerobic G3P dehydrogenase activity or function (122). Similarly, insertion into the *glpA* gene did not affect the *glpT* activity. These results were observed for a number of independently isolated insertions which indicates that the two genes are not in the same operon. Subsequent studies utilized operon-fusion strains in which the *glpT* operator-promoter region was fused to the structural β -galactosidase gene so that expression of the *glpT* control region could be easily assayed (123). In this

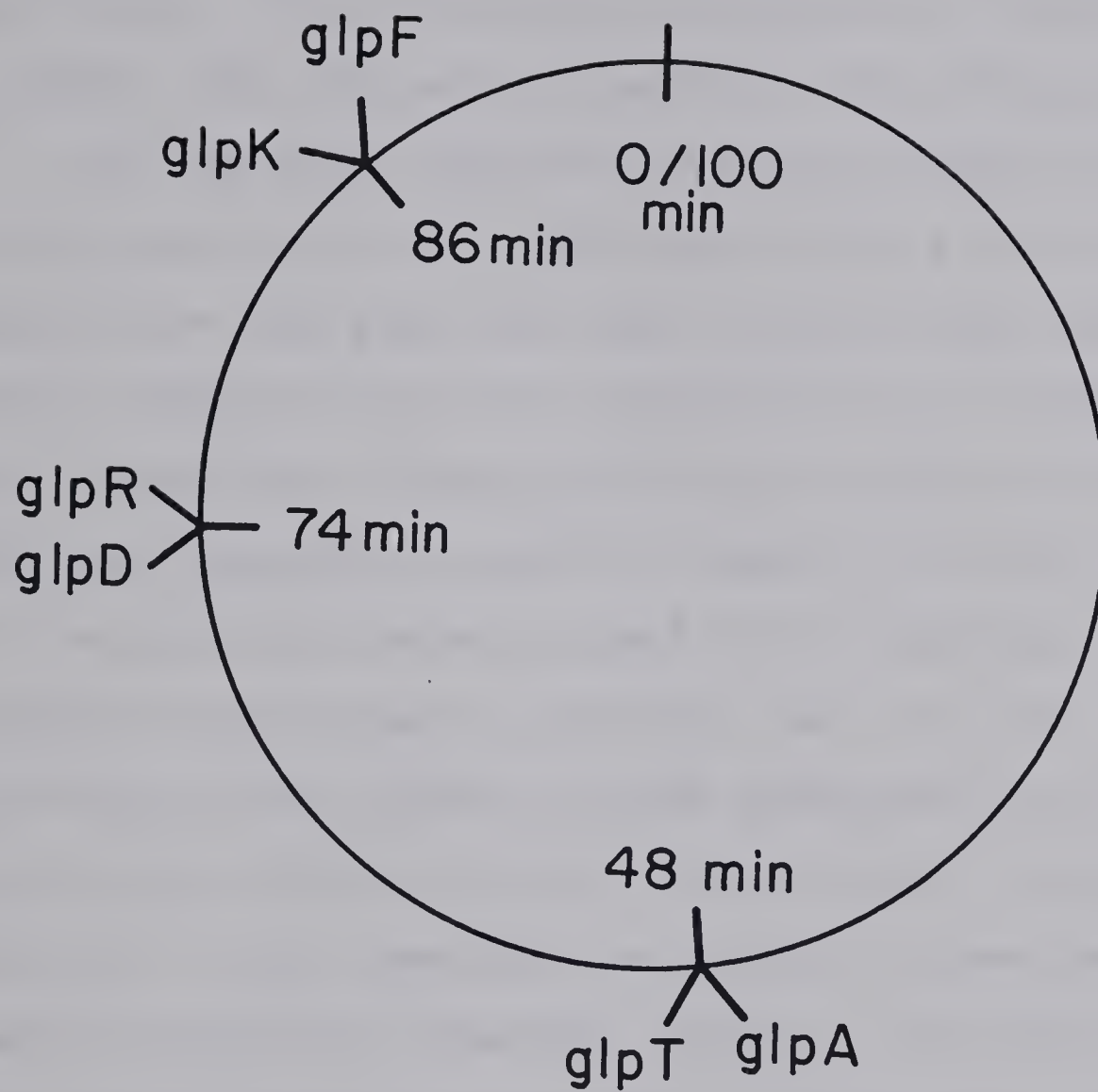


Figure 6. The Location of the *glp* Genes on the *E. coli* Chromosome.

study it was observed that the levels of the anaerobic dehydrogenase and β -galactosidase activities did not fluctuate in a parallel fashion with changes in the growth conditions. The differential expression of these two genes suggests that they are not part of the same operon.

All the known operons of the *glp* system are regulated by the product of the *glpR* locus which is adjacent to the *glpD* locus. The *glpR* gene specifies a repressor (124) which responds to glycerol-3-phosphate as effector (125). To study the effect of the *glpR* locus on the different *glp* operons, temperature-sensitive mutants and deletion mutants of the *glpR* gene were utilized (121). Synthesis of the aerobic dehydrogenase (*glpD* gene) was much more sensitive to repression than glycerol kinase (*glpK* gene) or G3P transport (*glpT* gene). When the effect of catabolite repression was studied, it was observed that glycerol kinase was much more sensitive than G3P transport which in turn was more sensitive than the aerobic G3P dehydrogenase (121).

The original studies on the effect on expression by the terminal electron acceptor present in the medium involved only the *glpD* and the *glpA* genes since there was no reason to suspect that the other gene products would fluctuate in response to these variations (121). In these studies it was observed that there were reciprocal fluctuations in the levels of the aerobic and anaerobic dehydrogenase. The aerobic dehydrogenase levels were high under aerobic conditions or under anaerobic conditions in the presence of

nitrate while the anaerobic dehydrogenase levels were low under these conditions. During anaerobic growth in the presence of fumarate the anaerobic dehydrogenase levels were much higher than the aerobic dehydrogenase levels. In a more recent study it was observed that the expression of the *glpT* gene was also affected by the terminal electron acceptor present in the growth medium (123). The pattern of expression is similar to that of the *glpA* gene but the fluctuations observed are much smaller, indicating that the *glpT* gene is less sensitive to this form of control than the *glpA* gene.

c. Characterization of the Proteins Involved in Glycerol and Glycerol-3-phosphate Catabolism

Glycerol-3-phosphate Transport Proteins

A periplasmic protein related to G3P transport, whose presence correlated with *glpT* function during genetic manipulations, has been identified by Silhavy *et al.* (126). However, the authors were unable to demonstrate binding activity towards G3P in crude shock fluid containing this protein. Subsequent purification of this protein indicated that the native protein was a tetramer of four identical 40,000 molecular weight subunits which did not exhibit any detectable G3P binding activity (127). The periplasmic protein was not present in membrane vesicle preparations that actively accumulated G3P, indicating that it was not involved in the active transport process across the cytoplasmic membrane. It is noteworthy that all the

transport-deficient mutants tested were deficient in transport in both vesicle preparations and whole cells (117).

The periplasmic protein was synthesized in a cell-free system directed by hybrid plasmid ColE1-*glpT* DNA (pLC3-46) dependent on cyclic AMP and induced by glycerol-3-phosphate (128). Although the product reacted with antibody prepared against the purified periplasmic protein, it was of a slightly larger size, indicating that it was likely the *in vivo* precursor. In addition, a 33,000 molecular weight polypeptide, whose synthesis was dependent upon cyclic AMP and which associated with the particulate fraction, was presumed to be the cytoplasmic *glpT* protein.

Recent reports in the literature on the purification and characterization of a periplasmic G3P binding protein (129) are related to a second transport system for G3P that was induced by selection for growth on G3P of a *glpT* mutant (130). The new G3P transport system appears to be regulated in a similar fashion as alkaline phosphatase (131).

Aerobic Glycerol-3-phosphate Dehydrogenase

Original studies on the aerobic G3PDH indicated that it could be distinguished from the anaerobic enzyme by its association with the particulate fraction and by its insensitivity to exogenous flavins (132). Subsequent purification of the enzyme by Weiner and Heppel (76) established that the enzyme had a non-covalently-bound FAD cofactor, an apparent molecular weight of 80,000, and was

composed of subunits of 35,000 molecular weight. In addition the authors reported that the K_m for DL-glycerol-3-phosphate was 0.8 mM for the purified enzyme compared to 23 mM for the membrane-bound activity.

Studies on the localization of the aerobic dehydrogenase indicated that the enzyme was present on the cytoplasmic surface of the membrane in whole cells and spheroplasts (133). This was concluded on the basis of a lack of G3P-energized active transport of amino acids in a G3P transport-deficient mutant and on the inability of whole cells or spheroplasts to utilize the impermeable electron acceptor, ferricyanide. Membrane vesicles prepared by the Kaback procedure (134) exhibited nearly half of the total G3P-dependent ferricyanide reductase activity prior to permeabilization, suggesting that partial inversion was occurring during preparation of the vesicles.

Anaerobic Glycerol-3-phosphate Dehydrogenase

Kistler and Lin (118) partially purified the anaerobic G3PDH and described a number of the properties of the enzyme preparation. Although the authors did not report the subunit composition, a native molecular weight of 80,000 was determined by gel filtration. They investigated the flavin stimulation of enzymatic activity and found that both FAD and FMN stimulated activity with K_m 's of 10^{-7} M and 10^{-4} M respectively. They also reported that the substrate dependence of the reaction rate was complex in the presence of FMN but was of the Michaelis-Menten type in its absence.

Enzymatic activity was also shown to be sensitive to treatments with p-chloromercuribenzoate, N-ethylmaleimide or iodoacetate.

B. The Thesis Problem

Although it is generally accepted that the energy intermediate in membrane-associated bioenergetic processes is the protonmotive force, the mechanism by which it is generated and utilized is still controversial. The ultimate understanding of this process will likely require characterization of the components involved and of their interactions at the molecular level. Considerable progress has been made with the respiratory chain components from beef heart mitochondria, but this system has certain features that make it less attractive to study than bacterial electron transport systems. The mammalian mitochondrial respiratory chain is more complex than individual bacterial electron transport complexes. For example, mammalian cytochrome oxidase has seven polypeptides (136) whereas nitrate reductase (93) and fumarate reductase (100) from *E. coli* consist of only two polypeptides. Furthermore, bacterial systems such as *E. coli* have the inherent advantage of well-characterized genetics and the additional advantage that many systems for genetic manipulation have been developed with this organism and are readily available.

The system that was chosen for study in our laboratory involves the proteins responsible for glycerol-3-phosphate catabolism in *Escherichia coli* and the components with which they interact. The reasons for choosing this particular system are the following:

1. The genetics of the *glp* system have been well established which should facilitate subsequent genetic manipulations.
2. The presence of an aerobic and an anaerobic dehydrogenase that interact with different electron transport pathways provide a unique approach for studying these systems.
3. The composition of the electron transport chain with which the anaerobic dehydrogenase interacts is relatively simple. This should aid in the eventual goal of reconstitution of the system.

The specific objectives of my graduate research were to purify and characterize the aerobic and anaerobic glycerol-3-phosphate dehydrogenases of *Escherichia coli*. I adopted a combined genetic and biochemical approach to this problem and thus the characterization and utilization of recombinant plasmids is also dealt with in the body of this thesis.

The first section of the thesis involves the characterization of a group of ColE1:*E. coli* hybrid plasmids carrying the *glpT* and *glpA* genes. In addition, determination of the polypeptide products coded by these plasmids is

included.

The second section involves the characterization of the aerobic glycerol-3-phosphate dehydrogenase. This study was carried out as a joint research endeavour by Miss Elke Lohmeier and myself under the supervision of Dr. Joel H. Weiner. It includes a physical, chemical and kinetic characterization of the purified enzyme and also involves reconstitution studies with the purified enzyme.

The third section of my studies deals with the purification and characterization of the anaerobic glycerol-3-phosphate dehydrogenase.

The purification and characterization of the aerobic and the anaerobic glycerol-3-phosphate dehydrogenase is a necessary step in determining the structural and functional organization of the glycerol-3-phosphate-oxygen and glycerol-3-phosphate-fumarate electron transport pathways. Reconstitution experiments with native vesicles or ultimately with the additional isolated components can be carried out with either of the purified dehydrogenases. This comparative approach may prove useful in studying the specificity of interactions that are involved in the electron transfer reactions and in the concomittant generation of a protonmotive force.

II. Materials and Methods

A. Materials

1. Chemicals

L-(U-¹⁴C)glycerol-3-phosphate, L-(U-¹⁴C) proline, L-(U-¹⁴C) glutamine, and L-U-¹⁴C-labelled amino acids were obtained from New England Nuclear, Boston, Ma. Phenyl Sepharose CL4B was from Pharmacia Fine Chemicals, Dorval, Quebec. Hydroxylapatite for protein purification was from Clarkson Chemical Co., Williamsport, Pa. Hydroxylapatite used in subunit separation (Bio-Gel HTP), acrylamide, bis-acrylamide, DTT, SDS, TEMED and ammonium persulfate were obtained from Bio-Rad Laboratories, Richmond, Ca. Gel electrophoresis grade agarose and lambda DNA were obtained from Bethesda Research Laboratories, Bethesda, Md. Dimethyl suberimide was obtained from Serva Biochemicals, Heidelberg, F.R.G. DTNB was obtained from Calbiochem-Behring Corp., San Diego, Ca.

Phosphonomycin was a generous gift from Dr. B.G. Christensen of Merck, Sharp and Dohme Research Laboratories, Rahway, N.J. 1-deazariboflavin, 5-deazariboflavin, and 1,5-dideazariboflavin were generous gifts from Dr. W.T. Ashton of Merck, Sharp and Dohme Research Laboratories, Rahway, N.J. Colicin E1 was isolated from *E. coli* W3110/ColE1 by the Schwartz and Helinski procedure (137).

2. Enzymes

Chymotrypsin was obtained from Worthington Biochemicals Corp., Freehold, N.J. Soybean trypsin inhibitor and nucleotide pyrophosphatase (Type III: from *Crotalus atrox* venom) were obtained from Sigma Chemical Co., St. Louis, Mo. Restriction endonucleases Eco RI, Bam HI, Hind III, Bgl I, Alu I, and Hinf I were obtained from Bethesda Research Laboratories, Bethesda, Md. Kpn I, Ava I, and Pvu II were obtained from New England Biolabs, Beverly, Ma. Pst I and Hpa I were obtained from Boehringer Mannheim, Dorval, Quebec.

3. Bacterial Strains and Plasmids

The bacterial strains and plasmids utilized in this study are listed in Tables 1 and 2. Strains 7, 13, 105 and 122 were originally isolated by E.C.C. Lin (Harvard University) and were provided by Dr. B. Bachmann (Yale University). JW14 is a spontaneous *glp D⁺* revertant isolated from strain 122. X1197 was provided by Dr. R. MacMacken (John Hopkins University). CSR603 was originally isolated by Sancer *et al.* (138) and was provided by Dr. B. Bachmann. MV12 and the hybrid plasmids listed in Table 1 were obtained from Clarke and Carbon (139) in the form of a collection of hybrid plasmid-containing isolates.

TABLE 1

E. coli Strains Utilized

Strain	Genotype	Reference (Source)
7	HfrC, glpR, phoA, relA, tonA22	219 (from strain 1)
13	F ⁺ , glpR, glpD, his, mal, bioB	118
105	F ⁻ , glpR, glpD, thr, leu, thi, gal, lac, str	141
122	F ⁻ , glpD, glpT, glpR, thr, leu, arg, lac, gal, str	144
JW14	F ⁻ , glpT, glpR, thr, leu, arg, lac, gal, str,	140 (from strain 122)
X1197	F ⁻ , thr, leu, arg, lacY, gal, minA, minB, lambda ⁻ , thi, recA1, strR	(from R. MacMacken)
MV12	F ⁺ , recA, trpD, thr, leu	139 (from strain C600)
CSR603	F ⁻ , recA, thr, leu, pro, arg, thi, phr, ara, lac, gal, tyr, mtl, strA, tsx, SupE44	138 (from B. Bachmann)

TABLE 2

Recombinant Plasmids Utilized

Plasmid	Description	Plasmid Size ¹
pLC3-46	Carries glpT, glpA	24.2 kb
pLC8-24	Carries glpT, glpA	25.0 kb
pLC8-29	Carries glpT	N.D.
pLC14-12	Carries glpT, glpA	14.6 kb
pLC19-24	Carries glpT, glpA	21.6 kb
pLC42-17	Carries glpT	15.0 kb
pLC16-43	Carries frdA	18.5 kb ²

¹ Plasmid size determined from summing fragment sizes during restriction endonuclease digestion analysis.

² From (203).

N.D.= not determined

B. Microbiological Methods

1. Storage of Strains and Growth Conditions

Bacterial strains were prepared for long-term storage by sterilely suspending cells in 50% glycerol and storing the suspension at -70° C. Prior to utilizing a strain in an experiment, the stored culture was streaked onto a complete medium plate (Luria Broth, 142) and individual isolates were tested for the correct phenotype by utilizing appropriate selective plates or by growth in liquid culture followed by appropriate manipulations for enzymatic or transport assays.

The growth media utilized for aerobic growth were either a complete medium (Luria Broth, 142) or a minimal medium described by Tanaka *et al.* (143), containing either 0.6% glycerol, 0.4% succinate, 0.5% pyruvate, or 0.2% glucose and 20 ug/ml of required amino acids. Cells grown for isolation of plasmid DNA were grown on a minimal medium described by Clewell (144).

The minimal medium utilized for anaerobic growth conditions is described by Spencer and Guest (145) and contained 40 mM fumarate, either 40 mM glycerol or 40 mM pyruvate, 0.05% caseamino acids and 20 ug/ml of required amino acids.

Cells grown aerobically in liquid culture were grown in sterile Erlenmeyer flasks with no greater than 25% of total volume occupied and rotated at 130 r.p.m. Anaerobic growth was attained by filling screw cap flasks completely and sealing the flask with parafilm. The cultures were either

agitated by utilizing a sterile magnetic stirring bar and a stirring box, or by rotation at 300 r.p.m. with intermittent inversion.

When strains containing hybrid ColE1:*E. coli* plasmids were utilized, Colicin E1 at 1 unit/ml was normally present in the growth medium.

For the preparation of aerobic dehydrogenase, Strain 7 was grown in a 300-liter fermentor with aeration on a growth medium containing 70 mM potassium phosphate, pH 7.0, 1% Difco yeast extract, 0.5% glycerol and 50 ug/ml thiamine. The bacteria were grown to an absorbance of 4 at 600 nm. For the preparation of anaerobic dehydrogenase, strain MV12/pLC14-12 was initially grown aerobically to stationary phase in 4 liters of complete medium containing 1 unit/ml Colicin E1. This culture was used to inoculate a 300-liter fermentor containing the anaerobic glycerol-fumarate minimal medium and the bacteria were grown without aeration to late log-early stationary phase of growth ($A_{600}=0.6$). The cells were harvested with a CEPA continuous-flow centrifuge and then frozen in liquid nitrogen and stored at -70°C .

2. Screening the Clarke and Carbon Strain Collection

One-hundred microlitres (10^8 cells) of a stationary phase culture of JW14 (selection for *glpT*) or strain 105 (selection for *glpD*), grown on M63 medium (142) plus required supplements, were spread on each of 44 minimal media (M63) plates. The plates contained 0.2% glycerol-3-phosphate as a carbon source, 10 ug/ml of

required amino acids or thiamin and 100 ug/ml streptomycin sulfate. Fresh patches of the 2000 donor F⁺ strains were grown at 37°C on L broth plates (142) containing 1 unit/ml Colicin E1 and were replicated with sterile velvets onto the recipient plates. The plates were then incubated at 37°C for 48 h. Patches of growth were observed where the donor had transferred the ColE1 hybrid plasmid containing a *glpT* gene to strain JW14. The ColE1:*glpT* plasmid-containing isolates were reisolated from the master plate, rescreened, and stored at -70°C in L broth containing 1 unit/ml Colicin E1 and 8% dimethylsulfoxide.

3. Transfer of Recombinant Plasmids to Recipient Strains

The hybrid plasmids were transferred to X1197 and CSR603 by mating the F⁺ MV12 donor strains with the F⁻ recipient strains. Donor and recipient strains were grown to mid-log phase ($A_{600}=0.5$) in Luria broth (142) and 0.5 ml aliquots of each were added to 9 ml of Luria broth in a 125 ml Erlenmeyer flask. The mating mixture was incubated for 60 minutes at 37°C with very gentle mixing and then were diluted and plated onto selective plates. The selective plates contained appropriate amino acid and vitamin supplements in addition to 100 ug/ml streptomycin sulfate, 1 unit/ml Colicin E1 and 0.5% glycerol-3-phosphate. A number of isolates were selected from each mating and those demonstrating elevated levels of G3P uptake were retained.

C. Isolation Procedures and Preparation of Cellular Extracts

1. Preparation of Membrane Vesicles

Membrane vesicles were prepared as described by Kaback (134) from cells grown aerobically on Tanaka minimal medium (143) containing either 0.4% succinate or 0.6% glycerol to mid-log phase.

2. Isolation of Minicells

Cultures were grown overnight in L broth with Colicin E1 at 1 unit/ml (except X1197) and the minicells were isolated essentially by the procedure of Inselburg (146).

3. Labelling Plasmid-coded Proteins

The washed minicell pellet was resuspended in 40 volumes (w/v) of labelling medium which consisted of Tanaka medium with 10 ug/ml each of threonine, leucine, thiamine, 0.001% caseamino acids, and either 0.2% glucose or 0.4% glycerol as a carbon source. The minicell preparation was incubated for 15 min at 37°C (shaking) and then a L-U-¹⁴C-labelled amino acid mixture was added to 20 uCi/ml. One hour after the addition of the label, a portion of the sample was precipitated by the addition of cold trichloacetic acid to 10% final concentration, and after 10 min on ice, the precipitate was spun down and washed with cold 10% trichloroacetic acid. This pellet was retained as the total minicell protein fraction.

4. Preparation of Membranes from Minicells

Two-hundred ug/ml lysozyme and 10 mM EDTA were added to the labelled minicell preparation pre-equilibrated on ice.

After incubating on ice for 1 hour, the minicell suspension was sonicated for 4 min at maximum output in a Raytheon bath-type sonic oscillator. Debris was removed by centrifuging at 3000 x g for 15 min and then the membrane vesicles were collected by centrifuging at 183,000 x g for 1 h in a Beckman Ti50 rotor. The membrane pellet was resuspended in Tanaka medium, trichloroacetic acid was added to 10%, and the precipitate collected and washed with cold 10% trichloroacetic acid.

5. Preparation of Crude Shock Fluid from Minicells

Crude shock fluid was obtained by the small-scale osmotic shock procedure described by Weiner and Heppel (147). To precipitate crude shock fluid protein, bovine serum albumin was added to 0.1 mg/ml and then trichloroacetic acid to 10% final concentration. The precipitate was collected by centrifuging in a Beckman JA20 rotor at 9000 rpm for 5 min.

6. Purification of the Aerobic Glycerol-3-phosphate Dehydrogenase

The procedure described below was adapted from a previous purification scheme (76). It is based on 100 gm wet weight of *E. coli* cell paste, yields 30 mg of homogeneous enzyme, and is adaptable to large scale purification.

Step I - Broken Cell Fraction

One hundred grams of frozen cell paste were thawed at room temperature in 550 ml of 50 mM Tris-HCl, pH 8.0, containing 50 mg/liter of phenylmethylsulfonyl fluoride (Buffer A). To

this was added EDTA to 10 mM and lysozyme to 0.5 mg/ml. The lysozyme was allowed to act for 20 min at 37° and then the sample was diluted to 900 ml with Buffer A. The suspension was frozen in liquid nitrogen and immediately thawed in a water bath at 37°. MgCl₂ was added to 25 mM followed by deoxyribonuclease and ribonuclease to 10 ug/ml each. The suspension was incubated a further 30 min at 37° then centrifuged at 40,000 x g for 30 min at 2°. The supernatant was discarded and the broken cells resuspended by homogenization in 800 ml of Buffer A and centrifuged as before. The washed preparation was resuspended by homogenization in 700 ml of 50 mM Tris-HCl, pH 7.5, containing 10% glycerol and 0.25 M NaCl to yield Fraction I.

Step II - Deoxycholate Extraction

Sodium deoxycholate was added to 0.2% to Fraction I and the suspension was stirred at room temperature for 20 min. If the sample became viscous, 10 mM MgCl₂ and 10 ug/ml deoxyribonuclease were added. The deoxycholate extract was spun at 40,000 x g for 60 min at 2°. The pellet was discarded and the supernatant (Fraction II) was made 20% in ethylene glycol and 0.2% in Brij 58 (Fraction IIA).

Step III - Biorex-70 Chromatography

Fraction IIA was immediately diluted 1 to 3 with 50 mM imidazole-HCl, pH 6.8, 20% ethylene glycol, 0.2% Brij 58 (Buffer B) and applied to 6x12 cm (350 ml) column of Biorex-70 equilibrated in Buffer B. The column was washed with 600 ml of Buffer B containing 0.35 M NaCl and activity was

eluted with 1 liter of Buffer B containing 0.65 M NaCl.

Active fractions were pooled to yield Fraction III.

Step IV - Phosphocellulose Chromatography

Fraction III was diluted 1 to 6 with 20 mM potassium phosphate, pH 6.6, containing 20% ethylene glycol, 0.2% Brij 58 (Buffer C) and was applied to a 6 x 7 cm (200 ml) column of Phosphocellulose P-11 equilibrated in Buffer C; activity was eluted with a linear gradient of 0.35 to 0.8 M NaCl in Buffer C. Active fractions were pooled to yield Fraction IV.

Step V - Hydroxylapatite Chromatography

Fraction IV was diluted 1 to 4 with 20% ethylene glycol, 0.2% Brij 58 and applied to a 2 x 9 cm (30 ml) column of hydroxylapatite. The column was washed with 60 ml of 5 mM potassium phosphate, pH 7.5, 20% ethylene glycol, 0.2% Brij 58 and then eluted with a linear gradient of 6 to 60 mM potassium phosphate in 20% ethylene glycol, 0.2% Brij 58; active fractions were pooled and stored at -70°. Fraction V was stable for at least 1 month at 4° and -70°.

7. Preparation of Cell Fractions for Anaerobic Dehydrogenase Identification

Chloramphenicol was added to late-log phase cultures at a final concentration of 150 ug/ml prior to harvest. When preparing cells for SDS-PAGE analysis, the cells were centrifuged and washed with 50 mM Tris-HCl, pH 7.5, containing 150 ug/ml chloramphenicol. The cells were resuspended in the same buffer containing 50 ug/ml phenylmethylsulfonyl-fluoride (PMSF) to an approximate

protein concentration of 20 mg/ml and were passed twice through a French Pressure cell at 16,000 p.s.i. Aliquots of the crude lysates were retained as the whole cell protein samples. The crude lysates were centrifuged at 3,000 X g for 5 min to remove cellular debris and the resulting supernatants were centrifuged at 195,000 X g for 1 hour. The supernatants from this high-speed spin were retained as the crude cytoplasmic fractions. The pellets were resuspended and washed in the same buffer, and resuspended in a small volume of buffer as the crude membrane fractions.

When preparing samples for transport assays the procedure described in section F of this chapter was followed except that chloramphenicol at 150 ug/ml was present in the wash and resuspension buffers.

In preparation for enzymatic assay, portions of the cultures were centrifuged and the cells resuspended in 100 mM potassium phosphate buffer (pH 7.5) containing 150 ug/ml chloramphenicol to a final protein concentration of 0.5 to 1.0 mg/ml. The cell suspension was sonicated (Biosonic III sonicator, full output for small probe) for a total of 1.5 min (with intermittent cooling) at 0°C and then centrifuged at 20,000 X g for 10 min. Aliquots of the supernatants were assayed as described in section F of this chapter.

8. Isolation of Plasmid DNA

Growth conditions and amplification of plasmid levels were carried out according to the procedure of Clewell (148). The cells were lysed and crude plasmid preparations

were prepared by the procedure of Guerry *et al* (149). The plasmid DNA was precipitated with ethanol, resuspended in TES buffer (50 mM NaCl, 5 mM disodium EDTA, 30 mM Tris-HCl, pH 8.0) and purified on a CsCl-ethidium bromide gradient as described by Clewell (148). The plasmid band was isolated and ethidium bromide removed by successive extractions with TES-saturated isobutanol. After 3-fold dilution with TES buffer, plasmid DNA was precipitated with ethanol, resuspended in a small volume of TES buffer, and stored at 4°C.

9. Isolation of the Subunits of the Anaerobic Dehydrogenase

The enzyme subunits were isolated by the procedure of Ziola and Scraba (150) which involves separation by SDS-PAGE, electrophoresis into hydroxylapatite and elution from the hydroxylapatite. Samples containing anaerobic dehydrogenase labelled with Remazol Brilliant Blue R by the procedure of Griffith (151) were used to follow migration of the subunits during the electrophoresis steps.

D. Physical Methods

1. SDS-Polyacrylamide Gel Electrophoresis

SDS-polyacrylamide gel electrophoresis was routinely performed utilizing the discontinuous gel system and the Tris-glycine buffer system described by Laemmli (152). Liquid samples for SDS-PAGE analysis with the Laemmli system were treated to obtain the following final sample concentrations: 1% SDS, 15% glycerol, 30 mM DTT, 50 mM

Tris-HCl (pH 6.8) and 0.001% bromophenol blue. When the sample was in the form of a pellet from trichloroacetic acid precipitation, it was resuspended in a minimum volume of sample buffer (1% SDS, 100 mM β -mercaptoethanol, 30% glycerol, 0.4 M Tris-base, and 0.01% bromophenol blue) and the mixture was left standing at room temperature for 10 min. The solution was neutralized by adding a small amount of 1 N HCl (5-10 μ l/50 μ l sample).

Alternatively, a fast-polymerizing, fast-running system described by Jovin *et al.* (153) was utilized. A sample mix (45% glycerol, 1.1% SDS, 55 mM DTT, 0.01% bromophenol blue, 59 mM Tris, and 59 mM Glycine, pH 8.8) was added to samples ranging in size up to 2/3 the volume of the added sample mix.

Samples were heated at 95°C for 5 minutes prior to adding the sample to the gel. After electrophoresis, gels were stained with 0.25% Coomassie blue in methanol/acetic acid/water (5:1:5) and destained in 7% methanol, 10% acetic acid.

2. Slicing and Counting Radioactive SDS-PAGE Gels

Destained gels were frozen on dry ice and sliced into 2-mm slices; each slice was incubated in a scintillation vial for 4 hours at 50°C with 0.5 ml of NCS solubilizer (Nuclear Chicago, Chicago, Il) containing 6% water. The vials were cooled to room temperature and 17 μ l of glacial acetic acid followed by 10 ml of Aquasol (New England Nuclear, Boston, Ma.) were added in the dark, then the vials

were shaken and counted.

3. Electrophoresis of DNA

Horizontal agarose gel electrophoresis was performed with gels containing between 0.7 and 1.2% agarose, depending on the experiment, in 40 mM Tris-acetate, 20 mM sodium acetate, 2 mM disodium EDTA, pH 8.1 (154). Electrophoresis was carried out for 12-16 hours at 35-40 volts. Vertical polyacrylamide gel electrophoresis was performed with gels containing 6% acrylamide, 0.2% bisacrylamide in 0.1 M Tris-borate, 2.5 mM disodium EDTA, 13% glycerol, pH 8.3. Electrophoresis was carried out for 12-16 hours at 80-100 volts. After electrophoresis, agarose and acrylamide gels were stained with 3 ug/ml ethidium bromide, transilluminated with long wave ultraviolet light, and photographed through a red filter using Polaroid type 667 Coaterless Land film.

The size of restriction fragments was determined relative to appropriate standards that were present in the stained gel. Fragment sizes from 800 to 20,000 base pairs were analyzed on agarose gels. Hind III-cleaved lambda DNA was routinely used as a standard for agarose gels and the larger fragments from Hinf I or Alu I-digested pBR322 DNA were used as standards in the smaller size range of fragments. Restriction fragments from 50-1,600 base pairs were analyzed by polyacrylamide gel electrophoresis. Hinf I or Alu I-digested pBR322 DNA was used as a standard in this gel system.

4. Electron Microscopy

Plasmid DNA was isolated, prepared for electron microscopy and micrographs were analyzed by Joel Weiner as described previously (140).

5. Sedimentation Studies

In preparation for sedimentation studies, samples of purified enzyme were dialyzed overnight against 80 mM potassium phosphate, pH 7.5, with or without 20% ethylene glycol (v/v) present. Sedimentation velocity experiments were carried out at 60,000 rpm at 13.3°C in a Beckman Model E Analytical Ultracentrifuge.

In the sedimentation equilibrium experiments the rotor speed was 11,000 rpm and the temperature was 11.4°C. Calculation of $S_{20,w}$ and molecular weight from the experimental data utilized an estimated value for \bar{v} of 0.73 ml/g.

6. Circular Dichroism

Circular dichroism measurements were performed by Kim Oikawa using a Cary model 6001 CD attachment to a Cary 60 recording spectropolarimeter according to the procedure described by Oikawa *et al.* (155).

7. Determination of Endogenous Flavin

Analysis of endogenous FAD in the anaerobic dehydrogenase required that exogenous FAD be removed prior to assay. This was achieved by passing 0.2 ml of purified enzyme through a 1 x 30 cm Sephadex G50 Superfine column. Aliquots of enzyme or of a standard FAD solution were added

to 80 mM potassium phosphate , pH 7.5, buffer containing 3.3 mg/ml of delipidated bovine serum albumin. 0.6 ml of cold 20% trichloroacetic acid was added to 0.6 ml of the solution and the suspension was incubated on ice for 20 minutes. The suspensions were centrifuged at $11,000 \times g$ for 15 minutes and 0.5 ml aliquots of the supernatant were either added to 1.5 ml 0.56 M K_2HPO_4 (final pH=7) or 1.5 ml 0.147 M KH_2PO_4 (final pH=3.0). The fluorescence of the samples and the standards were determined on a Turner Model 430 Fluorimeter exciting at 435 nm and measuring at 535 nm.

E. Chemical Methods

1. Determination of Protein Concentration

Protein concentration was normally determined utilizing the method of Lowry *et al* (156) using Biorad protein standard (Biorad Laboratories, Richmond, CA.). The protein concentration of solutions of the purified anaerobic glycerol-3-phosphate dehydrogenase was occasionally determined by utilizing the molar extinction coefficient at 271 nm ($136,000 \text{ cm}^{-1} \text{ M}^{-1}$).

2. Amino Acid Analysis

Samples were dialyzed for 24 hours against 50 mM NH_4HCO_3 , pH 7.5, buffer or for 72 hours if they contained SDS. Aliquots containing 1 nmole of enzyme or subunit were transferred to small (10 x 75 mm) pyrex tubes and lyophilized. The samples were subjected to acid hydrolysis in 6N HCl at 110°C in evacuated, sealed tubes for periods

of 24, 48, 72, and 96 hours (157). Samples containing 2 nmoles of enzyme or subunit were subjected to performic acid oxidation followed by 24-hour acid hydrolysis for determination of cysteine (158). The hydrolysates were evaporated to dryness, dissolved in 0.1 ml of 0.2 M, pH 2.2, sodium citrate buffer and then chromatographed on a Durrum Model D-500 Amino Acid Analyzer. Values of serine and threonine were obtained by extrapolation to zero time and the plateau values for valine and isoleucine were used. The number of tryptophan residues was determined by absorption at 280 and 288 nm in 6M guanidine-HCl according to Edelhoch (159).

3. Chemical Crosslinking of the Anaerobic Dehydrogenase

Chemical crosslinking of the purified enzyme was carried out with dimethylsuberimide according to the procedure of Davies and Stark (160) except that 20% ethylene glycol was present in the buffer. Purified anaerobic dehydrogenase (3.3 mg/ml) was dialyzed overnight against 200 mM sodium phosphate (pH 8.0), 20% ethylene glycol. Reaction mixtures containing 5 mg/ml dimethylsuberimide and between 0.3 and 3.0 mg/ml of dialyzed enzyme were incubated for three hours and then analyzed by SDS-PAGE using 7% acrylamide gels with a Tris/glycine buffer system (153). The gels were stained and destained as described in section D of this chapter and the destained gels were scanned at 550 nm with a Gilford 250 spectrophotometer with a gel scanning attachment.

4. Iron Analysis

Non-heme iron content was determined by Kelly Dabbs as described by Brumby and Massey (161, Method B). Total iron was determined by the ashing method described by Brumby and Massey (161, Method C) or the extraction method (Method D).

5. Acid-Labile Sulfide Analysis

Samples were analyzed for acid-labile sulfide by Kelly Dabbs using the procedure of King and Morris (162).

6. Inactivation of the Anaerobic Dehydrogenase

0.2 ml of purified enzyme (10 mg/ml) was passed through a 1 x 30 cm Sephadex G50 superfine column equilibrated in 100 mM potassium phosphate, pH 7.5, containing 20% ethylene glycol. Aliquots of the pooled enzyme (0.85 mg/ml) were mixed with an equal volume of potassium phosphate buffer, pH 6.5, containing either 4 mM 1,10-phenanthroline, 50 μ M PCMS, 50 μ M or 2 mM DTNB. The mixtures were incubated at 23°C and aliquots were assayed for enzymatic activity either in the presence or absence of added flavins. Quantitation of titration of the sulfhydryl groups by DTNB was determined by following the change in absorbance at 412 nm (163). The molar extinction coefficient of the *p*-nitrothiophenol anion in this buffer system ($27,600 \text{ cm}^{-1} \text{ M}^{-1}$) was determined by reacting DTNB with excess cysteine in this buffer system.

7. Preparation of Dideazaflavin Analogs

The FAD synthetase complex was purified from *Brevibacterium ammoniagenes* as described by Spencer *et al.* (164) except that the cells were grown on Luria Broth (142)

at 37°C, the cells were lysed by passing a concentrated cell suspension (0.3 g/ml) through a French Pressure cell (Aminco Instruments, Silver Spring, Md.) at 16,000 p.s.i. and the crude lysate was stored at -70°C.

The 1,5-dideazariboflavin analogue (165) was converted to dideazaFAD by incubation with the FAD synthetase complex and purified by DEAE-Sephacel and Biogel P2 chromatography (164). The preparation of the FAD synthetase complex and preparation and purification of the dideazaFAD was performed by Corrine Lobe.

The dideazaFAD was converted to dideazaFMN by incubating 3.5 micromoles of dideazaFAD in 60 mls of 50 mM Tris-HCl (pH 7.5), 5 mM MgCl₂, with 3 units of nucleotide pyrophosphatase for 25 min at 37°C. The dideazaFMN was purified by Biogel P2 chromatography (164) after reducing the volume by rotary evaporation.

F. Enzymatic Methods and Transport Assays

1. Transport Assays with Whole Cells

Cultures were grown to late log-early stationary phase and the cells were washed three times at room temperature in phosphate-free (A-P) medium (166) and suspended to 1 g/20 ml in A-P medium. A portion of the cell suspension was incubated for 5 minutes in the presence of 10 mM glucose and 80 µg/ml chloramphenicol. To start the reaction, an aliquot (20 µl) of the cell suspension was added to 0.5 ml (final volume) of a minimal medium consisting of 50 mM HEPES, pH

7.0, 15 mM KCl, 0.4 mM MgSO₄, 20 mM Ca(NO₃)₂, 10 mM glucose, 40 ug/ml chloramphenicol and either 12 uM L-(U-¹⁴C) glutamine (25 mCi/mmole), 10 uM L-(U-¹⁴C) glycerol-3-phosphate (25 mCi/mmole), or 10 uM L-(U-¹⁴C) proline (25.4 mCi/mmole). A 0.2 ml portion was removed at 15 and 30 sec and filtered on a 24-mm diameter presoaked nitrocellulose filter (0.45-microm pore size, Millipore Corp., Bedford, Ma.). Filters were immediately washed with 10 ml of wash buffer (10mM Tris-HCl, pH 7.3, 150 mM NaCl, 0.5 mM MgCl₂), dried, and counted as described previously (133).

2. Transport Assays with Membrane Vesicles

Vesicle transport assays were performed as follows: 10 ul of 80 mM D-lactate, 10 ul of 80 mM MgSO₄, and 10 ul of membrane vesicles of about 3-5 mg/ml protein were preincubated for 2 min, followed by addition of 10 ul of L-(U-¹⁴C) glycerol-3-phosphate (0.182 mM, 25 mCi/mmole) or L-(U-¹⁴C) proline (0.03 mM 25.4 mCi/mmole). 10 ul samples were taken at 15 and 30 sec, filtered directly on a nitrocellulose filter, washed immediately with 5 ml of 0.1 M LiCl, dried, and counted.

3. Assay of Enzyme Activity

Aerobic or anaerobic G3PDH activity was routinely monitored by following the G3P-dependent reduction of the tetrazolium dye, MTT. PMS was present in the assay mixture to transfer reducing equivalents from the enzyme to the terminal dye. For enzymatic assay of the aerobic

dehydrogenase the assay mixture contained the following final concentrations: PMS, 350 μ M; MTT, 75 μ M; Triton X-100, 0.2%; DL-glycerol-3-phosphate, 25 mM; 50 mM imidazole-HCl, pH 7.0, in a final volume of 1 ml. In studies involving the assay of whole cells or crude membrane preparations, 9 mM KCN was present in the assay mixture.

In routine assays of the anaerobic dehydrogenase, FAD and FMN were present to obtain maximal activity. The assay mixture contained the following final concentrations: PMS, 600 μ M; MTT, 75 μ M; DL-glycerol-3-phosphate, 20 mM; Triton X-100, 0.2%; FAD 10 μ M; FMN, 1 mM and 100 mM potassium phosphate, pH 7.5, in a final volume of 1 ml. When methylene blue was present in place of PMS its final concentration was 100 μ M.

4. Restriction Endonuclease Digestions

Digestion with restriction endonucleases was routinely carried out at 37°C for several hours in a standard restriction enzyme buffer (50 mM NaCl, 6 mM MgCl₂, 1 mM DTT, 10 μ g/ml bovine serum albumin, 30 mM Tris-HCl, pH 7.5) except for Kpn I, where the buffer recommended by the supplier was found to be necessary. The cleavage patterns obtained with lambda DNA or pBR322 DNA were observed to ensure that the reaction conditions and the restriction endonuclease preparations were satisfactory. When performing double or triple digestion experiments, the incubation mixture was heated at 65°C for 20 min to inactivate the first enzyme and then cooled to 37°C prior to adding the

next restriction enzyme. When digestion was complete the reactions were terminated by adding 0.2 volumes of stop mix (24% Ficoll 400, 4% SDS, 0.02% bromophenol blue, 0.02% Xylene Cyanole FF, 85 mM disodium EDTA) and heating at 65°C for 10 min.

The samples were split into two aliquots; one to be analyzed by horizontal agarose gel electrophoresis and the other to be analyzed by vertical polyacrylamide gel electrophoresis.

5. Proteolysis of the Anaerobic Dehydrogenase

Proteolysis was carried out in 50 mM Tris-HCl, pH 7.5, containing 0.25 ug/ml chymotrypsin and 240 ug/ml purified enzyme. To observe the effect of ethylene glycol on proteolytic degradation of the enzyme, the 20% ethylene glycol present in the purified enzyme preparation had to be removed. This was achieved by dilution with ethylene glycol-free buffer followed by ultrafiltration. This step was repeated many times to effectively remove the ethylene glycol. Where indicated, ethylene glycol was included at 20% (v/v). Reactions were incubated at room temperature and aliquots were immediately assayed for enzymatic activity or injected into 95°C SDS-PAGE sample buffer for electrophoretic analysis. Gel electrophoresis using 12% acrylamide gels was performed as described in the chemical crosslinking section. When the samples were analyzed for the presence of the flavin cofactor, the proteolytic reaction was terminated by the addition of a 10-fold excess of

soybean trypsin inhibitor.

6. Determination of K_m and V_{max}

The K_m and V_{max} values were obtained from the Wilkinson statistical fit of initial rate measurements at varying glycerol-3-phosphate concentrations (167) with calculations being performed by an APL program developed by D. Scott Hagen.

III. Recombinant ColE1:*E. coli* Plasmids

A. Introduction

The approach I adopted for the purification and characterization of the aerobic and anaerobic G3P dehydrogenases of *E. coli* was a combined genetic and biochemical one. It involved the use of recombinant ColE1:*E. coli* plasmids, prepared by Clarke and Carbon (139), in the form of a bank of strains each containing a hybrid plasmid with a random segment of the *E. coli* chromosome.

One advantage of utilizing recombinant plasmids is that they permit easy identification of plasmid-coded polypeptides and in this way the polypeptide composition of the gene product being studied can be determined. Knowledge of the polypeptide composition of the anaerobic dehydrogenase provided an additional criterion for evaluating potential steps in the purification protocol. A number of relatively simple systems for the identification of plasmid-coded polypeptides have been developed to be utilized instead of the traditional *in vitro* coupled transcription-translation systems. One procedure utilizes a mutant *E. coli* strain, X1197, aberrant in the cell division process, that produces miniature cells free of chromosomal DNA but containing normal amounts of most cellular components (168). Plasmid DNA can be incorporated into these minicells (146) and plasmid-coded polypeptides are synthesized (169,170). Specific labelling of plasmid-coded

proteins in a minicell system has been used to identify a number of gene products including the chemotaxis gene products (171) and the F sex factor proteins (172).

A second advantage of utilizing recombinant ColE1:*E. coli* plasmids is the fact that these are multicopy plasmids and there are normally 24 copies of the ColE1 plasmid per cell (173). Thus, genes present on recombinant ColE1:*E. coli* plasmids will have a greater number of copies per cell than chromosomal genes and consequently the gene products will also be elevated. The extent of amplification that has been observed under these circumstances is approximately 5 to 15-fold and further manipulation of the cloned genes can result in considerably higher levels of amplification. Increasing the level of enzyme by cloning and genetic manipulation has the obvious advantage of reducing the number of steps that are required for purification and increasing the yields of final product. This feature was particularly important for purification of the anaerobic G3PDH, as earlier purification attempts were only partially successful (118) due to the lability of this enzyme.

An additional benefit of recombinant plasmids carrying the gene of interest is that one can determine the physical structure of the DNA to yield information on the expression and structure of the gene products. Restriction endonuclease digestion analysis can provide information on the structural organization of the gene(s) and DNA sequence analysis of the gene yields the primary structure of the gene product.

B. Results

1. Selection of Recombinant Plasmids

The Clarke and Carbon colony bank of strains was prepared by mechanically shearing *E. coli* chromosomal DNA, inserting the fragments into EcoR1-cleaved ColE1 plasmid using a poly dA:poly dT annealing method, and then transforming an *recA*⁻, *F*⁺ strain with the hybrid plasmids (139). The average size of the chromosomal fragments was 8.5×10^6 daltons and 2,100 strains were selected for the colony bank. Thus the chance of finding a particular gene in the bank should be greater than 99% (139). The presence of the *F*⁺ sex factor facilitates transfer of the ColE1:*E. coli* hybrid plasmid so that the colony bank can be screened for a particular gene by utilizing an *F*⁻ mutant strain and appropriate selective media.

At the time that the studies with these recombinant plasmids were being initiated, we were also interested in studying the G3P transport carrier and thus the initial screening of the colony bank was designed to detect recombinant plasmids carrying the *glpT* gene. This was achieved by mating the isolates with strain JW14 and then selecting on a minimal medium for growth on glycerol-3-phosphate as the carbon source and resistance to the antibiotic streptomycin. The donor strains are selected against on this medium by the presence of streptomycin and also by the lack of tryptophan which is an auxotrophic requirement of the donor cells. JW14 cannot grow because the

glpT deficiency prevents uptake of G3P directly and a deletion in the alkaline phosphatase gene prevents uptake by conversion to glycerol externally.

The screening of the colony bank was initially performed by Joel Weiner and indicated that the plasmids pLC3-46, pLC8-12, pLC8-24, pLC8-29, pLC14-12, pLC19-24 and pLC42-17 corrected the *glpT* deficiency in JW14 (139). When the isolates were retested it was observed that the results with pLC8-12 were marginal and this plasmid was eliminated from further study. In order to determine whether the closely-linked *glpA* gene was present on any of these recombinant plasmids, the strains were analyzed for the levels of activity of the aerobic and the anaerobic G3PDH. The results of this study (which was performed by Elke Lohmeier) are listed in Table 3. The levels of anaerobic dehydrogenase were below the detection limit of the experiment in French Press lysates prepared from strains carrying random hybrid plasmids or from two *glpT* plasmid-carrying strains (pLC8-29 and pLC42-17). However, four of the *glpT* recombinant plasmid strains had substantial levels of the enzyme, indicating that these plasmids were carriers of the *glpA* gene. The level of the aerobic enzyme was the same in all the strains tested.

The colony bank was screened in a similar fashion for recombinant plasmids carrying the *glpD* gene utilizing strain 105 . However, despite several attempts by different individuals in our laboratory, no isolates were observed

TABLE 3

Glycerol-3-phosphate Dehydrogenase Levels in Strains
Carrying Recombinant Plasmids

Strain MV12/pLC	Aerobic Dehydrogenase (units/mg)	Anaerobic Dehydrogenase (units/mg)
3-46 <i>glpT</i>	0.12	0.034
8-24 <i>glpT</i>	0.10	0.025
8-29 <i>glpT</i>	0.12	<0.005
14-12 <i>glpT</i>	0.11	0.086
19-24 <i>glpT</i>	0.12	0.039
42-17 <i>glpT</i>	0.13	<0.005
8-2 control	0.10	<0.005
19-42 control	0.11	<0.005
20-6 control	0.16	<0.005

Assays performed as described in the methods chapter.
One unit is defined as 1 micromole MTT reduced per
minute.

that corrected the *glpD* deficiency. This result was not anticipated as the chance of a particular gene not being represented in the collection should be less than 1%. It is possible that the *glpD* gene is closely linked to a gene that is lethal at elevated levels and would thus not be represented in the strain collection.

2. Identification of Recombinant Plasmid-Coded Polypeptides

a. Glycerol-3-phosphate Transport Proteins

The study on the G3P transport function was carried out in conjunction with Elke Lohmeier and some of the data I will be presenting was obtained from experiments performed by her. However, only the results that are a necessary component of this section will be included and her contributions will be specifically mentioned.

The level of G3P transport in the six previously identified isolates and in control strains was determined by Elke Lohmeier. The results in Table 4 demonstrate that the levels of G3P transport, but not glutamine or proline uptake, are elevated in strains carrying the recombinant plasmids containing the *glpT* gene. Furthermore, kinetic studies indicated that the V_{max} but not the K_m was increased in these strains (140) which is consistent with there being an increase in the number of transport carrier polypeptides rather than affecting existing carriers. To establish that the plasmids resulted in increased levels of cytoplasmic carrier polypeptides rather than just the periplasmic binding protein component, Elke Lohmeier carried out

TABLE 4

Active Transport in MV12/pLC Isolates

Strain MV12/pLC	G3P Uptake (units/mg)	Proline Uptake (units/mg)	Glutamine Uptake (units/mg)
3-46 <i>glpT</i>	200	9.2	6.8
8-24 <i>glpT</i>	182	ND	ND
8-29 <i>glpT</i>	267	14.8	7.9
14-12 <i>glpT</i>	133	5.4	7.3
19-24 <i>glpT</i>	200	5.2	7.3
42-17 <i>glpT</i>	133	ND	9.8
8-2 control	ND	3.0	7.7
19-42 control	36	ND	5.6
20-6 control	36	14.8	7.1
Strain 7	54	12.0	7.9

Transport assays were performed as described in the methods chapter. ND, not determined.

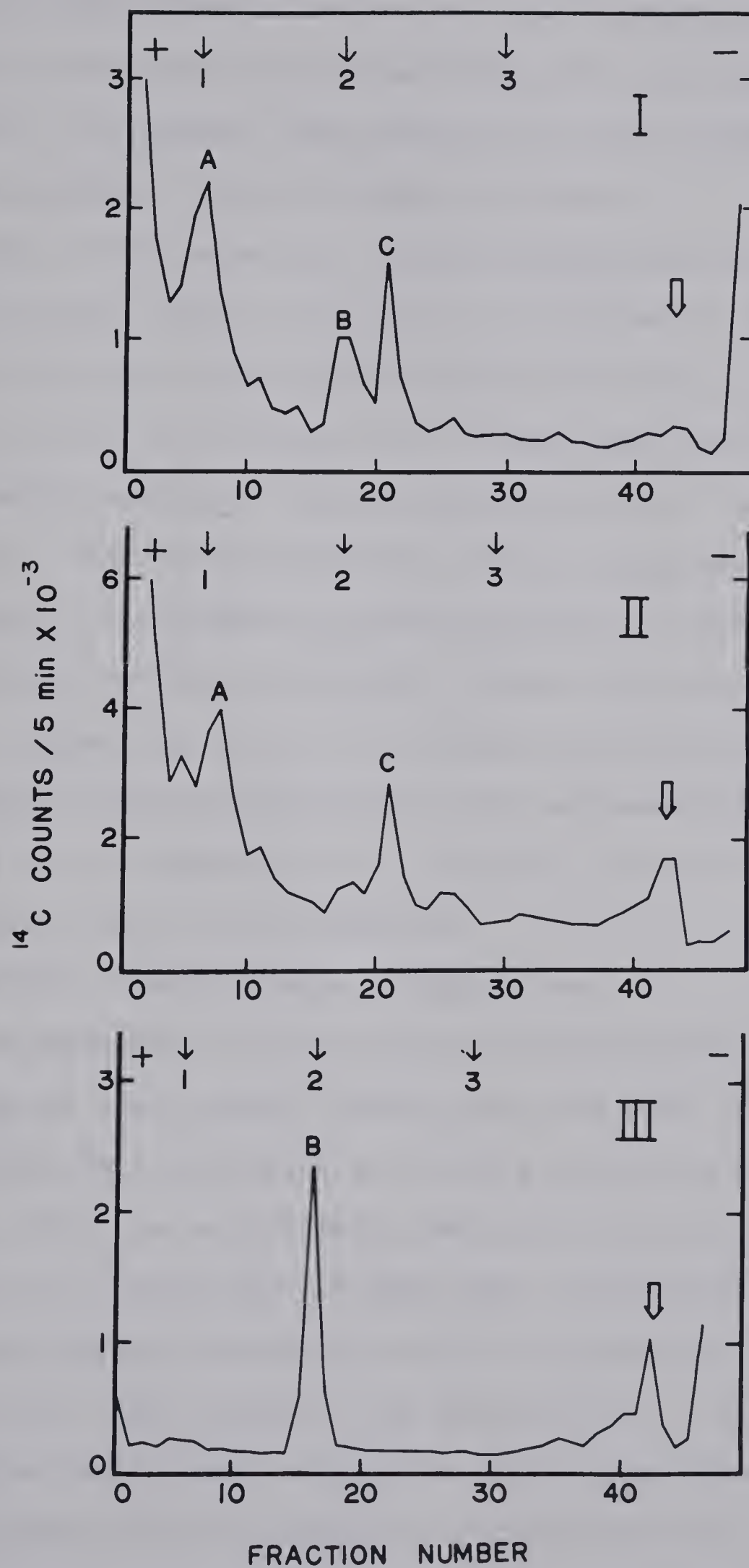
transport studies with isolated membrane vesicles. Elevated levels of transport were observed in vesicles prepared from strains carrying recombinant plasmids containing the *glpT* gene (140) indicating that the cytoplasmic carrier levels were indeed increased.

In order to identify the *glpT* polypeptides, I chose to utilize the minicell system described in the Introduction instead of a cell-free protein synthesizing system for the following reasons:

1. The minicell system requires fewer manipulations and fewer components to be added, which increases the chances of initial success.
2. In a minicell system, proteins are processed and compartmentalized as they are in whole cells, thus allowing one to distinguish cytoplasmic proteins from membrane proteins or periplasmic proteins.

The recombinant plasmids carrying the *glpT* gene were mated into the minicell-producing strain, X1197. Minicells were isolated, newly synthesized protein was labelled and cellular fractions were obtained as described in the methods chapter. When the total minicell protein fraction was analyzed by SDS-PAGE and scintillation counting as described in the methods chapter, two polypeptides were observed that were common to all the plasmid isolates. These polypeptides are labelled as peaks A and B in Figure 7I and have molecular weights of 40,000 and 26,000 respectively. The label observed at the ion front in Figure 7 presumably is

Figure 7. SDS-Polyacrylamide Gel Electrophoresis of Plasmid-coded Proteins from Minicells. The polypeptides programmed by pLC42-17 which were expressed in minicells were isolated and subjected to electrophoresis as detailed in the methods chapter. I, Total minicell protein fraction. A 50 μ l sample derived from 200 μ l of labelled minicells was applied to the gel. Internal standards used were the following: (1) goat immunoglobulin light chains, 25,000; (2) aldolase, 40,000; (3) bovine serum albumin, 68,000. The Rf values of the prominent bands are the following: (A) 0.86; (B) 0.62; (C) 0.53. The wide arrow indicates the stacking gel-resolving gel interface. II, Membrane protein fraction. A 50 μ l sample derived from 0.5 ml of labelled minicells was applied to the gel. Standards and Rf values as in I. III, Periplasmic protein fraction. A 50 μ l sample derived from 1 ml of osmotic shock fluid was applied to the gel. Standards and Rf values as in I.



due to charged tRNA molecules and small polypeptides and the label at the stacking gel-resolving gel interface (indicated by arrow) is probably high molecular weight aggregates undissociated in the conditions utilized.

The 26,000 molecular weight polypeptide observed in the total minicell protein fraction is observed in the membrane protein fraction (Figure 7II), but not in the periplasmic protein fraction (Figure 7III), suggesting that it is the cytoplasmic membrane carrier polypeptide involved in G3P transport. The 40,000 molecular weight polypeptide is not observed in the membrane protein fraction (Figure 7II), but is observed in the periplasmic protein fraction (Figure 7III), suggesting that it is the periplasmic *glpT* component. It should be mentioned that the two components discussed above are not observed when a minicell preparation carrying the plasmid pLC20-30 is utilized.

b. Anaerobic Dehydrogenase Polypeptides

The approach to identifying the *glpA*-coded polypeptides involved an even simpler system that had been recently developed. This technique utilized a strain of *E. coli*, CSR603, which is particularly sensitive to ultraviolet light because it is deficient in DNA repair mechanisms (138). Exposing plasmid-containing cells to appropriate levels of ultraviolet light leads to the destruction of the host chromosome while only a fraction of the plasmid molecules are affected. After a period of incubation only plasmid-coded polypeptides are produced and thus

specifically labelled.

In preparation for the identification experiments, plasmid pLC14-12 was mated into strain CSR603. Clearly, the *glpA* polypeptides might be identified by comparing SDS-PAGE profiles and enzyme activities in crude extracts from different strains and different growth conditions. The strains CSR603, CSR603/pLC14-12, MV12/pLC16-43 and MV12/pLC14-12, grown under aerobic and anaerobic conditions, were utilized in this experiment. This allowed me to evaluate the effect of the plasmid, the growth condition and the genetic background on the observed activities and SDS-PAGE profiles. Assaying for G3P transport activity in these experiments allowed comparison of expression of the *glpA* and *glpT* genes and thus unambiguous identification of the *glpA* polypeptides.

Total cell, crude cytoplasmic and crude membrane fractions were analyzed by SDS-PAGE to ensure that the enzymatic activity and the identified polypeptides were associated with the same cell fraction.

The enzyme and transport activities obtained in this experiment are listed in Table 5 and the SDS-PAGE analysis of the crude cytoplasmic fraction is illustrated in Figure 8. It is evident from Table 5 that the highest levels of anaerobic dehydrogenase activity are observed in the presence of the plasmid, in both genetic backgrounds, under anaerobic conditions. Similarly, two polypeptides of 62,000 and 43,000 molecular weight are observed in Figure 8 in

TABLE 5

Expression of Anaerobic Dehydrogenase and
Glycerol-3-phosphate Transport Activity

Strain	Glycerol-3-phosphate Transport (nmoles/min/mg)		
	Aerobic Growth	Anaerobic Growth	Ratio Anaerobic/ Aerobic
CSR603	4.4	11.7	2.7
CSR603/pLC14-12	23.9	60.8	2.5
MV12/pLC16-43 ¹	7.8	4.4	0.6
MV12/pLC14-12	51.0	35.5	0.7
Strain	Anaerobic G3P Dehydrogenase (umoles/min/mg)		
	Aerobic Growth	Anaerobic Growth	Ratio Anaerobic/ Aerobic
CSR603	0.02	0.17	8.5
CSR603/pLC14-12	0.13	2.10	16.2
MV12/pLC16-43 ¹	0.04	0.16	3.8
MV12/pLC14-12	0.30	1.90	6.3

¹pLC16-43 is a control plasmid which does not carry either the *glpA* or *glpT* genes.

Figure 8. SDS-PAGE Analysis of Crude Cytoplasmic Fractions from Control and pLC14-12-Carrying Cells Grown Under Aerobic and Anaerobic Conditions. Growth conditions, preparation of extracts and SDS-PAGE were performed as described in methods chapter. The Laemmli gel system (152) was utilized in this experiment. The dark arrows indicate the positions of the 62,000 and 43,000 molecular weight polypeptides. Molecular weight standards used were the following: 1st well- bovine serum albumin (68,000) and chymotrypsinogen (25,000); 2nd well- aerobic G3P dehydrogenase (58,000), aldolase (39,500) and lactate dehydrogenase (33,500); 11th well- IgG heavy chains (50,000), ovalbumin (45,000) and IgG light chains (25,000).



anaerobically-grown cells containing pLC14-12 which are not evident in cells lacking pLC14-12 or in cells grown aerobically. The results in Table 5 and Figure 8 illustrate that the expression of the 62,000 and 43,000 molecular weight polypeptides closely parallels the levels of anaerobic G3PDH activity and not G3P transport activity. Furthermore, these polypeptides are observed in whole cell extracts and are found predominantly in the crude cytoplasmic fraction which parallels the distribution of anaerobic dehydrogenase activity but not transport activity. Finally, these two polypeptides are also observed in extracts from anaerobically-grown cells containing the plasmids pLC3-46, pLC8-24 and pLC19-24 but not in cells containing pLC42-17.

The data in Table 5 also allowed me to make some observations on the effect of anaerobiosis on the expression of the *glpT* and *glpA* genes. The ratio of activities observed under anaerobic versus aerobic conditions is different for the two genes, suggesting that they are not coordinately controlled. This is the same conclusion reached in expression studies by Miki and Lin (123) and is consistent with the recent demonstration that the two genes are in separate operons (122).

A second observation that can be made from the data in Table 5 is that there is an apparent difference in the extent of the respiratory control in the two genetic backgrounds (i.e. compare anaerobic/aerobic ratios in MV12

and CSR603). Furthermore, the pattern of expression of the plasmid genes appears to reflect the expression of the chromosomal genes, suggesting that the plasmid genes have retained their control regions. The control of expression of genetic loci in the presence of different terminal electron acceptors is poorly understood and could involve both repression and induction systems. Thus it is difficult to draw any conclusions from the data in Table 5 as to whether the *glpT* and *glpA* loci are affected by the same controlling elements or the possible extent of such interactions.

3. Physical Characterization of the Recombinant Plasmids

The size of the recombinant plasmids pLC3-46, pLC8-24, pLC8-29, pLC14-12, pLC19-24 and pLC42-17 was determined by measurements of electron micrographs prepared by Joel Weiner and the lengths of the inserts are reported elsewhere (140). Restriction endonuclease cleavage analysis of these plasmids was pursued for the following reasons:

1. The analysis would identify the regions of overlap between the various plasmids and could potentially determine the regions containing the *glpT* and *glpA* genes.
2. This analysis would provide information useful for subsequent attempts at recloning the *glpA* and *glpT* genes for further amplification of activities.
3. The restriction endonuclease cleavage analysis is a necessary first step in the nucleotide sequence determination of the two genes which was being

considered in our laboratory.

The recombinant plasmids pLC3-46, pLC8-24, pLC14-12, pLC19-24 and pLC42-17 all carry the *glpT* gene and all except pLC42-17 amplify anaerobic G3PDH, indicating that they also apparently carry an intact *glpA* gene (Table 2 and 3). Restriction endonuclease cleavage analysis was performed on these five recombinant plasmids in order to identify the regions of overlap and thus determine the regions of DNA containing the *glpT* and *glpA* genes.

Some restriction fragments migrated anomalously during gel electrophoresis. That is, their position relative to other fragments differed on the two gel systems. Although we did not investigate this phenomenon, it in fact was useful in several instances. When a restriction endonuclease digestion experiment produced two fragments of nearly identical size, one could not always confidently deduce this from relative fluorescence intensities of the bands. However, if the two fragments migrated differently on the second gel system one could not only be confident that there were two fragments but also could identify each one in subsequent combinations of restriction endonuclease digestions.

The fact that the anomalous migration resulted in different estimates of size did not present any great problem since the true size could be deduced from the sum of the fragments that were produced in further restriction endonuclease digestions. In most experiments, all five

recombinant plasmids were subjected to identical restriction endonuclease digestion conditions and run on the same gel so that common fragments could be readily identified. It is also noteworthy that triple restriction endonuclease digests proved to be very useful in some instances for unambiguously establishing the relative positions of restriction sites.

These restriction endonuclease cleavage analyses involved nine different restriction endonucleases in various combinations used on five different recombinant plasmids. These experiments provided a very large amount of data on fragment sizes obtained from various combinations of digestions from which restriction maps of all five plasmids were constructed. I have chosen to summarize the information by presenting a restriction map of pLC14-12 (Figure 9), a composite restriction map of the inserts in all five plasmids (Figure 10), and two representative tables listing the results from some of the digestions performed on pLC14-12 and pLC42-17 (Tables 6 and 7).

The approximate location of the *glpT* and the *glpA* genes can be deduced from the regions of overlap of the recombinant plasmids. However, the location of the *glpA* gene indicated in Figures 9 and 10 is more precise than can be determined from the overlap data alone. It was deduced from the results of SDS-PAGE analysis of total and crude cytoplasmic extracts of strains carrying pLC42-17 or pLC19-24 (Figure 11). pLC42-17 produced neither a functional *glpA* product nor the 43,000 or 62,000 subunits. However, a

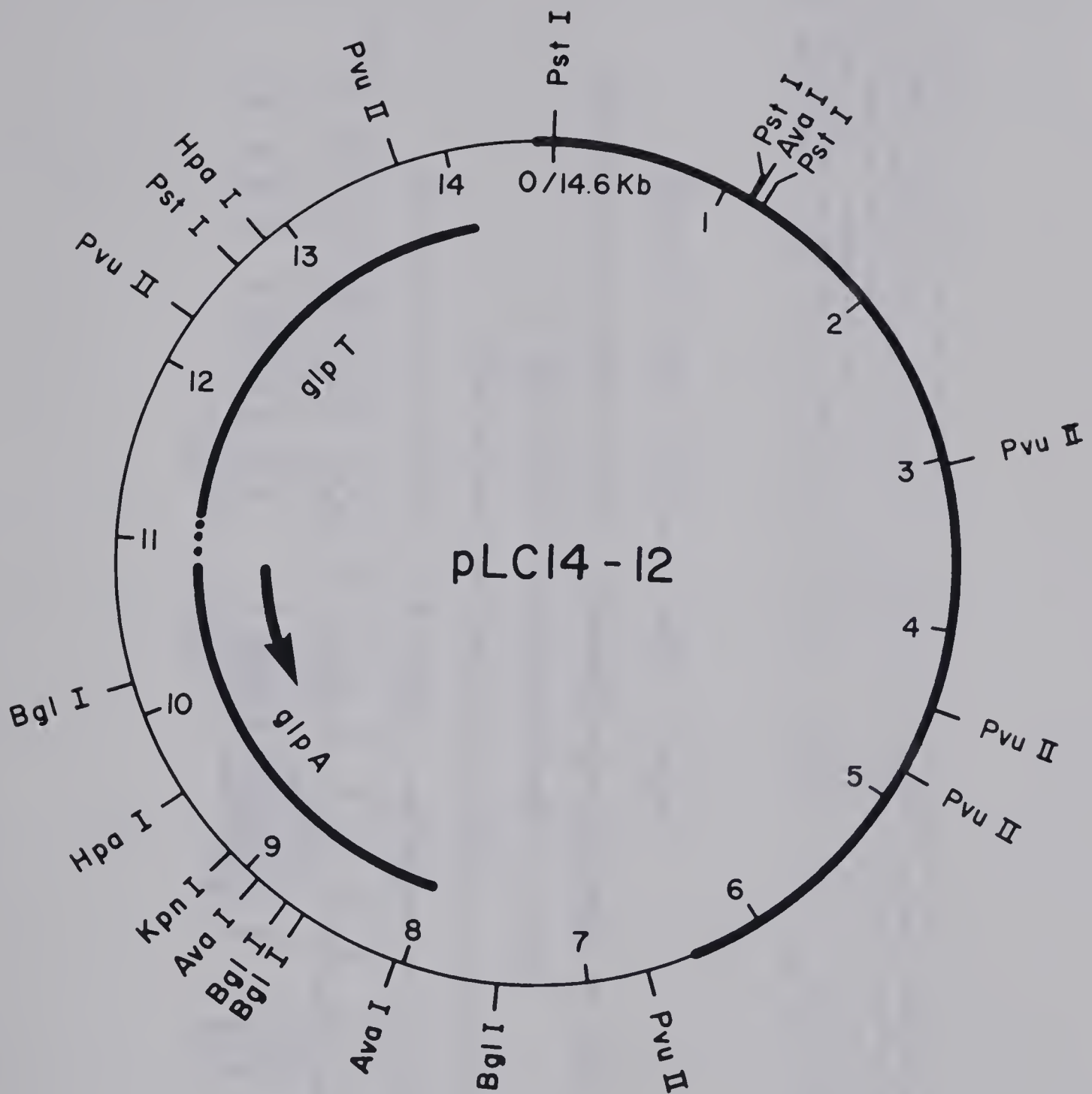


Figure 9. Restriction Endonuclease Cleavage Map of pLC14-12. The thicker portion of the circle represents the ColE1 vector DNA and the thinner portion represents the inserted chromosomal DNA. The bars along the inner contours of the circle indicate the regions of DNA carrying the *glpA* or *glpT* gene. The dark arrow indicates the proposed direction of transcription.

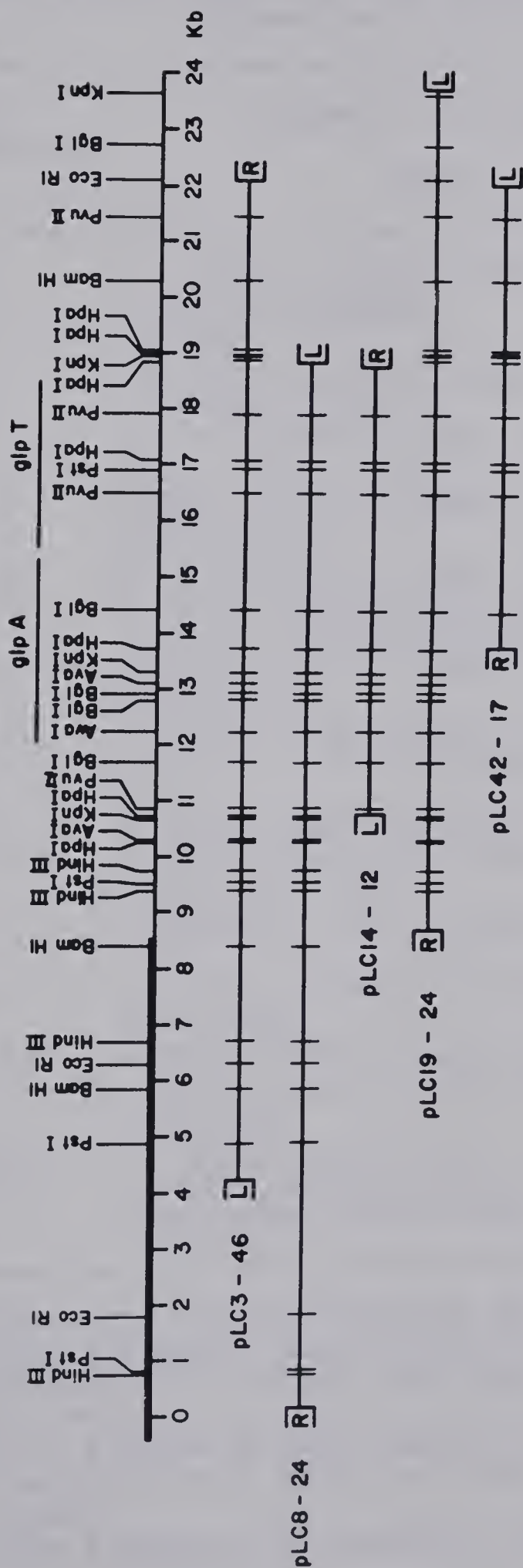


Figure 10. Restriction Endonuclease Cleavage Maps of the Inserts in PLC3-46, PLC8-24, PLC14-12, PLC19-24 and PLC42-17. A composite restriction map of the appropriate *E. coli* chromosomal region is illustrated at the top of the figure. The darkened line at the left is to indicate that only Bam HI, Eco RI, Hind III and Pst I sites are mapped within this region. The relative orientation of the Hpa I site and the Kpn I site centered around 19 kilobases has not been firmly established. Below are illustrated the regions that are found in the inserts in the individual recombinant plasmids. The boxed ends represent the ColE1 vector and L and R indicate the left and right ends of the ColE1 vector. The convention followed is that the end of ColE1 vector containing a Pst I site is designated as the right end (compare with Figure 2).

TABLE 6
Fragment Sizes Obtained from Restriction Endonuclease
Digestion of pLC14-12

Restriction Endonuclease(s) Used	Fragment Sizes(base pairs) pLC14-12
Pst I	(11,500) ¹ ; 1,920; 1,170 ² ; 84 ²
Ava I	6,900; 6,800; 880 ³
Kpn I	(14,600)
Bgl I	(11,900); 1,480 ³ ; 1,170 ³ ; 120 ³
Hpa I	(11,000); 3,300 ³
Pvu II	5,700 ³ ; 4,000; 1,830; 1,450 ³ ; 1,420 ² ; 390 ²
Pst I/Ava I	6,800; 3,600 ³ ; 1,920; 1,170 ² ; 880 ³ ; 68 ² ; 16 ⁴
Pst I/Kpn I	8,100; 3,400 ³ ; 1,920; 1,170 ² ; 84 ²
Pst I/Bgl I	6,300; 2,400 ³ ; 1,920; 1,480 ³ ; 1,170 ³ ; 1,170 ² ; 120 ³ ; 84 ²
Pst I/Hpa I	8,200; 3,050 ³ ; 1,700; 1,170 ² ; 200 ³ ; 84 ²
Pst I/Pvu II	5,700 ³ ; 1,830; 1,800 ² ; 1,420 ² ; 1,170 ² ; 1,100 ³ ; 900; 390 ³ ; 390 ² ; 84 ²
Ava I/Kpn I	6,900; 6,600; 880 ³ ; 200 ³
Ava I/Bgl I	6,400; 5,500; 1,300 ³ ; 570 ³ ; 570 ³ ; 190 ³ ; 120 ³
Kpn I/Bgl I	(12,000); 1,170 ³ ; 1,090 ³ ; 410 ³ ; 120 ³
Bgl I/Hpa I	(9,100); 2,580 ³ ; 1,170 ³ ; 800 ³ ; 680 ³ ; 120 ³
Bgl I/Pvu II	4,000; 2,070 ³ ; 1,830; 1,480 ³ ; 1,450 ³ ; 1,420 ² ; 1,170 ³ ; 820 ³ ; 390 ² ; 120 ³
Kpn I/Hpa I	(11,000); 3,300 ³ ; 410 ³
Hpa I/Pvu II	4,000; 2,900 ³ ; 2,750 ³ ; 1,830; 1,420 ² ; 840 ³ ; 600 ³ ; 390 ²

¹ The lengths shown in parenthesis are approximate values.

² Restriction fragments also found in digests of pLC3-46, pLC8-24, and pLC19-24 which are from totally within the ColE1 region.

³ Restriction fragments also found in digests of pLC3-46, pLC8-24, and pLC19-24 which are not from the ColE1 vector region.

⁴ Restriction fragment not actually observed.

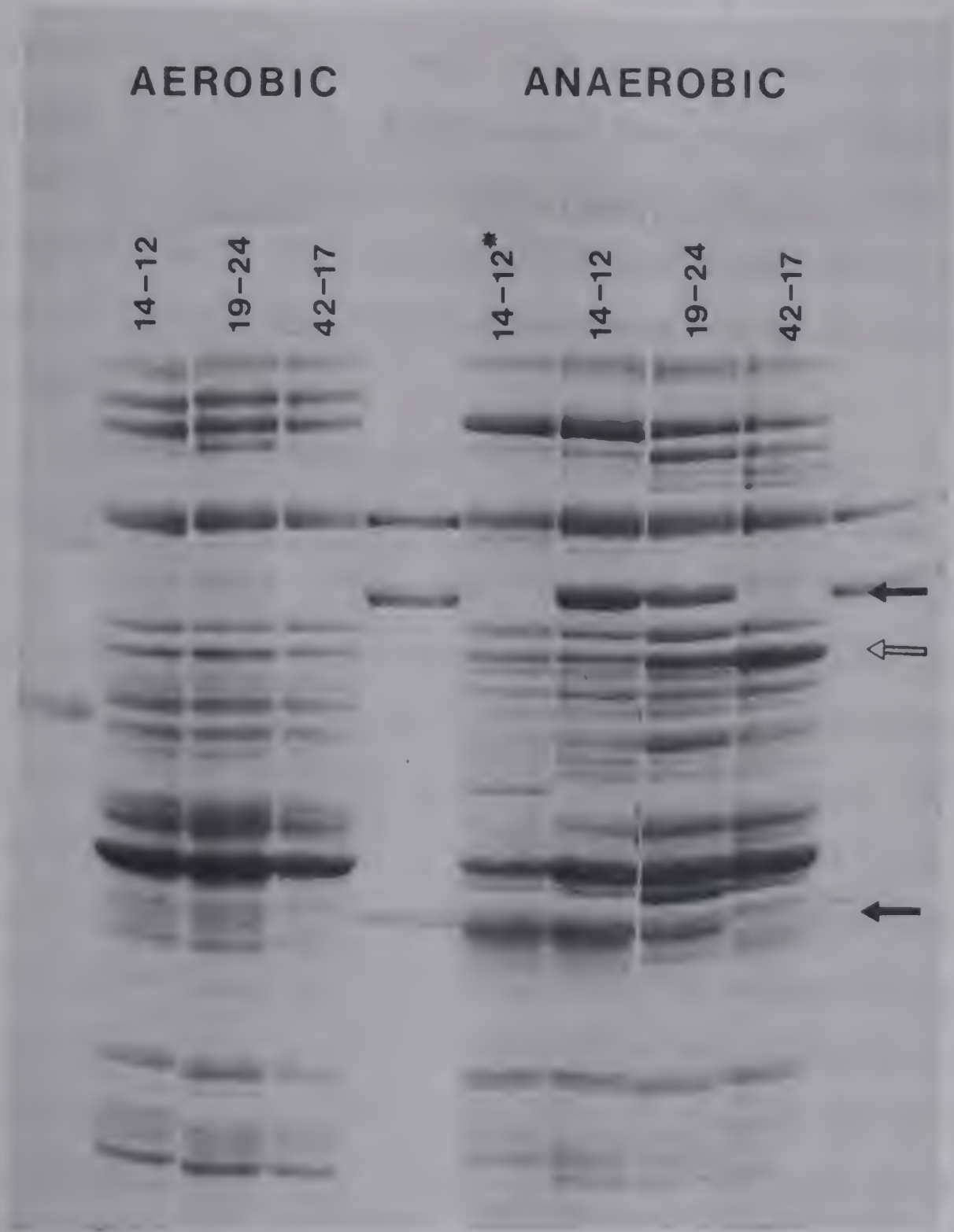
TABLE 7

Fragment Sizes Obtained from Restriction Endonuclease
Digestion of pLC42-17

Restriction Endonuclease(s) Used	Fragment Sizes(base pairs) pLC42-17
<i>Pst</i> I	(10,300);3,100;1,170 ² ;84 ²
<i>Ava</i> I	(14,400)
<i>Kpn</i> I	(14,800)
<i>Bgl</i> I	(14,600)
<i>Hpa</i> I	(12,300);1,750;130;68
<i>Pvu</i> II	6,000;3,700;2,200;1,450 ³ ; 1,420 ² ;390 ²
<i>Bam</i> HI	(14,700)
<i>Pst</i> I/ <i>Ava</i> I	(10,000);3,100;1,170 ² ;68 ² ; 16 ⁴
<i>Pst</i> I/ <i>Kpn</i> I	8,200;3,100;2,100;1,170 ² ; 84 ²
<i>Pst</i> I/ <i>Bgl</i> I	(10,200);2,200;1,170 ² ;850; 84 ²
<i>Pst</i> I/ <i>Hpa</i> I	8,500;3,100;1,750;1,170 ² ; 200 ³ ;130;84 ² ;68
<i>Pst</i> I/ <i>Pvu</i> II	3,700;2,900;2,200;1,800 ² ; 1,420 ² ;1,170 ² ;1,100 ³ ;390 ³ ; 390 ² ;84 ²
<i>Pst</i> I/ <i>Bam</i> HI	7,000;3,100;3,050;1,170 ² ;84 ²
<i>Ava</i> I/ <i>Kpn</i> I	8,300;6,300
<i>Ava</i> I/ <i>Bgl</i> I	(12,500);1,940
<i>Ava</i> I/ <i>Bam</i> HI	7,600;6,900
<i>Kpn</i> I/ <i>Bgl</i> I	(10,200);4,500
<i>Bgl</i> I/ <i>Hpa</i> I	(9,700);2,580 ³ ;1,750;130; 68
<i>Bgl</i> I/ <i>Pvu</i> II	4,000;3,700;2,200;2,070 ³ ; 1,450 ³ ;1,420 ² ;390 ²
<i>Kpn</i> I/ <i>Hpa</i> I	(12,400);1,750;120;68;10 ⁴
<i>Hpa</i> I/ <i>Pvu</i> II	6,000;2,500;2,200;1,420 ² ; 840 ³ ,600 ³ ,390 ²

¹⁻⁴As indicated in Table 6.

Figure 11. SDS-PAGE Analysis of Crude Cytoplasmic Extracts from pLC14-12, pLC19-24, and pLC42-17. Growth conditions, preparation of extracts and SDS-PAGE were performed as described in the methods chapter. The fast-running gel system (153) was used in this experiment. The dark arrows indicate the positions of the 62,000 and the 43,000 molecular weight polypeptides and the light arrow indicates the position of the 58,000 molecular weight polypeptide produced in pLC42-17.* Incubated in the presence of 40 ug/ml pancreatic DNAase, containing contaminating trypsin and chymotrypsin, for 30 minutes at 37 °C. Molecular weight standards used were: 1st well- bovine serum albumin (68,000) and IgG heavy chain (50,000); 5th and 10th wells- fumarate reductase (69,000) and anaerobic G3P dehydrogenase (62,000 and 43,000).



58,000 molecular weight polypeptide was produced, and only under conditions in which the anaerobic dehydrogenase would be optimally expressed. We believe this was a product of the incomplete *glpA* locus in pLC42-17. When extracts from MV12/pLC19-24 were analysed, this polypeptide was not observed. Since pLC19-24 contained the entire region of DNA that was found in pLC42-17 (see Figure 10) the possibility that synthesis of this polypeptide was directed by any other region of DNA in the insert other than the *glpA* locus was excluded.

A tentative assignment of the direction of transcription can be made on the basis of the above results taken in conjunction with what is known about the structure of the vector DNA. Transcription of the *glpA* gene in the direction from right to left in Figure 10 would extend from the partial *glpA* gene in pLC42-17 into the vector ColE1 DNA. The extension into the vector DNA is at the end of the Colicin E1 gene, which is transcribed in the opposite direction (174). Thus the probability of encountering a termination codon would be fairly high and the extension into the ColE1 vector would contribute only a relatively small amount to the molecular weight of the partially completed polypeptide. Transcription of the *glpA* locus in the direction from left to right proceeds into regions of DNA common to all the plasmids and would not result in a polypeptide of altered molecular weight in pLC42-17.

C. Discussion

In earlier studies on the expression of the *glp* genes it was observed that the expression of the *glpT* and *glpA* genes seemed to fluctuate in a parallel fashion, suggesting that the two genes shared a common operator-promoter region (121). The results from the present study, however, indicate that the two genes respond differently to changes in the terminal electron acceptor present in the growth medium. Non-coordinate control of the *glpA* and *glpT* genes with respect to the catabolite and *glpR* repression systems was also observed in a recent study by Miki and Lin (123). In this study the authors monitored expression from the *glpT* promoter by assaying for β -galactosidase utilizing an operon-fusion strain in which the structural gene for β -galactosidase had been fused to the *glpT* promoter. The observation that bacteriophage Mu insertions into one of the two genes did not affect the other is a more direct demonstration that the *glpA* and *glpT* genes are in separate operons (122).

We can conclude from our present studies that the recombinant plasmids pLC3-46, pLC8-24, pLC8-29, pLC14-12, pLC19-24 and pLC42-17 carry the *glpT* gene. Cells carrying these recombinant plasmids appear to have an increased number of transport polypeptides present in the cytoplasmic membrane. Furthermore, our *in vitro* studies enabled us to tentatively identify the periplasmic component as a 40,000 molecular weight polypeptide and the membrane component as a

26,000 molecular weight polypeptide. These results are consistent with those of other workers who have identified and purified the 40,000 molecular weight periplasmic component (126,175) and tentatively identified the membrane carrier polypeptide (128).

The levels of anaerobic G3PDH activity that were attained in anaerobically-grown cells containing a recombinant plasmid carrying the *glpA* gene were sufficient to permit identification of the *glpA* polypeptides in crude cell extracts. The presence of the 62,000 and 43,000 molecular weight polypeptides observed in SDS-PAGE profiles closely paralleled the levels of anaerobic G3PDH activity. Furthermore, these polypeptides were found predominantly in the cytoplasmic fraction after cell lysis, in agreement with activity studies and were observed in cells containing plasmids pLC3-46, pLC8-24, pLC19-24 which carry a functional *glpA* gene but were not observed in pLC42-17. Finally, the results in chapter 5 verify that these two polypeptides are the subunits of the purified enzyme.

Having identified the *glpA* polypeptides I did not feel that it was necessary to carry out any *in vitro* labelling experiments to directly show that the plasmids carried the structural information for the anaerobic G3PDH. I felt that the plasmids did not code for some protein which induces the synthesis of the enzyme for the following reasons:

1. All the independently derived *glpA* mutations that have been tested map at the same region, closely linked to

the *glpT* locus (91,124,125). Thus it is unlikely that there is a separate locus responsible for specifically inducing the synthesis of the anaerobic dehydrogenase polypeptides. Furthermore, the plasmids that we utilized in this study all contained the closely linked *glpT* locus.

2. The production of a 58,000 molecular weight polypeptide by pLC42-17 is consistent with the plasmid possessing a portion of the structural polypeptide information but is not consistent with it containing a portion of an inducer locus.

In two separate studies discussed in this chapter recombinant ColE1:*E. coli* plasmids are utilized to identify the *glpT* polypeptides and the *glpA* polypeptides respectively. The probable reason that the anaerobic dehydrogenase polypeptides were not identified in the minicell labelling experiments designed to identify the *glpT* polypeptides is that the experiments were carried out under aerobic conditions in which the *glpA* locus is repressed (121). Similar *in vitro* labelling experiments performed by Schumacher and Bussman (128) utilizing pLC3-46 also identified the *glpT* polypeptides but did not detect the *glpA* polypeptides. On the other hand, the transport polypeptides were not observed in the experiments identifying the *glpA* polypeptides because they were present at too low a level to be detected by Coomassie Blue staining of crude extracts. The *glpT* polypeptides were not even evident in Coomassie

Blue stained gels from the minicell labelling experiments and were only identified after slicing and counting the gels.

The recombinant plasmids utilized in this study vary considerably in size, with inserts ranging from 8.2 to 16.8 kilobases (see Table 2, ColE1 vector 6.4 kb). The smallest plasmid, pLC14-12, has sufficient DNA to code for the *glpA* and *glpT* polypeptides with little excess DNA. The *glpA* polypeptides of 62,000 and 43,000 would together require 2.8 kb of DNA whereas the *glpT* locus, which codes for a 40,000 molecular weight periplasmic component (128,175) and a 26,000 cytoplasmic membrane component (128), would require 1.8 kb. The total insert is 8.2 kb, of which 4.6 kb is required for *glpA* and *glpT* structural polypeptide information. This feature was helpful in defining the location of the *glpT* and *glpA* genes by restriction analysis. The identification of a 58,000 molecular weight polypeptide produced by pLC42-17 under conditions similar to those needed to express the *glpA* polypeptides allowed us to assign a more precise location for the *glpA* structural gene. In addition, it predicts the direction of transcription and thus indicates the region in which the *glpA* promoter-operator should be located.

The anaerobic G3PDH is composed of two subunits indicating that either there are two complementing genetic loci involved or that post-translational processing of a primary product occurs. This argument can be also applied to

the *glpT* gene which results in the production of a 40,000 molecular weight periplasmic component and a 26,000 molecular weight cytoplasmic membrane component. Although earlier genetic experiments implicated a single locus for the *glpA* gene (90), two immediately adjacent genetic loci (both located within a 4 kb region, see Figures 9 and 10) would probably not have been detected in these experiments. If the two subunits of the anaerobic dehydrogenase were the result of a post-translational cleavage event, it would be the first example of this type of processing occurring in prokaryotes of which I am aware. Nucleotide sequence analysis of the *glpA-glpT* region, which is in progress in our laboratory, should clarify the situation.

IV. Characterization of the Aerobic Dehydrogenase

A. Introduction

The aerobic glycerol-3-phosphate dehydrogenase has been purified (76) and shown to be located on the inner surface of the cytoplasmic membrane (133). However, the preliminary characterization of the enzyme was not very extensive and many of the physical, chemical and enzymatic properties of the enzyme were not known. Thus a more extensive characterization of this enzyme was initiated.

The purification and characterization of the aerobic glycerol-3-phosphate dehydrogenase was a joint study in which both Elke Lohmeier and I were involved and in which Joel Weiner contributed extensively in directing the emphasis of the research. In order to give a complete description of this enzyme for comparison with the anaerobic enzyme, I will be discussing the results of some experiments that were not performed by myself. However, contributions by Elke and Joel will be specifically mentioned.

B. Results

1. Molecular Weight

SDS-PAGE analysis of the purified enzyme, carried out by Elke Lohmeier and described elsewhere (176), established that the polypeptide molecular weight was 58,000. The earlier reported value of 35,000 (76) was in error due to the insufficient concentrations of SDS used in those

experiments thus underestimating the true subunit molecular weight. Analytical gel filtration experiments indicated that the native enzyme was an α_2 dimer. This conclusion was strengthened by the fact that quantitation of the amount of FAD cofactor present, also performed by Elke Lohmeier, showed that there was 0.5 mole FAD/mole 58,000 polypeptide.

2. Optical Properties

The absorption spectrum of the purified enzyme exhibited three absorption maxima at 278 nm, 380 nm and 455 nm. The 380 nm and 455 nm peaks were bleached by the addition of substrate (Figure 12), in agreement with earlier observations that a 450 nm peak was bleached by substrate (76).

The enzyme has an A_{280}/A_{455} ratio of 11 and an A_{280} of 1.15/mg protein. Using the extinction coefficient for free FAD of $11.3 \text{ cm}^{-1}\text{mM}^{-1}$ (177), the calculated stoichiometry for FAD cofactor to 58,000 polypeptide was 0.55 mole/mole. This agreement with the value obtained by fluorometric determination of endogenous flavin indicated that the absorption properties of the membrane-bound FAD were not significantly altered relative to free FAD.

3. Amino Acid Composition

The results of amino acid analysis performed as described in the methods chapter is listed in Table 8. The enzyme has 41% nonpolar amino acids (glycine classified as polar).

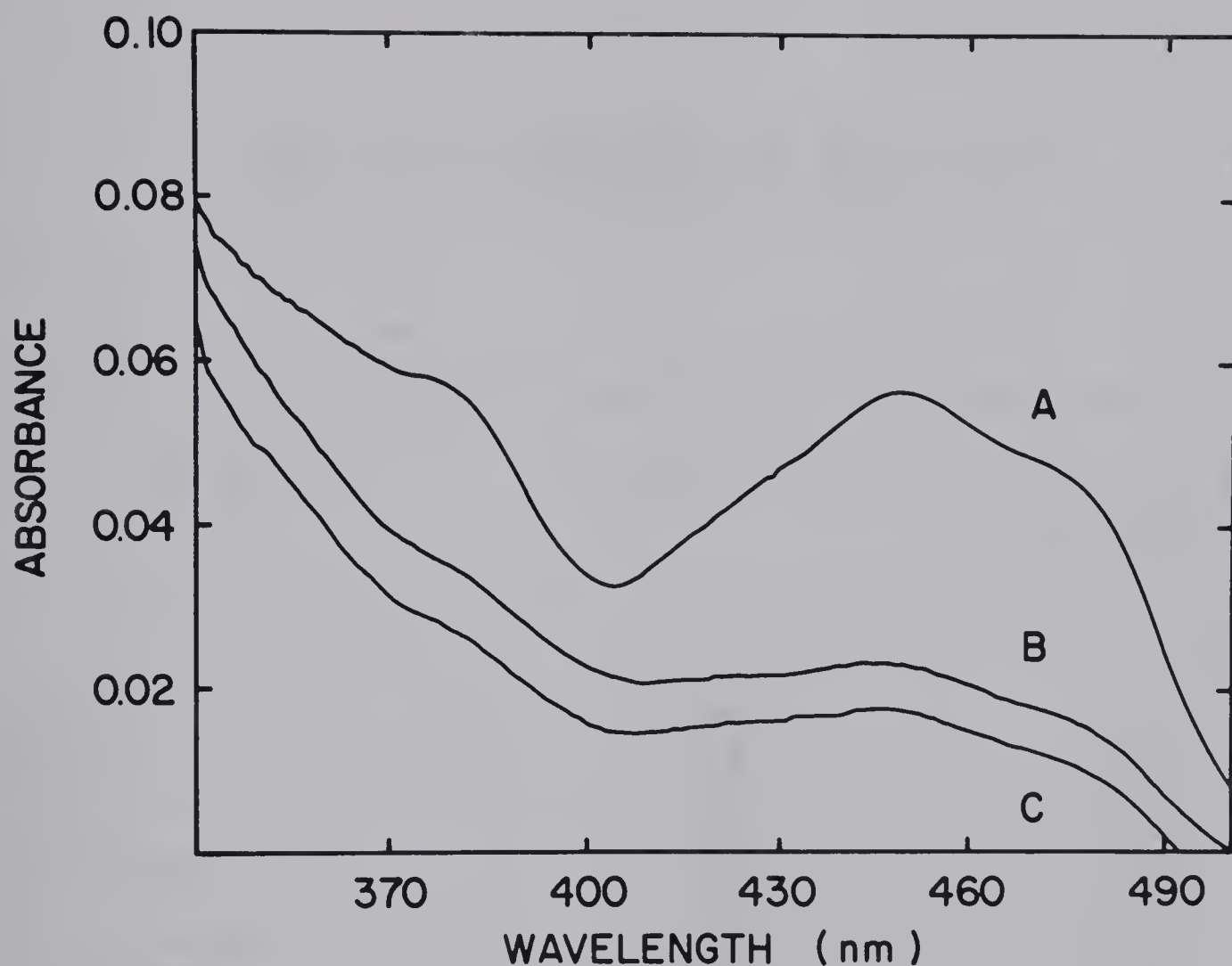


Figure 12. Absorption Spectrum of the Aerobic Dehydrogenase. The absorption spectrum of 0.4 ml of detergent-depleted (176) enzyme (0.55 mg/ml) was determined with a Gilford 2600 spectrophotometer before and after additions of 3.0 M DL-glycerol-3-phosphate. Curve A, no additions; curve B, DL-glycerol-3-phosphate, 15 mM; curve C, 45 mM.

TABLE 8

Amino Acid Composition of the Aerobic
Glycerol-3-phosphate Dehydrogenase

Amino Acid	Moles/58,000 g	% of Total Residues
Glycine	44	8.4
Alanine	45	8.7
Valine	33	6.4
Leucine	55	10.5
Isoleucine	26	5.0
Proline	18	3.5
Phenylalanine	16	3.1
Tryptophan	8	1.5
Methionine	13	2.6
Serine	32	6.2
Threonine	29	5.5
Cysteine	4	0.8
Tyrosine	21	3.9
Aspartate, Asparagine	50	9.7
Glutamate, Glutamine	47	9.0
Lysine	27	9.3
Arginine	38	7.2
Histidine	15	2.8

4. Comparison of Purified and Membrane-bound Enzyme

To assess whether any drastic changes in the aerobic G3PDH occurred during purification, the crude and purified enzyme were compared. The K_m for substrate was determined to be 1.1 mM, 10 mM and 21 mM for the purified enzyme, the crude membrane preparation and toluene-permeabilized whole cells respectively. This may be a reflection of the relative accessibility of the active site to substrate in the different preparations rather than an alteration in binding properties of the enzyme. The effects of pH on the enzymatic activity of the membrane-bound and purified enzyme were similar, both enzymes exhibiting a rather broad optimum between pH 7.0 and 9.5 (Figure 13). Above pH 9.5 autoredox of MTT made enzymatic assay difficult. The effect of increasing temperature on enzymatic activity is a balance between the increasing rate due to increased thermal kinetic energy and the lability of the enzyme at higher temperatures. The membrane-bound and purified enzyme had similar temperature-activity profiles (Figure 14).

5. Electron Acceptors for the Aerobic Dehydrogenase

The enzymatic assay for glycerol-3-phosphate dehydrogenase was originally developed for whole cells and crude extracts. The lipid solubility of PMS was desirable for this purpose and the lack of autooxidizability of the reduced MTT made enzymatic assay convenient. However, it was of interest to determine the relative effectiveness of other electron acceptors in the assay of G3PDH activity.

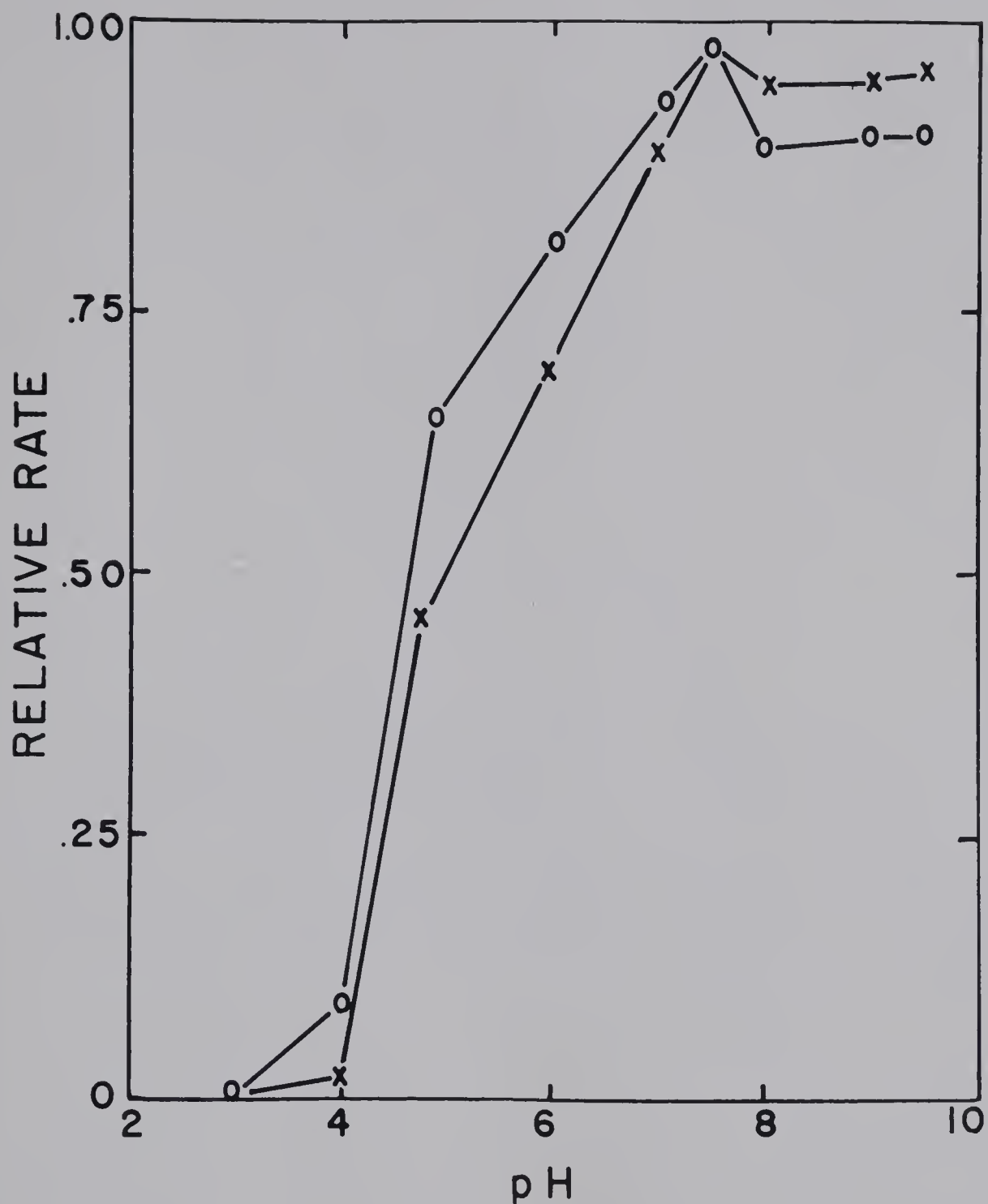
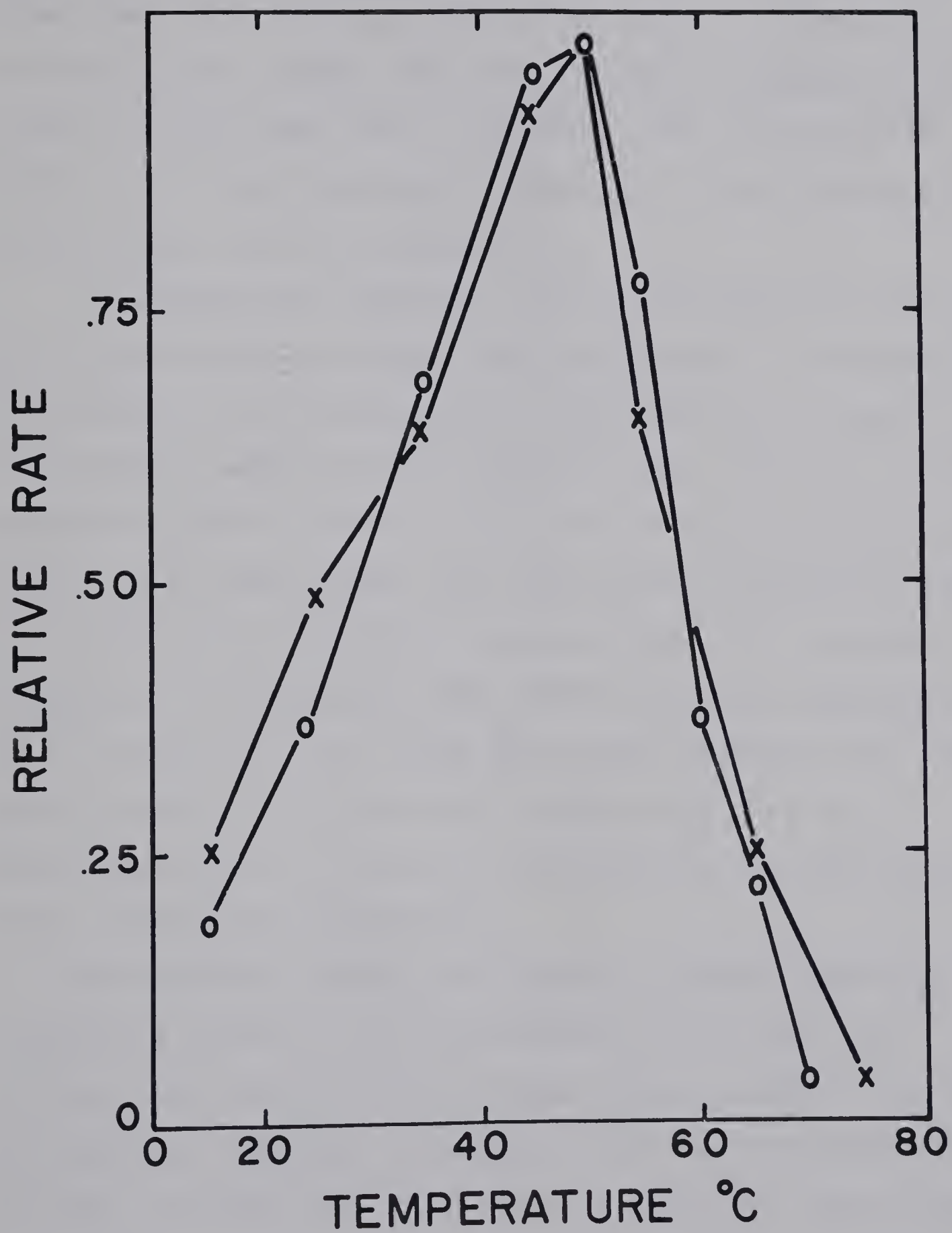


Figure 13. pH Profile of Aerobic Dehydrogenase Activity. Aliquots of crude membrane preparation (Fraction I) or purified enzyme were assayed in the standard assay mixture (9 mM KCN included), except that the 50 mM imidazole buffer was replaced by the following 50 mM buffers for the indicated pH ranges: sodium citrate, pH 2.5-5.0; sodium cacodylate, pH 5.0-7.0; HEPES, pH 7.0-8.5; Glycine-NaOH, pH 8.5-9.5. Open circles, membrane preparation; x's, purified enzyme.



Figure 14. Temperature Profile of Aerobic Dehydrogenase Activity. Aliquots of crude membrane preparation (Fraction I) or purified enzyme were incubated at the various temperatures in the standard assay mixture (without added glycerol-3-phosphate) for 5 minutes in a Cary dual-beam spectrophotometer to achieve temperature equilibration. The reaction was initiated by addition of substrate and the rate measured.



Ferricyanide could be directly reduced by the enzyme at rates equivalent to those attainable with redox-coupling dyes (Table 9). Although DCPIP could also be directly reduced by the enzyme, the rate was nearly doubled by the redox-coupling dyes PMS or menadione. MTT, on the other hand, showed only negligible reduction in the absence of intermediate electron acceptors.

To compare the different electron acceptors in Table 9, it is necessary to consider the stoichiometries involved. The oxidation of one molecule of G3P produces 2 reducing equivalents, which in turn results in the reduction of one molecule of MTT or DCPIP or two molecules of ferricyanide (178). It is thus evident that the maximal reduction rates with these dyes are within the same range. The resulting sequence of ferricyanide, MTT, DCPIP which was observed may be a reflection of the redox potentials of these dyes. The direct reduction of the redox couplers could not be determined under the aerobic conditions of the assay due to their rapid autooxidizability.

Cytochrome c was not an electron acceptor under any conditions tested. It is interesting to note that the quinone analogue, menadione, could support reduction of MTT but the yeast quinone, coenzyme Q6, and the mitochondrial quinone, coenzyme Q10, were inactive. Although the natural quinones were used at concentrations known to be active with G3PDH solubilized from inner mitochondrial membranes (179), no positive controls were available in this experiment and

TABLE 9

Electron Acceptors for the Aerobic Dehydrogenase

Electron coupler	Electron Acceptor			
	MTT	Ferricyanide	DCPIP	Cytochrome c
None	0.28	37.7	6.7	0
PMS	15.0	30.1	12.8	0
Methylene blue	11.7	35.7	7.1	0
Menadione	12.0	33.7	10.4	0
CoQ6	0.4	31.0	6.3	0
CoQ10	0.5	33.0	6.5	0

Results are expressed as micromoles of reducing equivalent accepted per min per mg of protein. Assays were performed as described under Methods, except that MTT and PMS were replaced by the electron acceptors listed. The concentrations used were: MTT, 72.4 μ M; ferricyanide, 1 mM; DCPIP, 150 μ M; cytochrome c, 30 μ M; PMS 326 μ M; methylene blue, 15 μ M; menadione, 1.5 mM; CoQ6, 60 μ M; CoQ10, 50 μ M. The reaction was followed in a Gilford model 250 spectrophotometer at 570 nm for MTT, 420 nm for ferricyanide, 600 nm for DCPIP, and 550 nm for cytochrome c.

thus the activity of these commercially supplied compounds could not be determined.

6. Inhibition by Structural Analogs

The effect of various structural analogs of G3P on enzymatic activity was studied and the results are summarized in Table 10. The product of the enzymatic reaction, dihydroxyacetone phosphate, is a potent inhibitor of G3P reduction. The inhibition by dihydroxyacetone phosphate is competitive with a K_I of 0.5 mM. Phosphoenol pyruvate, phosphoglycolic acid, D,L-glyceraldehyde-3-phosphate, and D-3 and D-2 phosphoglyceric acid are also fairly effective competitive inhibitors with K_I 's in the 1 mM range. β -glycerolphosphate and phosphonomycin, the phosphonate analogue of glycerol-3-phosphate, have no effect on activity. The pattern of inhibition observed is fairly similar to that of mitochondrial G3PDH (180).

7. Inhibition of Activity by Purine Nucleotides

The purified enzyme activity was inhibited by purine nucleotides but not by pyrimidine nucleotides (Table 11). ATP, dATP, and GTP are effective inhibitors whereas UTP and dTTP (data not shown) are without effect. There appears to be specificity for the nucleoside triphosphate as both ADP and AMP do not inhibit enzymatic activity. The effect of ATP on enzyme activity was studied further by Danielle MacBeth who found that inhibition by ATP is complex with a slight stimulation being observed at low concentrations (0.5 mM).

TABLE 10

Effect of Substrate Analogues on the Aerobic
Glycerol-3-phosphate Dehydrogenase

Analogue	Relative Rate	KI (mM)
None	1.00	
Dihydroxyacetone phosphate	.01	0.5
Phosphoenol pyruvate	.13	0.6
Phosphoglycolic acid	.09	N.D.
D,L Glycerinaldehyde-3-phosphate	.15	N.D.
D-3 Phosphoglyceric acid	.16	0.7
D-2 Phosphoglyceric acid	.21	1.4
Glucose-6-Phosphate	.73	
β -Glycerophosphate	1.01	
Ribose-5-phosphate	.93	
Fructose-1,6-diphosphate	.88	
Phosphonomycin	.98	
Glycerol	.91	
2,3 Diphosphoglyceric acid	1.19	

N.D. = Not Determined

Assays were performed as described in Methods with 2 ug G3P dehydrogenase, 2 mM DL-G3P and 10 mM analogue. KI values were obtained from Lineweaver-Burk plots using at least 3 concentrations of inhibitor. 100% activity is 22 nmoles MTT reduced per minute.

TABLE 11

Inhibition by Purine Nucleotides

Inhibitor	Inhibitor Concentration	Relative Rate	% Inhibition
None	-	1.0	0
ATP	10 mM	0.27	73
dATP	10 mM	0.35	65
GTP	10 mM	0.36	64
UTP	10 mM	1.03	0
ATP	2.5 mM	0.58	42
ADP	2.5 mM	1.01	0
AMP	2.5 mM	1.04	0

Assays were performed as described in methods except that the substrate concentration was 2 mM DL-G3P and the indicated concentration of inhibitor was added.

The effect is not thought to be via enzyme phosphorylation as the β,γ -methylene analogue of ATP is also an inhibitor.

Since ATP is the product of electron transport via oxidative phosphorylation the inhibition observed may indicate an as yet unknown regulation of electron transport via the primary dehydrogenase. However, although physiological levels of nucleotides were tested, Mg^{+2} ions were not added to the assay mixtures to ensure that the physiological species, Mg-ATP, was present.

8. Inactivation of Aerobic Dehydrogenase

The effect of various ions on enzymatic activity indicated that several divalent cations were inhibitors of enzyme activity when included in the assay mixture (Table 12). These effects were observed in the 10-100 μM concentration range with the relative effectiveness following the series: Cu^{++} , Co^{++} > Mn^{++} > Zn^{++} . The divalent cations Ca^{++} and Mg^{++} had no effect on activity at these concentrations. This observation led us to suspect that there may be an essential sulfhydryl group necessary for maintaining enzymatic activity. In order to test this possibility, the effect of several sulfhydryl reagents on enzymatic activity was determined. The results in Table 13 are consistent with there being an essential sulfhydryl involved in enzymatic activity. However, the relatively high concentrations of PCMB required for inactivation (17 moles PCMB/mole 58,000 polypeptide at 0.1mM) suggest that it is not a readily accessible and reactive sulfhydryl. Addition

TABLE 12

Inhibition of Aerobic Dehydrogenase
Activity by Divalent Cations

Divalent Cations	Concentration (uM)	% Inhibition	
		MTT Reduction	Ferricyanide Reduction
Zn ⁺⁺	100	40	70
	10	0	
Cu ⁺⁺	100	100	30
	10	14	
Mn ⁺⁺	100	60	55
	10	0	
Co ⁺⁺	100	100	0
	10	12	

Assays performed as described in the methods chapter except that the indicated concentration of divalent cation (chloride salt) was present in the assay mixture.

TABLE 13

Inactivation of the Aerobic Dehydrogenase

Reagent	Concentration (mM)	% Inhibition
PCMB	0.1	52
	0.3	97
N-Ethylmaleimide	20.0	39
	50.0	63
1,10-Orthophenanthroline	1.0	0
PCMB plus 10 mM G3P	0.3	97

Purified enzyme (0.34 mg/ml) was incubated for 15 minutes at 30°C with the indicated concentration of reagent, after which time 2 ug of the treated enzyme was assayed under the standard conditions. Control enzyme solutions were diluted and incubated appropriately.

of substrate did not protect against inactivation under these conditions.

The iron chelator, 1,10-phenanthroline, reduced the level of enzymatic activity, suggesting that there may be iron present which is essential for activity. This result has been confirmed in subsequent experiments performed by John Robinson (unpublished results). However, the iron content of the purified enzyme has not been determined and the possibility that inhibition by 1,10-phenanthroline is due to some other mode of action cannot be eliminated.

9. Effect of Phospholipids

To test the effect of phospholipids on enzymatic activity, it was necessary to remove the detergent associated with the enzyme. In an initial attempt to achieve this goal, the purified enzyme (which contains 0.2% Brij 58) was subjected to hydroxylapatite chromatography (Step V) in which the 0.2% Brij 58 was replaced by 0.5% sodium cholate. The cholate form of the enzyme showed a slight stimulation (40%) by addition of egg yolk phospholipids but an attempt to remove excess cholate by dialysis resulted in irreversible inactivation of the enzyme. This problem was overcome when Elke Lohmeier obtained a detergent-depleted form of the enzyme by exchanging the detergent for the chaotrope, sodium perchlorate (176). Although there was a dramatic drop in specific activity during preparation of the detergent-depleted enzyme (11.5 units/mg to 1.5 units/mg), this activity could be restored by the addition of

detergents or phospholipids (176).

10. Reconstitution of Aerobic Dehydrogenase with Membrane Vesicles

The aerobic G3PDH was purified on the basis of its enzymatic activity without regard to its allotopic site, the portion of the protein which interacts with the membrane. It was therefore of interest to determine if our homogeneous preparation was active in reconstitution experiments.

As a measure of reconstitution Elke Lohmeier assayed the ability of our preparation to stimulate G3P-dependent active accumulation of L-proline into vesicles. For these studies we prepared membrane vesicles from *E. coli* Strain 8, which lacks a functional membrane-associated G3PDH and therefore cannot utilize G3P to support active transport, unless active enzyme is added back.

The preparation of detergent-depleted enzyme was a necessary first step in the reconstitution procedure as very low concentrations of detergent destroy vesicle integrity (181). Reconstituted vesicles were prepared by incubating vesicles with detergent-depleted enzyme, centrifuging and resuspending the vesicle pellet. The stimulation of G3P-dependent proline accumulation in Strain 8 vesicles by the addition of enzyme is shown in Figure 15. The maximal uptake observed was even greater than that observed with control Strain 7 vesicles (8.2 nmole/min/mg) under the same conditions (176). Neither boiled enzyme nor enzyme containing detergent was effective in reconstitution.

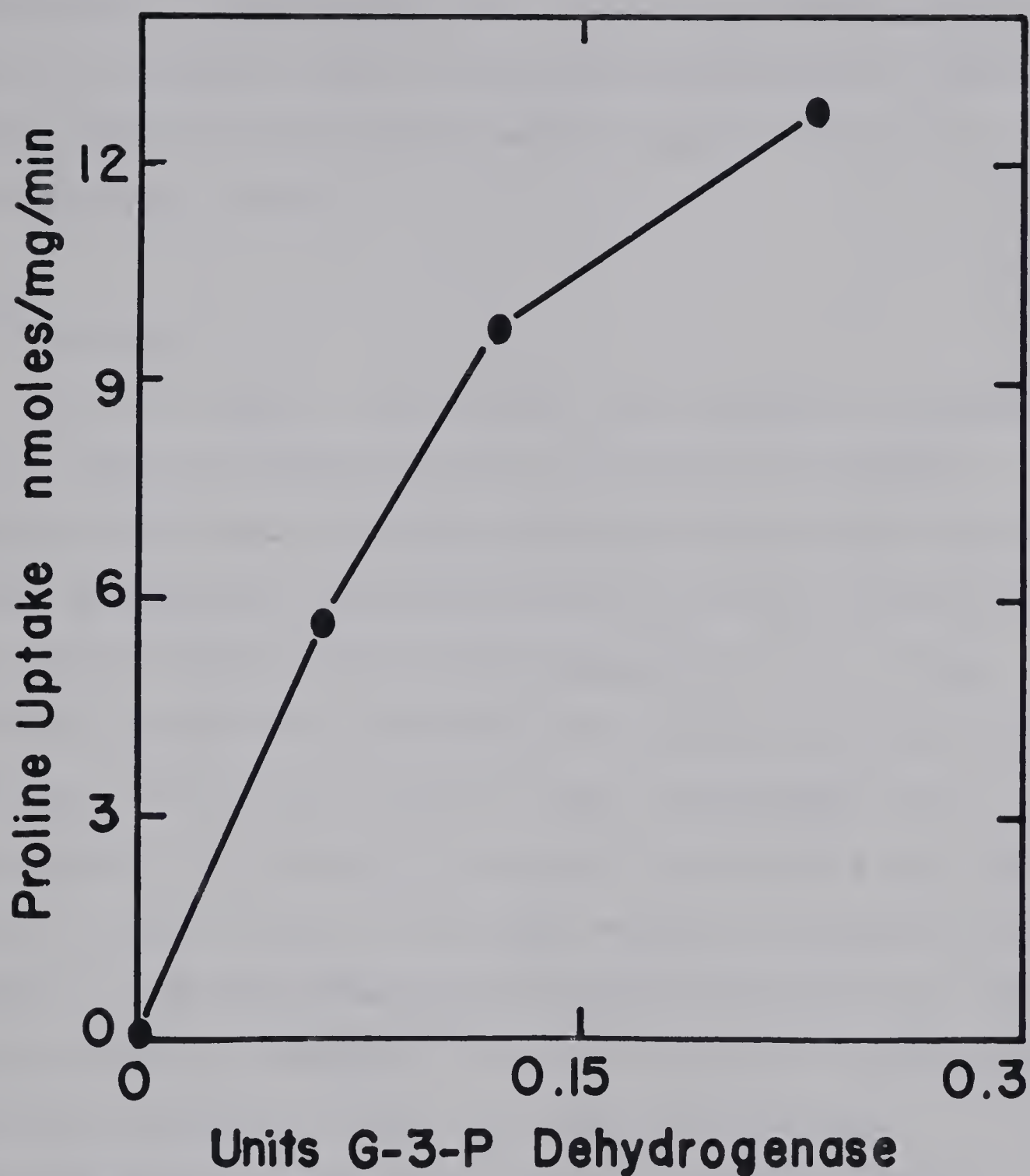


Figure 15. Reconstitution of Glycerol-3-phosphate-dependent Proline Transport. To 0.43 ml of membrane vesicles (0.4 mg/ml in 0.1 M potassium phosphate buffer, pH 6.6) was added detergent-depleted enzyme (0.05 to 0.2 units) and the volume was brought to 0.5 ml with buffer. Incubation was carried out for 15 min at 30°C and then the sample was centrifuged for 15 min at 40,000xg. The vesicle pellet was resuspended in 10 μ l of 0.1M potassium phosphate buffer, pH 6.6, and assayed for proline transport with glycerol-3-phosphate as energy source as described in the methods chapter.

Furthermore, the reconstituted transport showed a similar pattern of sensitivity to uncouplers and electron transport chain inhibitors as native vesicles using D-lactate as an energy source (176).

C. Discussion

In this chapter the chemical and functional properties of the aerobic, membrane-bound, glycerol-3-phosphate dehydrogenase were described. The purified enzyme was shown to be composed of a 58,000 molecular weight polypeptide and the native state of the enzyme appeared to be a dimer. Chemical crosslinking studies subsequently performed by John Robinson (182) have now more firmly established this conclusion. The similarity observed between the purified enzyme and the enzyme in a crude membrane preparation with respect to pH and temperature optima indicated that the enzyme had not undergone any drastic alterations during the isolation procedure. This conclusion was further strengthened by the reconstitution experiments which indicated that the purified enzyme interacted with the native electron transport chain.

In a previous study (133) on the topography of the aerobic dehydrogenase, evidence for localization on the cytoplasmic face of the membrane was obtained by enzymatic assay with the impermeable electron acceptor ferricyanide. The results presented in this study (Table 9) indicated that the purified enzyme could directly reduce ferricyanide which

substantiated the authors' conclusion that ferricyanide was interacting with the primary dehydrogenase and not some other component of the electron transport chain.

The fact that the activity of this enzyme was affected by purine nucleoside triphosphates, but not by pyrimidine nucleoside triphosphates or purine nucleoside mono- or diphosphates might suggest that ATP or GTP, or both, are natural effectors of this enzyme. However, the kinetics of these effects were quite complex and have not been studied in the crude, membrane-bound form of the enzyme thus making any projections to the *in vivo* situation questionable.

A number of divalent cations inhibited enzymatic activity (Table 12). The effect of these divalent cations depended upon whether ferricyanide or PMS-MTT was used to measure enzymatic activity. Subsequently, in a much more rigorous study, John Robinson was able to demonstrate specific inhibition of the PMS-MTT activity by Cu^{++} ions and specific inhibition of the ferricyanide assay with Zn^{++} ions (182). Furthermore, he demonstrated that cysteine protected the enzyme from inactivation by these ions which indicates that the effect of the ions is probably due to their interaction with essential sulfhydryls on the enzyme.

The G3PDH is an integral membrane protein and as such requires detergents or chaotropic agents to be solubilized. Removal of detergent results in a dramatic reduction in activity that can be restored by a variety of phospholipids or detergents (176,182). The results did not reveal any

apparent specificity for head group but showed a dependence on the fatty acid composition of the phospholipids and on the chain length of the detergent.

In subsequent studies on the effect of amphipaths on enzymatic activity, John Robinson showed that detergent depletion greatly affected the PMS-MTT assay but did not have any significant effect on the ferricyanide assay (182). The effect of added detergent increased both the V_{max} and the K_m for G3P in the PMS-MTT assay but had little effect on these parameters in the ferricyanide assay. Furthermore, he showed by crosslinking experiments that there was no apparent effect of detergent on the quaternary structure of the enzyme. Circular dichroism studies indicated that detergent caused a minor conformational change of the enzyme. Detergents also caused a decrease in intrinsic tryptophan fluorescence that occurred at the same detergent concentrations as the increase in enzymatic activity. He concluded on the basis of these experimental observations that amphipaths are necessary for the binding of PMS, but not ferricyanide, to the dehydrogenase (182).

V. Purification and Characterization of the Anaerobic Dehydrogenase

A. Introduction

Kistler and Lin (118) reported on a purification of the anaerobic G3PDH from an *E. coli* mutant deficient in the aerobic dehydrogenase. The enzyme was isolated from aerobically grown cells and partially purified by a combination of ammonium sulfate fractionation, gel filtration and DEAE-cellulose chromatography. Although they were unable to assess the purity of their preparation, its specific activity suggests that it was about 30%. The lability of the enzyme contributed to the low yields obtained at each step of the purification and probably was largely responsible for their inability to achieve purification to homogeneity. The authors did not determine the subunit composition of the enzyme but estimated a native molecular weight of 80,000, which was similar to the value obtained for the aerobic dehydrogenase in previous studies (76).

The product of the reaction catalyzed by their partially purified preparation was dihydroxyacetone phosphate. The authors determined that both exogenous FAD and FMN were stimulatory. The extent of stimulation by FAD and FMN (3-fold and 10-fold) and the concentration of half maximal stimulation (100 nM and 100 uM) for the two flavins were distinctly different. The authors also reported that

FMN caused the dependance of enzymatic activity on substrate to deviate from simple Michaelis-Menten kinetics.

In this chapter I will report on the purification to homogeneity of the anaerobic G3PDH from anaerobically grown cells containing a recombinant plasmid carrying the *glpA* gene. The physical, chemical and kinetic properties of the purified enzyme will also be presented.

B. Results

1. Purification of the Anaerobic Dehydrogenase

During the early stages of development of the purification protocol for the anaerobic dehydrogenase, Strain 13, which does not possess an aerobic G3PDH, was utilized as a starting material. It was observed that, in contrast to observations with other strains, the level of anaerobic enzyme was comparable in anaerobically and aerobically grown cells and even increased further in aerobically grown cells once stationary phase of growth was reached. This can perhaps explain why Kistler and Lin (118) used aerobically grown strain 13 as a starting material and why their initial specific activities were relatively high. However, the lability of the enzyme during purification made the prospect of purifying the enzyme from this strain an elusive goal.

The extent of amplification of anaerobic G3PDH activity in anaerobically grown cells carrying plasmid pLC14-12 (Table 5) convinced me to use this as the starting material

for purification of the enzyme. The purification procedure described below and listed in Table 14 is based on 100 grams wet weight of *E. coli* cell paste. All operations were carried out at 0-4°C.

The cell paste was thawed in 500 ml of 50 mM Tris-HCl (pH 7.5) containing 50 ug/ml phenylmethylsulfonylfluoride. After homogenization the suspension was passed twice through a precooled French Pressure cell (Aminco Instruments, Silver Spring, Md.) at 16,000 p.s.i. The lysate was then centrifuged at 48,000 x g for 1 hour and the supernatant was retained. Since the anaerobic dehydrogenase is an extrinsic membrane enzyme, virtually all the activity was present in the supernatant fraction at this stage. This was observed for both plasmid-containing and control strains and allowed us to purify the anaerobic dehydrogenase without resorting to any solubilization procedures. To stabilize enzyme activity the supernatant was made 20% (v/v) with ethylene glycol.

A saturated ammonium sulfate solution neutralized to pH 7.5 with ammonium hydroxide was slowly added to the crude supernatant to 44% (v/v) and the suspension was stirred for an additional 20 min. The suspension was then centrifuged at 15,000 x g for 15 min and the supernatant was retained. Saturated ammonium sulfate was then gradually added to the supernatant to 53% (v/v), allowed to stir for 20 min, and centrifuged as above. The supernatant was discarded and the pellet was resuspended in a final volume of 40 ml of 80 mM

TABLE 14

Purification of the Anaerobic Glycerol-3-Phosphate
Dehydrogenase from *E. coli*

Fraction	Total Activity (units)'	Total Protein (mg)	Specific Activity (units/mg)	Recovery (%)
Crude Supernatant	17,000	6,650	2.6	100
Ammonium Sulphate Pellet	8,200	1,250	6.6	48
Phenyl Sepharose Pool	3,560	230	15.5	21
HA Pool	3,160	80	39.5	18

'One unit is defined as 1 micromole of MTT reduced per min.
HA, hydroxylapatite.

Tris-HCl, pH 7.5, containing 20% ethylene glycol and 10 μ M FAD (Buffer A).

Hydrophobic exchange chromatography proved to be effective as the next step in the purification protocol. This had been anticipated since a membrane-associated protein would be expected to interact more strongly with the hydrophobic resin than the bulk of the cytoplasmic proteins. In hydrophobic exchange chromatography, in contrast to other forms of chromatography, the resolubilized ammonium sulfate pellet can be directly applied to the column without a desalting step. This was particularly important since it was essential to limit the number of steps and the duration of the purification procedure due to the lability of the enzyme.

The resuspended ammonium sulfate pellet was applied to a 3.2 x 15 cm (250 ml) Phenyl Sepharose CL4B column equilibrated with Buffer A. The column was washed with 450 ml of Buffer A and activity eluted with a 1.4 liter linear gradient of increasing ethylene glycol concentration (20 to 50%) and decreasing buffer concentration (80 to 20 mM Tris-HCl, pH 7.5) at a flow rate of 70 ml/hr. The elution profile from the Phenyl Sepharose column (Figure 16) indicated that the prediction of the binding properties of the anaerobic dehydrogenase was correct. The bulk of the protein did not bind to the hydrophobic resin in the low salt (80 mM) and moderate ethylene glycol concentrations (20%) present in the wash buffer. The anaerobic enzyme,

PHENYL SEPHAROSE CL4B CHROMATOGRAPHY

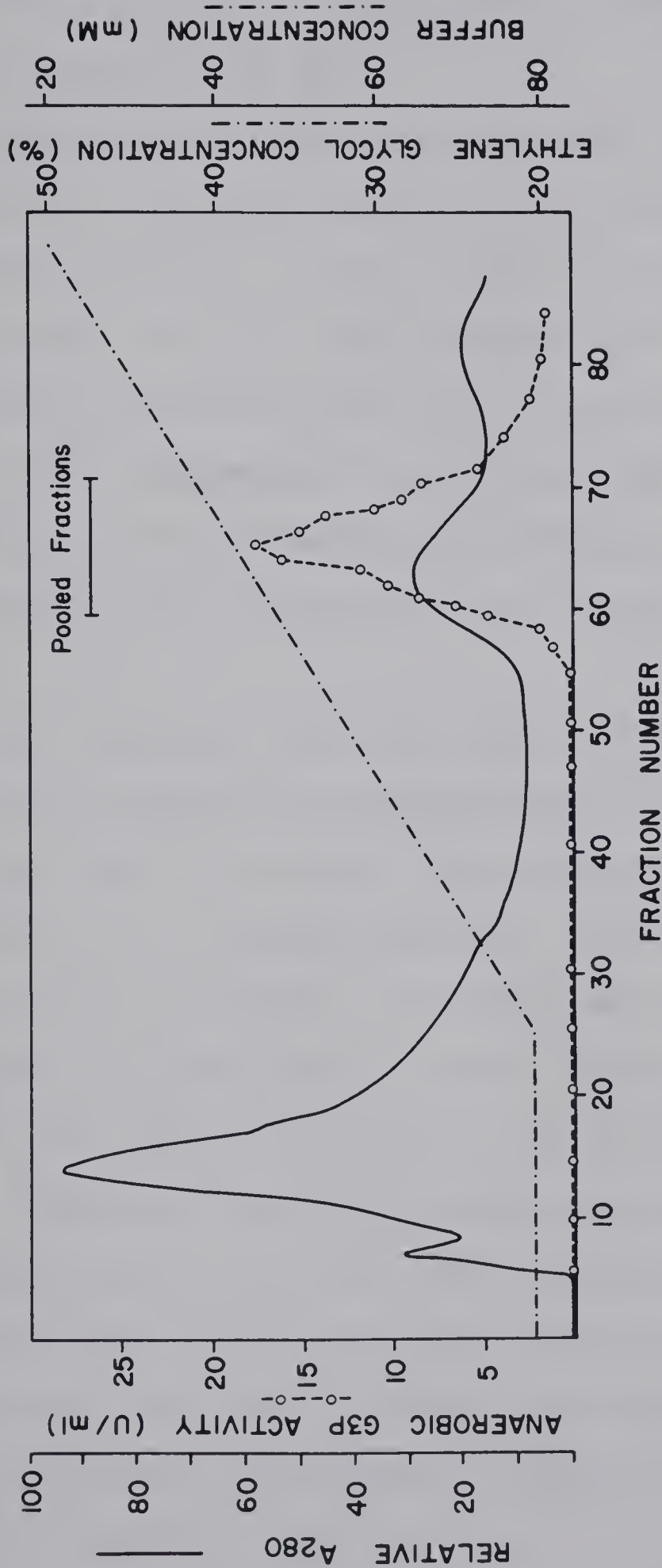


Figure 16. Phenyl Sepharose CL-4B Chromatography of Ammonium Sulfate Pellet Fraction from Cytoplasmic Fraction of MV12/pLC14-12. Experimental conditions and manipulations for chromatography are as described in text. A₂₈₀ was measured with a flow-through LKB Uvicord II and enzyme activity was measured as described in the methods chapter. The ethylene glycol and buffer concentrations were not measured but were estimated assuming a linear change in concentrations from the beginning to the end of the gradient.

however, did bind under those conditions and was eluted at the ethylene glycol concentration of 35% and the buffer concentration of 45 mM.

The enzyme preparation obtained from the Phenyl Sepharose column was nearly pure as judged by SDS-PAGE analysis. However, I felt it was necessary to remove the minor impurities from the preparation for the subsequent physical and chemical analyses I would be performing. Of the numerous chromatographic procedures that were tested hydroxylapatite chromatography produced the best results followed by Blue Sepharose, DEAE-Sephacel, Biorex-70 and CM-52.

The fractions from the Phenyl Sepharose column containing glycerol-3-phosphate dehydrogenase activity (greater than 12 units/ml) were pooled and applied to a 1.6 x 40 cm (75 ml) hydroxylapatite column equilibrated with 2 mM potassium phosphate, 18 mM Tris-HCl, pH 7.5, containing 20% ethylene glycol and 10 μ M FAD (Buffer B). The column was washed with 300 ml of Buffer B and activity eluted with a 1 liter linear gradient of increasing potassium phosphate concentration (2 to 40 mM) and decreasing Tris-HCl concentration (18 to 0 mM) at a flow rate of 50 ml/hr (Figure 17). The peak fractions were pooled, concentrated by ultrafiltration, and aliquots frozen in liquid nitrogen and stored at -70°C .

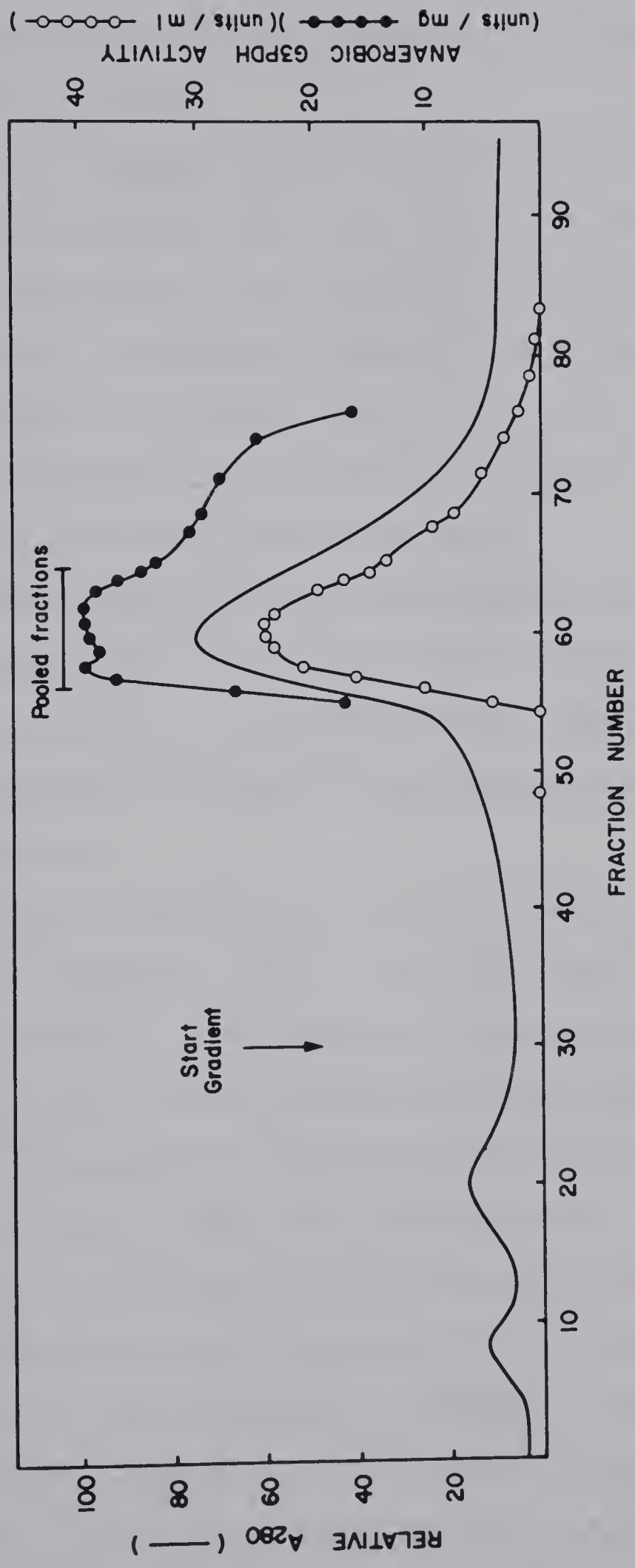


Figure 17.Hydroxylapatite Chromatography of Fraction Pool from Phenyl Sepharose CL-4B Column. Experimental conditions are as described in the text. A 280 was measured with a flow-through LKB Uvicord II and enzyme activity was measured as described in the methods chapter

2. Evidence for Purity

The purity of the preparation was assessed by the following criteria:

1. Only two polypeptides were observed by SDS-PAGE analysis over an acrylamide concentration range of 7% to 15%. Estimations of the relative amounts of the two subunits based on absorbance scans of Coomassie blue-stained gels yielded a 1:1 molar ratio. The ratio of these two polypeptides was the same across the peak which eluted from the Phenyl Sepharose resin.
2. The specific activity was constant across the peak eluting from the hydroxylapatite column (Figure 17).
3. The plot of r^2 vs concentration obtained from sedimentation equilibrium studies was linear (Figure 21).

3. Stability

Initial stability studies of the enzyme in crude extracts suggested that it was reasonably stable at 4°C (half-life=30 hr) and could be further stabilized by 20% glycerol (v/v) or more effectively by 20% ethylene glycol (v/v) (90% activity remaining after 60 hr). It was however destabilized by high salt concentrations (400 mM NaCl results in half-life=7 hr), divalent cations (half-life < 5 hr) or changes in pH (above pH 8.5 or below pH 6.0 half life < 8 hr). It was subsequently observed that there was significant loss of activity during column chromatography and that the presence of 10 μ M FAD in the buffers increased the yield of active enzyme. The purified enzyme that has

been concentrated to 4-10 mg/ml is quite stable at -70°C and even at 4°C . However, when the enzyme is diluted (0.2 mg/ml) and incubated at room temperature the loss of activity is significant (20% in 2 hours).

4. Quaternary Structure and Hydrodynamic Properties

The purified enzyme was shown to be a dimer of the 43,000 and the 62,000 molecular weight polypeptide subunits by chemical crosslinking studies and sedimentation equilibrium. Figure 18 shows the result of a crosslinking experiment with dimethylsuberimidate as the crosslinking agent. In this spectrophotometric trace of a Coomassie Blue-stained SDS-PAGE gel it is apparent that in addition to the individual subunits there is only one major crosslinked species whose molecular weight is approximately the sum of the two individual subunits. The profile is essentially the same when the concentration of protein in the crosslinking mixture is varied from 0.3 to 3.0 mg/ml.

Sedimentation equilibrium studies yielded a value of 93,500 for the molecular weight of the native enzyme (Table 15). The sedimentation coefficient ($S_{20,w}$) listed in Table 15 was determined from the sedimentation velocity experiment described in the methods chapter. The remaining hydrodynamic properties listed in Table 15 were calculated from experimentally determined values of molecular weight and sedimentation coefficient.

The value of $D_{20,w}$ was calculated from the experimentally determined values of $S_{20,w}$ and molecular

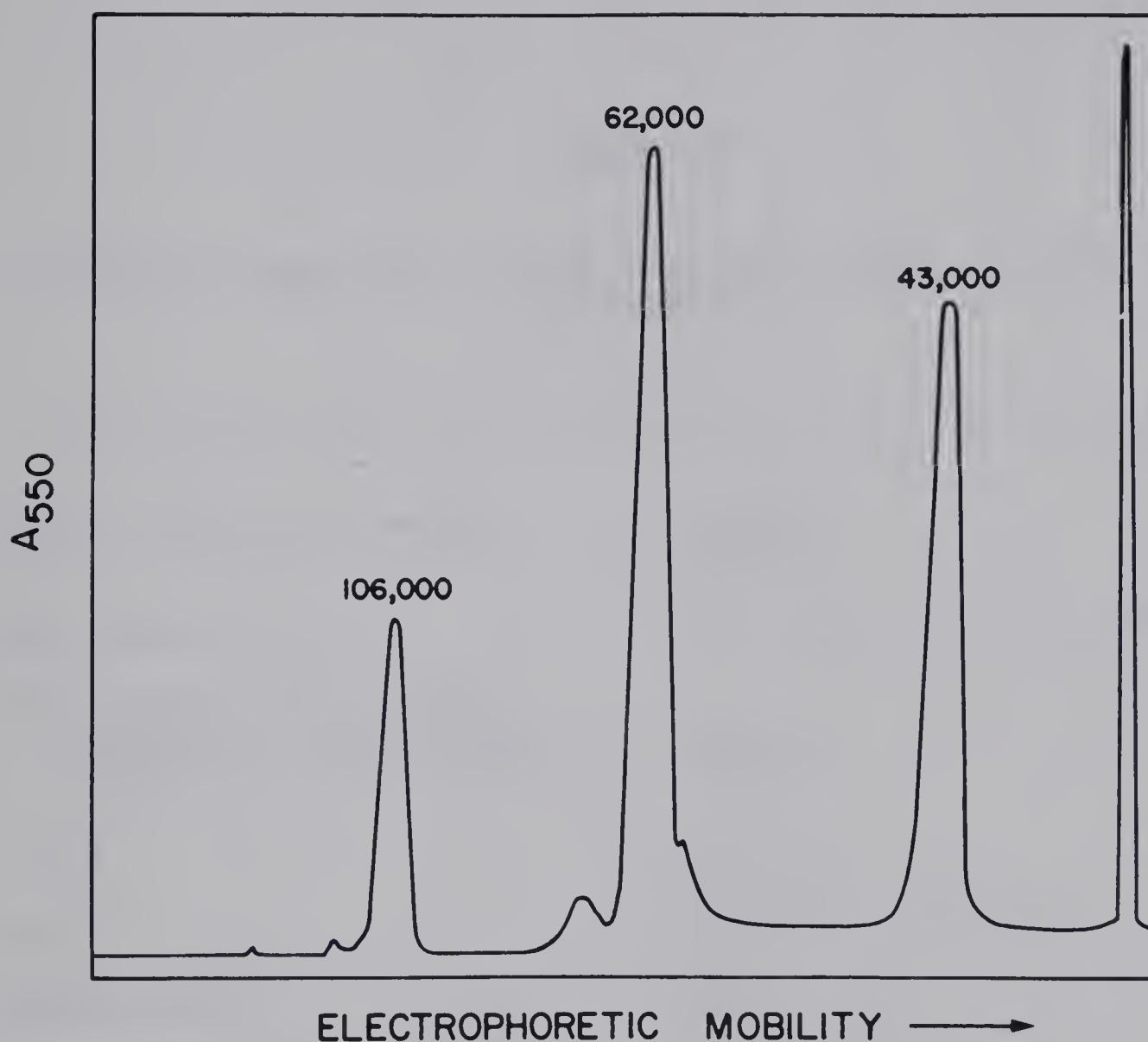


Figure 18. SDS-PAGE of Crosslinked Anaerobic Glycerol-3-phosphate Dehydrogenase. The profile is from a crosslinking reaction carried out as described in the methods chapter with 5 mg/ml dimethylsuberimide and 0.9 mg/ml enzyme. Molecular weights are based on parallel gel electrophoresis of standard proteins.

TABLE 15

Physical Properties of the Anaerobic Glycerol-3-Phosphate
Dehydrogenase

Subunit molecular weight	62,000 43,000
Quaternary Structure	1:1 molar ratio of subunits
Native Molecular Weight:	
Chemical Crosslinking	106,000
Sedimentation Equilibrium	93,500
$S_{20,w}$	5.16 S
$D_{20,w}^1$	5.0×10^{-7} cm ² /sec
Stokes radius ¹	43 Å
Frictional coefficient ¹	1.4

¹ Calculated from the experimentally determined values of $S_{20,w}$ and native molecular weight (from sedimentation equilibrium experiments) as described in the text.

weight using the equation (186):

$$D_{20,w} = RTS_{20,w}/M (1 - \bar{v}\rho)$$

where M is the molecular weight, R is the gas constant, T is the absolute temperature, ρ is the density of water at 20°C and a value for partial specific volume, \bar{v} , of 0.73 ml/g was assumed.

The value for Stokes Radius was calculated from the $D_{20,w}$ value determined above by using the equation (184):

$$a = kT/6\pi\eta D_{20,w}$$

where a is the Stokes Radius, k is the Boltzmann constant and η is the viscosity of water at 20°C.

The ratio, f/f_0 , was in turn calculated from the value of a by the equation (185):

$$f/f_0 = \frac{a}{\left(\frac{3M\bar{v}}{4\pi N} \right)^{1/3}}$$

where N is Avogadro's number and a value of 0.73 ml/g was assumed for partial specific volume.

The calculated values for the hydrodynamic properties listed in Table 15 are best considered as reasonable estimates since they were calculated from only two experimentally determined values rather than utilizing additional independently determined parameters such as Stokes Radius. However, the ratio f/f_0 is considerably greater than 1, indicating that the molecule is somewhat asymmetric in shape (equivalent to an axial ratio of 7 to 10 for a prolate ellipsoid) or that hydration of the molecule is unusual.

5. Circular Dichroism

Circular dichroism spectra were obtained of the purified enzyme in buffers containing ethylene glycol concentrations varying from 2% to 20%. It is evident in Figure 19 that changes in ethylene glycol result in small but significant changes in the secondary structure of the purified enzyme. The following discussion indicates how estimates of the percentage α -helix were obtained from circular dichroic spectra.

The mean residue ellipticity, $(\theta)_{\lambda}$, at a particular wavelength, λ , was calculated from the following equation (186):

$$(\theta)_{\lambda} = \theta_{\text{obs}} m / 100 l c$$

where:

1. m is the mean residue ellipticity (from amino acid analysis).
2. θ_{obs} is the measured ellipticity value at the wavelength, λ , of interest.
3. l is the light path in cm.
4. c is the protein concentration in g/ml.

The mean residue ellipticity can be expressed by the relationship (187):

$$(\theta)_{\lambda} = f_{\alpha}(\theta)_{\alpha} + f_{\beta}(\theta)_{\beta} + f_R(\theta)_R$$

where f_{α} , f_{β} and f_R represent the fractional values of α -helix, β -sheet and random coil structure in the protein and $(\theta)_{\alpha}$, $(\theta)_{\beta}$ and $(\theta)_R$ are the mean residue ellipticity contributions of the three types of secondary structure.

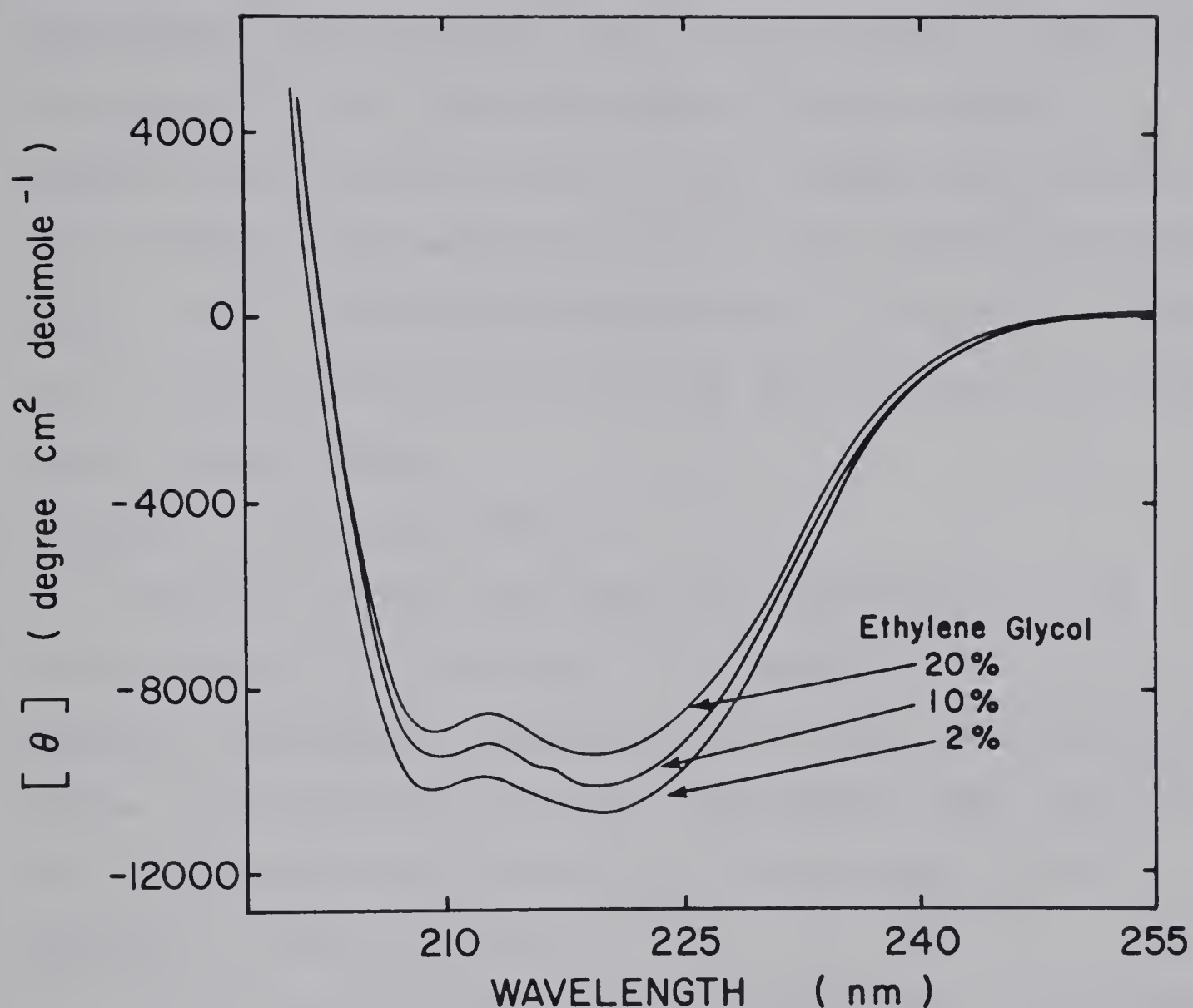


Figure 19. Circular Dichroism Spectra of the Anaerobic Glycerol-3-phosphate Dehydrogenase. Samples containing 1mg/ml enzyme in 50 mM potassium phosphate buffer, pH 7.5, with 2 to 20% ethylene glycol present were analyzed as described in the methods chapter.

Since the sum of f_{α} , f_{β} and f_R equals one it is possible to calculate f_{α} given values for $(\theta)_{\gamma}$ at two different wavelengths and values for $(\theta)_{\alpha}$, $(\theta)_{\beta}$ and $(\theta)_R$. Thus f_{α} was calculated for the three different ethylene glycol concentrations using values of mean residue ellipticity at 210 and 225 m μ and values for $(\theta)_{\alpha}$, $(\theta)_{\beta}$ and $(\theta)_R$ from Chen *et al.* (188). The values obtained were 32 (31.8), 33 (33.4) and 35 (34.9) per cent α -helix for 20%, 10%, and 2% ethylene glycol respectively.

6. Effect of Ethylene Glycol

Ethylene glycol was found to be necessary in the buffers during purification of the anaerobic glycerol-3-phosphate dehydrogenase in order to stabilize the enzyme. An explanation of this requirement came from a study of the sedimentation properties of the enzyme in the presence of ethylene glycol.

In the sedimentation velocity experiment illustrated in Figure 20 the two samples were treated identically except for the presence of 20% ethylene glycol in one sample. The boundary is relatively narrow and distinct in the sample containing ethylene glycol but is much broader in the sample without ethylene glycol. The plots of log concentration vs r^2 from sedimentation equilibrium are illustrated in Figure 21. The plot from the sample lacking ethylene glycol shows a considerable amount of curvature whereas the plot from the sample containing ethylene glycol is fairly linear. The molecular weight estimates obtained from the curve from the

Figure 20. Sedimentation Velocity Profile of Anaerobic Glycerol-3-phosphate Dehydrogenase. The sedimentation velocity experiments above were performed as described in the methods chapter. The two samples were transferred to separate cells in the same rotor and independently scanned at the indicated times. Zero time refers to the time at which the rotor has reached the running speed of the experiments.

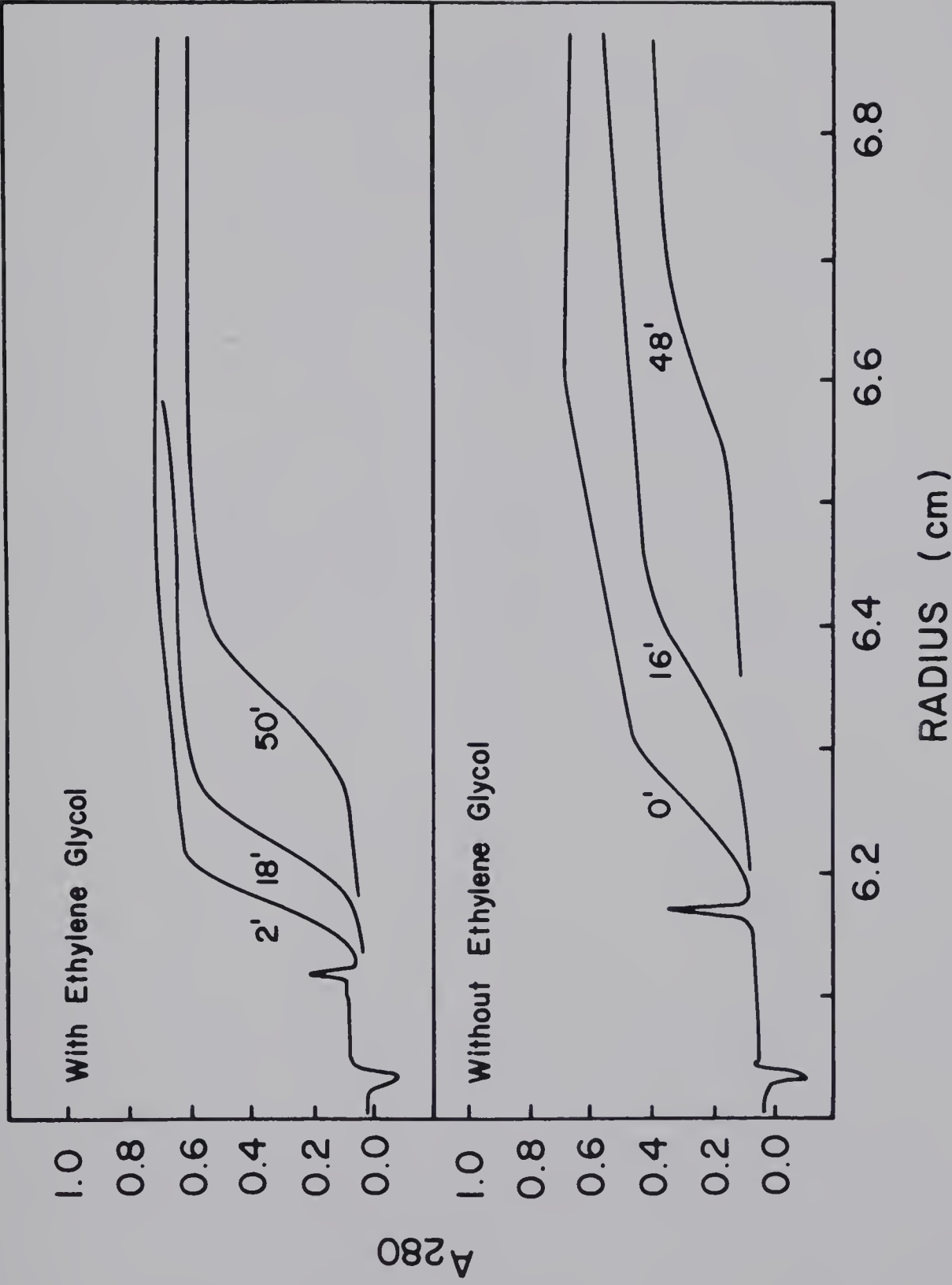
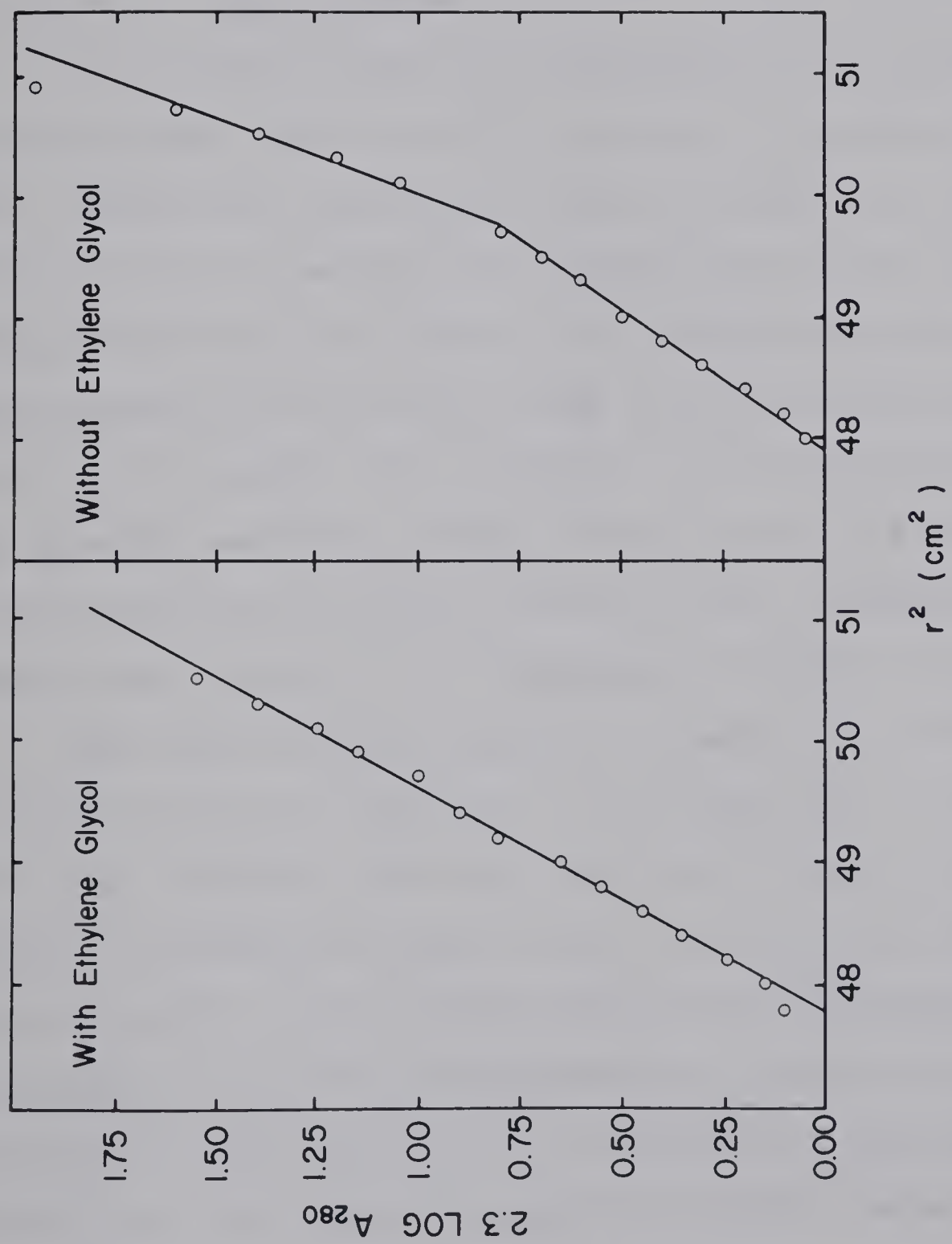


Figure 21. Sedimentation Equilibrium of Anaerobic Glycerol-3-phosphate Dehydrogenase. The sedimentation equilibrium experiments were performed as described in the methods chapter. The samples were scanned after 65 hours of centrifugation at 11,000 rpm.



sample lacking ethylene glycol suggest that dissociation rather than aggregation is occurring. For example, the slopes from the two arbitrarily-drawn lines in Figure 21 yield molecular weights of 59,000 and 107,000.

7. Cofactor Identification

The purified enzyme was subjected to gel filtration using Sephadex G-25 superfine to remove exogenous flavin and then assayed for endogenous flavin by measuring the trichloroacetic acid-soluble flavin fluorescence. The endogenous flavin was shown to be FAD by measuring the fluorescence as a function of pH (189) and quantitation relative to standard FAD solutions indicated that 1.04 mole was present per mole of dimer. When the gel filtration step was omitted and the buffer concentration of FAD merely subtracted, a value of 1.1 mole/mole of dimer was obtained.

When the purified enzyme was assayed for non-heme iron content a value of 1.6 moles of iron per mole of dimer was obtained. Since the non-heme iron assay is an extraction method I decided to compare this value to total iron determination by extraction and by total digestion methods. The values obtained by the extraction method were variable yielding an average value of 1.4 moles iron per mole of dimer. The total digestion method yielded a value of 1.9 moles iron per mole of enzyme. Assays for acid labile sulfur yielded a value of 1.04 moles of acid labile sulfur per mole of enzyme. I suspect that the iron is present in an iron-sulfur center (an Fe_2S_2 complex) for the reasons

discussed in the following section.

8. Optical Properties

The absorption spectrum of the enzyme (Figure 22) has maxima at 271 nm, 375 nm and 446 nm. The enzyme has an A_{271}/A_{260} ratio of 1.22, and A_{271}/A_{446} ratio of 7.0, an A_{446}/A_{375} ratio of 1.01 and a molar extinction coefficient at 271 nm of $136,000 \text{ cm}^{-1} \text{ M}^{-1}$.

The spectrum in the visible region has absorption maxima very near to those of free FAD but an equivalent amount of free FAD is not sufficient to account for the absorption spectrum in this region (57% and 46% of the 446 nm and the 375 nm maxima respectively). This indicates that either the absorption of the bound flavin is enhanced or another component is contributing to the spectrum in this region. An absorption spectrum of the enzyme with an equivalent amount of free FAD in the blank has the general appearance of an iron-sulfur spectrum (Figure 23) and has the amount of absorption expected for an Fe_2S_2 centre based on the average extinction coefficients of known iron-sulfur proteins (190). The absorption in this region was bleached upon addition of *p*-chloromercuriphenylsulfonic acid (Figure 23) which is a property observed in other iron-sulfur proteins (190).

Addition of substrate (sn-glycerol-3-phosphate) bleached the absorption spectrum in the visible region (Figure 24) indicating reduction of the FAD, whereas addition of β -glycerolphosphate had no effect. Under aerobic

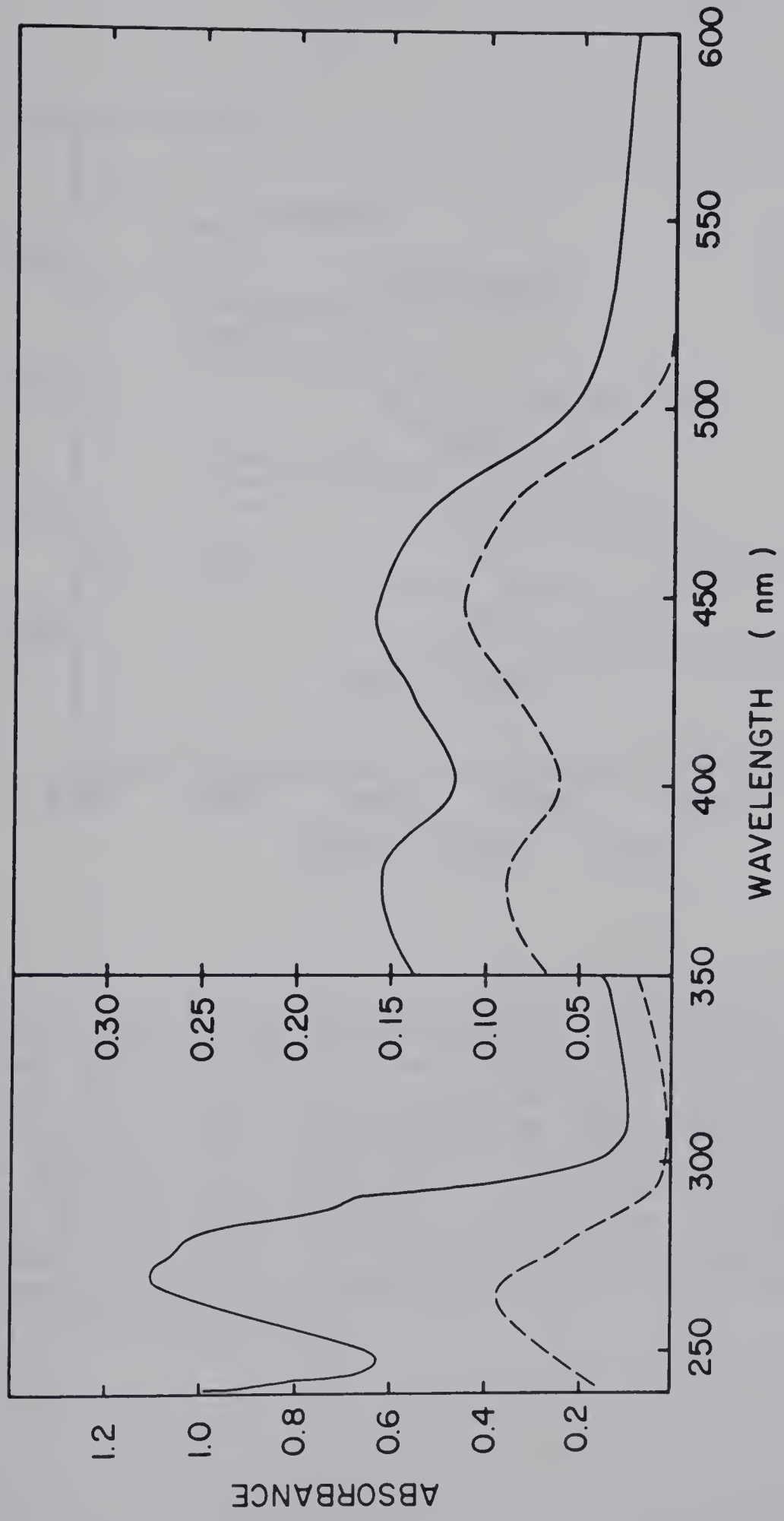


Figure 22. Absorption Spectrum of the Anaerobic Glycero1-3-phosphate Deydrogenase. 0.2 ml of purified enzyme (10 mg/ml) was applied to a 0.8x30 cm Sephadex G-25 Superfine column in order to remove exogenous flavin. The absorption spectrum of the pooled fractions (0.85 mg/ml) from 230 to 600 nm was recorded on a Varian Cary 219 spectrophotometer with elution buffer (100mM potassium phosphate, pH 7.5, 20% ethylene glycol) used as a blank (solid line). The spectrum of a 10 μ M solution of FAD is indicated by the dashed line.

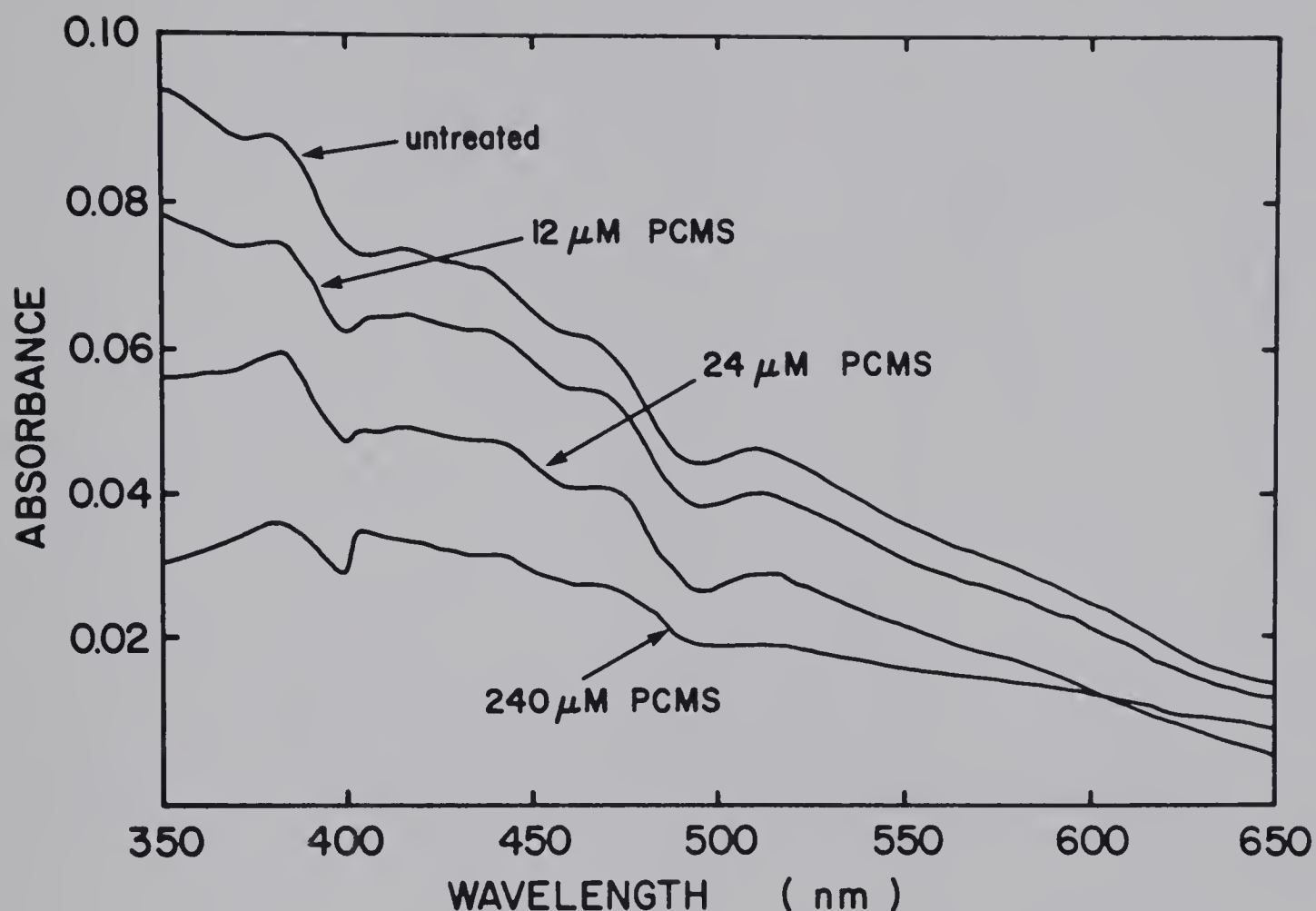
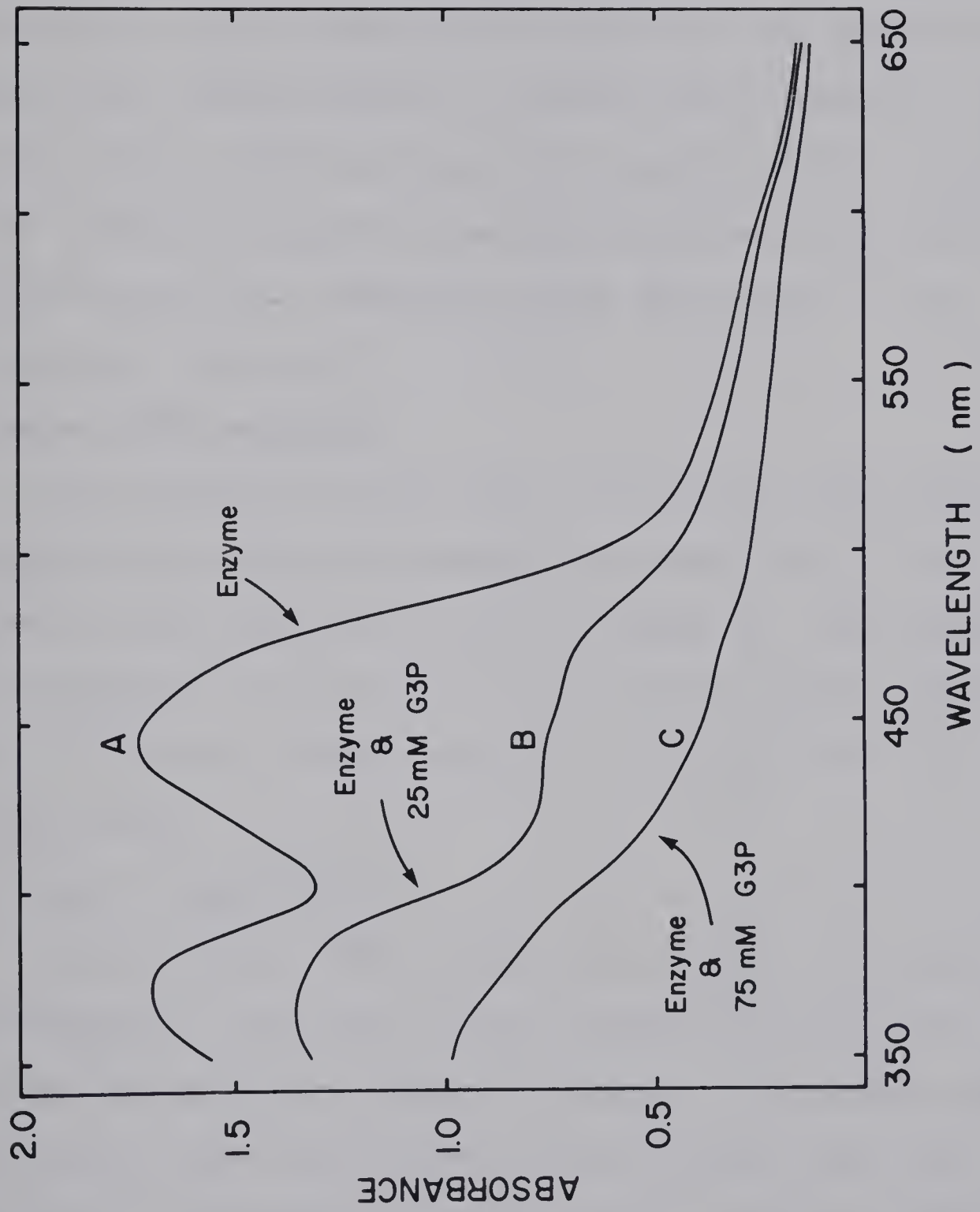


Figure 23. The Visible Absorption Spectrum of the Anaerobic Glycerol-3-phosphate Dehydrogenase. Exogenous flavin was removed as described in the methods chapter prior to spectral analysis. The absorption spectrum of a 0.97 mg/ml sample of anaerobic dehydrogenase was obtained before and after additions of 3mM PCMS to the indicated final concentrations. The absorption spectrum of an equivalent amount of free FAD was also recorded before and after treatment with PCMS. The recorded FAD spectra were then subtracted from the enzyme spectra and plotted on a Hewlett-Packard plotter.

Figure 24. Effect of Substrate on Absorption Spectrum of Anaerobic Glycerol-3-phosphate Dehydrogenase. The absorption of 0.8 ml of purified enzyme (10 mg/ml) was determined with a Varian Cary 219 Spectrophotometer before and after additions of aliquots of 2.85 M DL-glycerol-3-phosphate or β -glycerolphosphate (data not shown).



conditions this bleaching effect was only attained with relatively high concentrations of enzyme and substrate indicating that the flavin cofactor is readily auto-oxidizable. In fact, after performing the experiment (Figure 24) one can observe the color of the enzyme solution change from reddish-brown to golden-brown from top to bottom as the oxygen diffuses toward the bottom of the cuvette. After substrate-induced bleaching there was considerable visible absorption remaining which may be due to an iron-sulfur component.

9. Amino Acid Analysis

The purified subunits and the native enzyme were subjected to amino acid analysis as described in the methods chapter. The results are shown in Table 16. The proportion of hydrophobic amino acids in the native enzyme, the 62,000 subunit, and the 43,000 subunit is 45%, 43% and 47% respectively.

10. Kinetic Properties

The anaerobic G3PDH is usually assayed by measuring the G3P-dependent reduction of the tetrazolium dye, MTT, with the dye phenazine methosulfate present to transfer reducing equivalents from the enzyme to the terminal dye. As originally observed by Kistler and Lin (118), in this assay the presence of FAD or FMN stimulated the rate of the enzymatic reaction. The extent of stimulation that I observed by FAD was only 20% whereas for FMN it was approximately 6 fold. In general agreement with their

TABLE 16

Amino Acid Composition of Anaerobic Glycerol-3-Phosphate
Dehydrogenase

Amino Acid Residue	# of Residues/Subunit or Holoenzyme		
	43,000 subunit	62,000 subunit	Holoenzyme
glycine	33	41	70
alanine	34	53	84
valine	23	35	55
leucine	44	47	79
isoleucine	15	30	42
proline	23	20	46
phenylalanine	12	8	23
tryptophan	6	9	26
methionine	6	7	15
serine	19	23	37
threonine	15	32	50
cysteine, 1/2 cystine	5	10	18
tyrosine	2	7	12
aspartate, asparagine	25	44	65
glutamate, glutamine	44	52	90
lysine	8	13	24
arginine	19	43	60
histidine	8	13	21
Total molecular weight	42,888	62,016	104,818

earlier results (118), I found that the concentration of half maximal stimulation for FAD and FMN were very different; 200 nM for FAD and 130 μ M for FMN (Figure 25). Furthermore, I carried out experiments in which one flavin was present at a saturating concentration and the other was varied. I found that there was essentially no effect on the titration curve (Figure 26). When methylene blue replaced phenazine methosulfate, the stimulation by FAD was still observed but FMN no longer stimulated. Rather, it inhibited the enzymatic reaction (Figure 25). Interestingly, the half-maximal concentration for inhibition was 130 μ M, the same as the half-maximal concentration for stimulation of the phenazine methosulfate-coupled reaction.

In an earlier study with a partially purified preparation, Kistler and Lin (118) reported that the effect of substrate concentration on the rate of the enzymatic reaction was altered by the presence of exogenous FMN. In the absence of FMN the kinetics were simple Michaelis-Menten type whereas exogenous FMN resulted in the Lineweaver-Burk plot having two apparent linear portions. This was not observed in my studies with the purified enzyme. Figure 27 is a Lineweaver-Burk plot of data obtained from studies carried out in the presence or absence of exogenous FMN. In the presence of FMN there are no obvious deviations from a single linear relationship, even when the data is plotted on an Eadie-Hofstee plot (not shown). The data indicates that the maximal velocities in the presence and absence of FMN

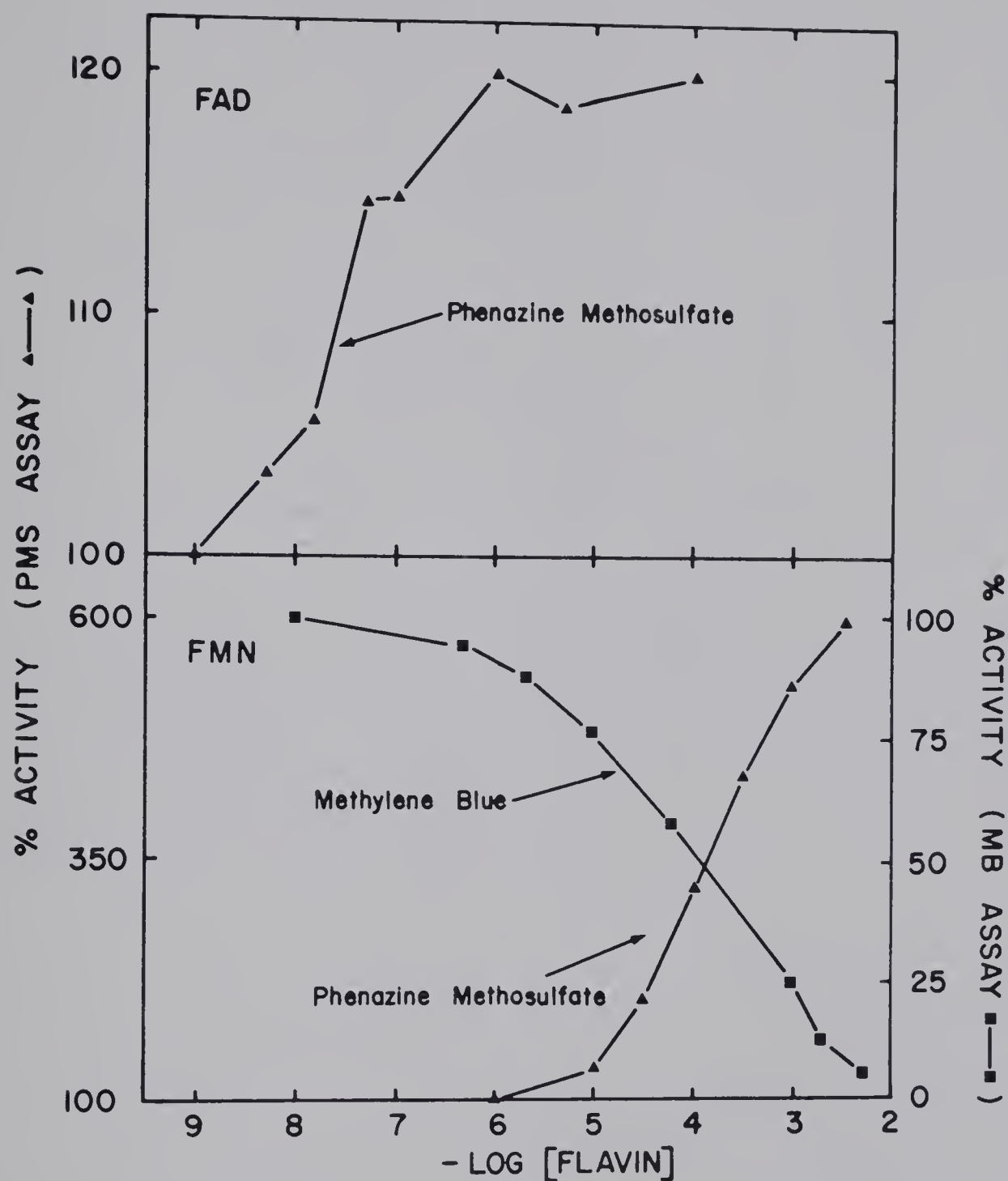
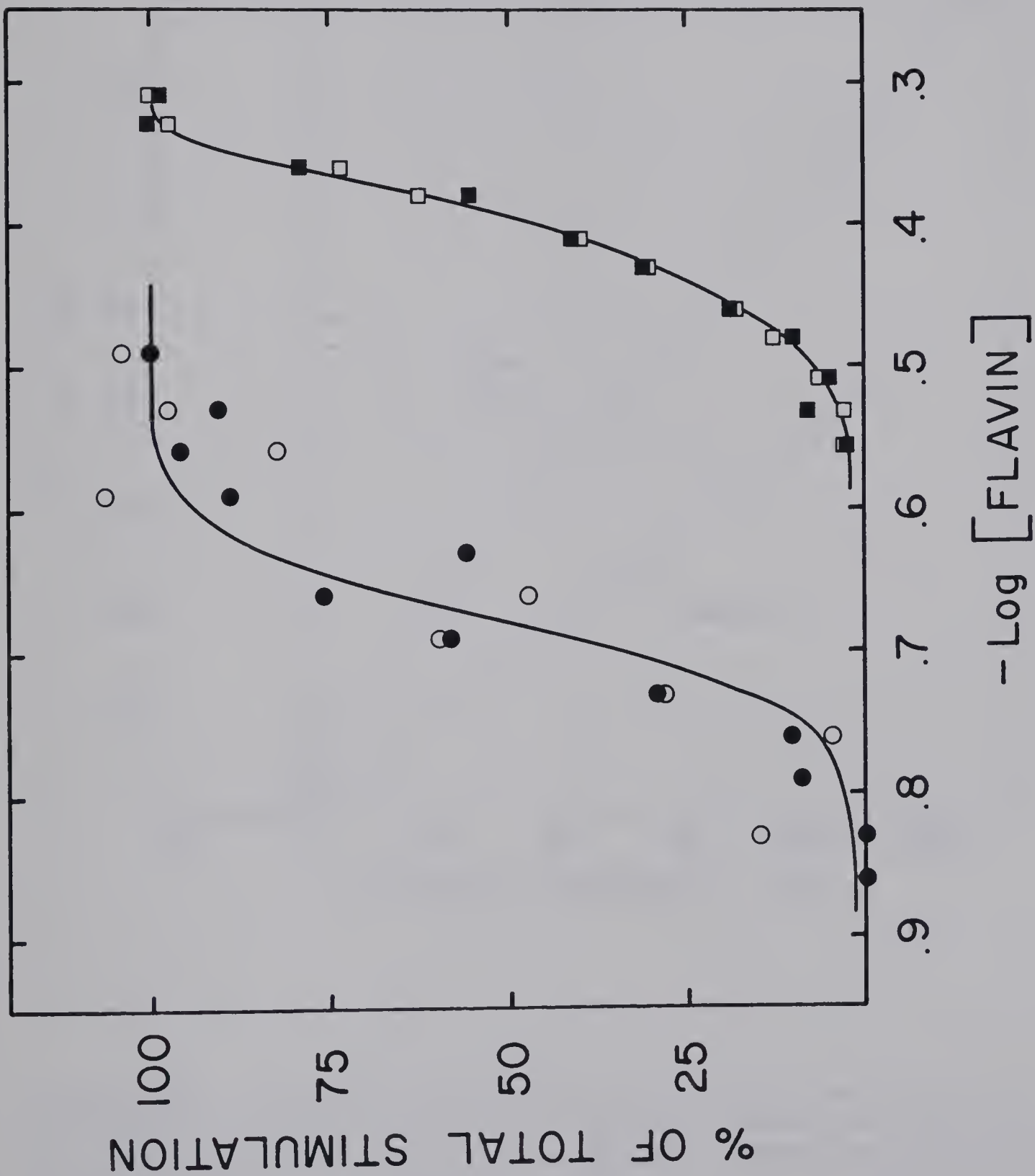


Figure 25. Effect of Exogenous Flavins on Anaerobic Glycerol-3-phosphate Dehydrogenase Activity. Enzymatic assays were performed as described in the methods chapter except that the exogenous flavin present in the assay mixture is as indicated in Figure 5. 100% activity is the activity obtained in the absence of exogenous flavins.



Figure 26. The Effect of Combinations of FAD and FMN on Enzymatic Activity. Enzymatic assay and removal of exogenous FAD prior to assay was performed as described in the methods chapter. Circles represent titration with FAD in the presence (open circles) or absence (closed circles) of 1mM FMN. Squares represent titration with FMN in the presence (open squares) or absence (closed squares) of 10 uM FAD.



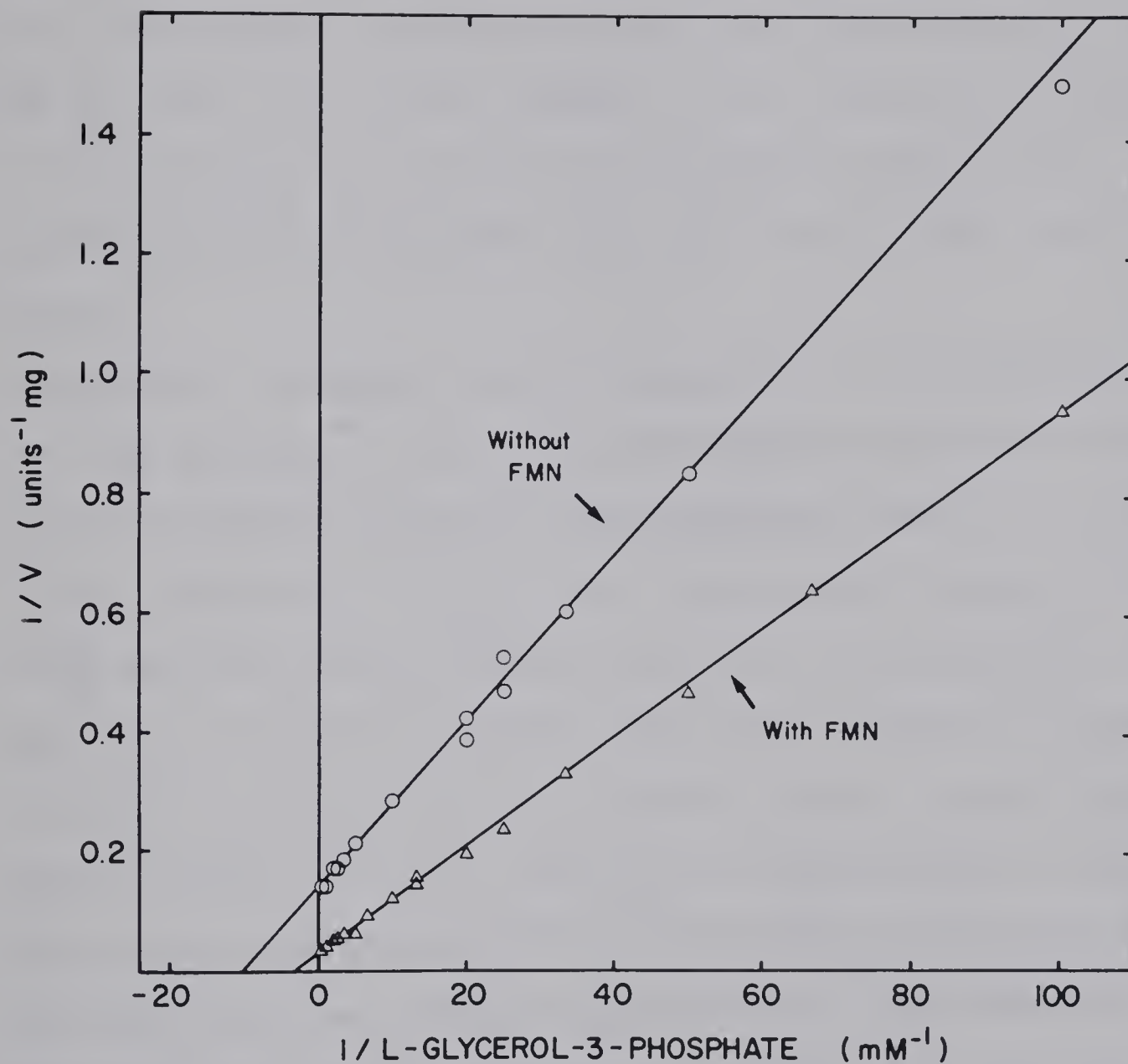


Figure 27. Lineweaver-Burk Plot of Initial Velocity of Anaerobic Glycerol-3-phosphate Dehydrogenase as a Function of Substrate Concentration. Enzymatic assays were performed as described in the methods chapter with 10 μM FAD present and with or without 1 mM FMN present.

are 34.4 ± 0.3 and 7.2 ± 0.1 units/mg respectively. The K_m for sn-glycerol-3-phosphate in the presence and absence of exogenous FMN is 0.34 ± 0.01 mM and 0.10 mM respectively. Thus the presence of FMN increases both the maximal velocity and the K_m . The turnover number in the presence of flavins is 2,000 molecules of glycerol-phosphate oxidized to dihydroxyacetone phosphate per molecule of enzyme per minute.

11. Electron Acceptors for the Anaerobic Dehydrogenase

The ability of the anaerobic dehydrogenase to reduce various electron acceptors was measured (Table 17) as part of the comparative studies with the aerobic enzyme. In this study anaerobic dehydrogenase activity was measured in the absence of exogenous flavins. As with the aerobic enzyme (Table 9) ferricyanide was directly reduced by the anaerobic enzyme but MTT was not. The aerobic dehydrogenase reduced DCPIP more effectively than the anaerobic enzyme. As also observed with the aerobic dehydrogenase, both PMS and methylene blue were efficient as intermediate electron acceptors.

The aerobic dehydrogenase showed maximal activity with ferricyanide as the direct electron acceptor, which was not increased by the addition of the intermediate electron-accepting dyes (Table 9). In contrast, the presence of PMS or methylene blue increased the rate of reduction of ferricyanide by the anaerobic dehydrogenase.

TABLE 17

Electron Acceptors for the Anaerobic Dehydrogenase

Electron Coupler	MTT	DCPIP	Ferricyanide
None	0.10	1.0	13.0
PMS	7.4	7.1	16.3
Methylene blue	3.2	1.8	19.4

Results are expressed as micromoles of reducing equivalent accepted per min per mg of protein. Assays were performed as described under Methods, except that MTT and PMS were replaced by the electron acceptor listed. The concentrations used were: MTT, 72.4 μ M; ferricyanide, 1 mM; DCPIP, 150 μ M; PMS, 600 μ M; methylene blue, 100 μ M. The reaction was followed in a Gilford model 250 spectrophotometer at 570 nm for MTT, 420 nm for ferricyanide, and 600 nm for DCPIP.

12. Effect of Detergent on Enzymatic Activity

When optimizing assay conditions for the anaerobic dehydrogenase I observed that Triton X-100 stimulated the rate of the PMS-coupled MTT reduction 2- to 3-fold. However, since the reduced form of MTT is somewhat insoluble in aqueous solutions, the detergent stimulation could be due to a direct effect on the enzyme turnover or to the enhanced solubility of the reduced MTT. In order to investigate this further the anaerobic enzyme was assayed using three different electron-accepting dyes in the presence or absence of 0.1% Triton X-100. The results from this study are listed in Table 18. It is evident that although Triton X-100 has the greatest effect on PMS-coupled MTT reduction, it also stimulates the rate of PMS-coupled DCPIP reduction and ferricyanide reduction. Since Triton X-100 would not affect the solubility of the reduced forms of these latter two dyes the detergent effect must be directly on the enzyme.

13. Effect of Dideazaflavins on Enzymatic Activity

The effect of exogenous flavins on enzymatic activity may be due to participation in the electron transfer reactions or they may act in some allosteric manner. These two possibilities might be distinguished by using flavin analogs with altered redox properties. Several riboflavin analogs, called deazariboflavins, have been synthesized in which one of the ring nitrogens involved in the electron transfer reactions is replaced by a carbon atom. The effect of this substitution is to prevent redox reactions involving

TABLE 18

Effect of Detergent on Anaerobic Dehydrogenase Activity

Electron Acceptor	Electron Coupler	Enzymatic Activity	
		minus Triton X-100	plus Triton X-100
MTT	PMS	2.9	7.4
DCPIP	PMS	4.4	7.1
Ferricyanide	None	9.7	13.0

Assays were performed essentially as described in Table 17 except that Triton X-100 was ommitted where indicated.

this ring position. Thus the 1,5-dideazariboflavin analog, which has both the ring nitrogens replaced, should be inert in typical flavin mediated redox reactions.

Dideazariboflavin was converted to dideazaFAD and dideazaFMN by the procedure of Spencer *et al.* (191) and the effect of these analogs on anaerobic dehydrogenase activity was determined. The results are listed in Table 19.

DideazaFMN inhibited the PMS-coupled reduction of MTT in approximately the same concentration range as FMN stimulated. This result is consistent with FMN acting as an intermediate electron acceptor. The effect of dideazaFAD on enzymatic activity seems to be similar to that of FAD. However, it appears that this stimulation is only observed at much higher concentrations with the dideazaFAD analog.

14. Inactivation Studies

The effect on enzymatic activity of preincubation with the sulfhydryl reagents PCMS and DTNB is summarized in Table 20. The results indicate that the activity assayed in the absence of exogenous flavins is relatively insensitive to this treatment, whereas the stimulation of activity by exogenous flavins is nearly eliminated. Incubation with the iron chelator, 1,10-phenanthroline, has no effect on either activity indicating that if iron is involved in the catalytic activity or in electron transfer to PMS, it must be tightly bound.

The titration of the enzyme with DTNB at the two concentrations was followed by measuring the release of

TABLE 19

Effect of Deazaflavin Analogs on Anaerobic
Dehydrogenase Activity

Concentration of Flavin	Exogenous Flavin Added	
	FMN	DideazaFMN
none	6.0	6.0
15 μ M	8.5	5.3
30 μ M	10.5	5.0
60 μ M	13.3	4.3
374 μ M	18.3	2.2
746 μ M	23.2	1.6
	FAD	DideazaFAD
5.8 nM	6.7	6.0
290.0 nM	7.1	6.2
1.1 μ M	7.4	6.1
2.9 μ M	7.5	6.3
5.8 μ M	7.3	6.6

Assays were performed as described in the methods chapter except that the indicated concentration of flavin was included in the assay mixture.

TABLE 20

Inactivation of the Anaerobic Glycerol-3-Phosphate
Dehydrogenase

Inhibitor	Concentration	% Activity Remaining'	
		Flavin- independent activity	Flavin- dependent activity
PCMS	25 μ M	80	6
DTNB	25 μ M	89	73
DTNB	1 mM	70	10
Orthophenanthroline	2 mM	97	97

'Reaction mixtures prepared as described in the methods chapter were incubated for 1 hour at 23°C and then assayed for enzymatic activity. Flavin-dependent activity refers to the activity assayed in the presence of 10 μ M FAD and 1 mM FMN.

thionitrobenzoic acid (163). Figure 28 shows the time course of the DTNB titration and Figure 29 shows the plot of residual activity versus number of SH- groups modified. There appears to be one very reactive sulfhydryl group in the enzyme which when modified results in a 25% loss in activity whether exogenous flavins are present in the assay mixture or not (Figure 28 and 29). Modification of up to 14 sulfhydryl groups in the enzyme does not result in a further decrease of the flavin-independent activity. When activity is measured in the presence of flavins, up to 3-4 additional sulfhydryl groups can be modified without reducing enzymatic activity further. However, modification of additional sulfhydryls results in a concomittant decrease of flavin-stimulated activity.

12. Proteolytic Studies

The large subunit of the anaerobic G3PDH was particularly susceptible to proteolytic cleavage by trypsin or chymotrypsin. When crude extracts from anaerobically grown recombinant plasmid-containing cells were subjected to limited proteolysis and analyzed on SDS-PAGE gels, we observed complete loss of the 62,000 molecular weight polypeptide band before any significant alteration of the remaining gel profile was observed (Figure 11). This preferential degradation of the large subunit by chymotrypsin could be carried out with the purified enzyme in the absence of ethylene glycol, resulting in a preparation of relatively intact small subunit (Figure 30,

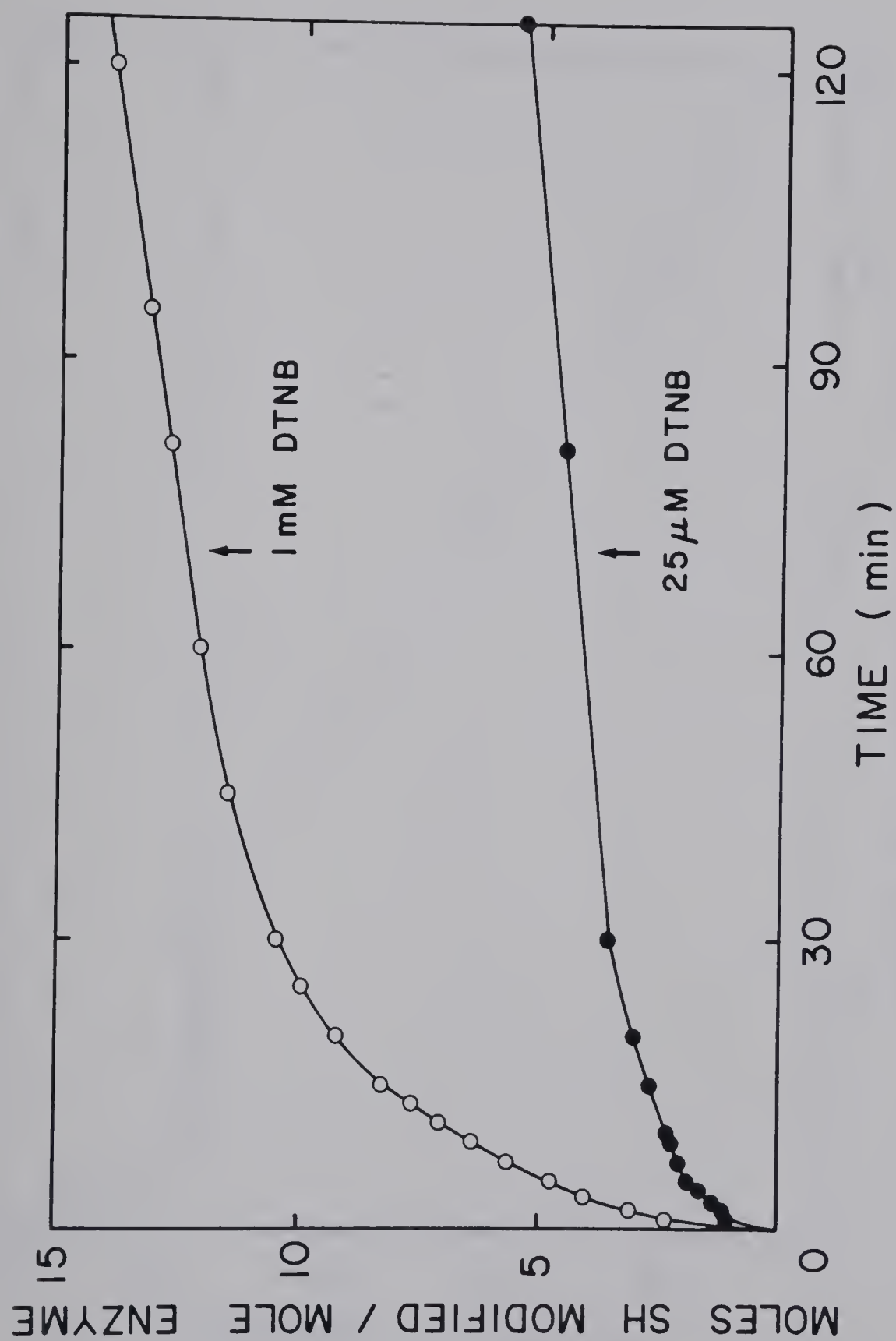


Figure 28. Time Course of DTNB Modification of Anaerobic Dehydrogenase. The number of sulphhydryls modified was determined as described in the methods chapter.

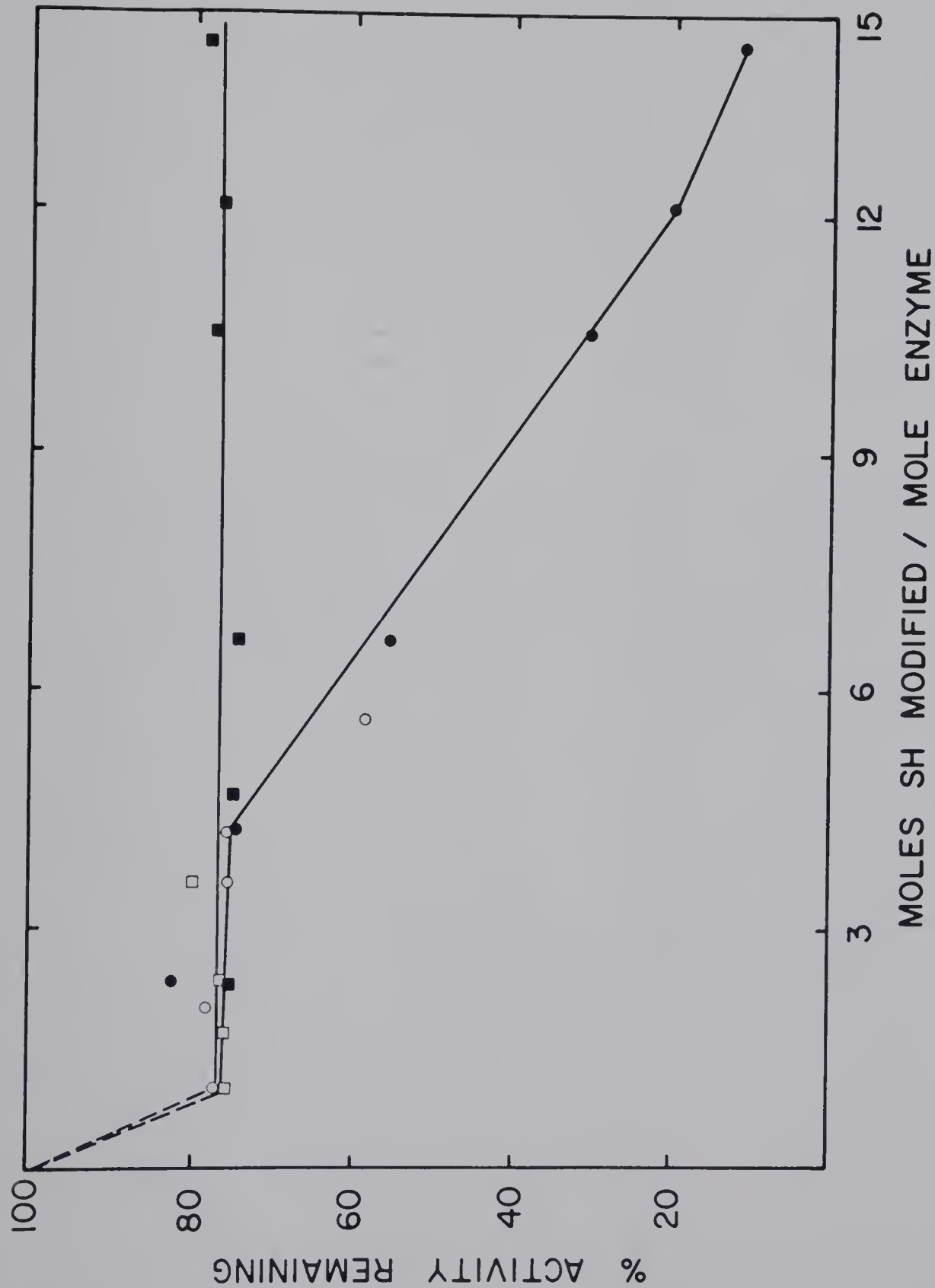
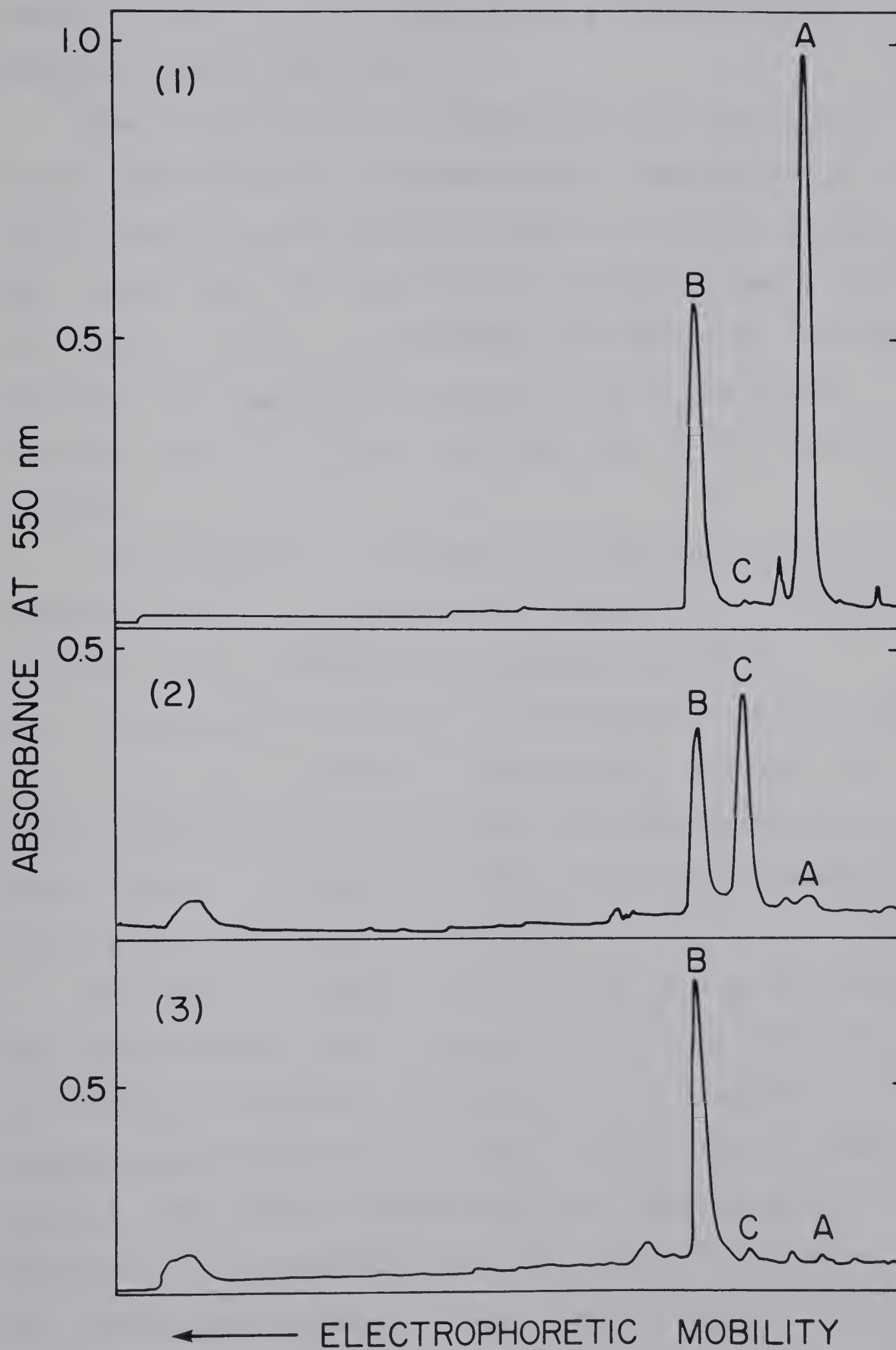


Figure 29.Correlation of Sulfhydryl Modification With Inactivation of Anaerobic Dehydrogenase. Determination of the number of sulfhydryls modified and of enzymatic activity is as described in the methods chapter. % activity remaining is relative to control enzyme solutions incubated for the same time period. Squares represent enzyme activity measured in the absence of exogenous flavins. Open and closed squares represent treatment with 25 uM and 1 mM DTNB respectively. Circles represent activity measured in the presence of exogenous flavins. Open and closed circles represent treatment with 25 uM and 1 mM DTNB respectively.

Figure 30. Products of Proteolysis of the Anaerobic Dehydrogenase. Proteolysis was carried out as described in the methods chapter except that the concentration of chymotrypsin was 1.8 ug/ml. Panel 1 is untreated enzyme. Panel 2 is enzyme in 20% ethylene glycol after 5 min of proteolysis. Panel 3 is enzyme in buffer lacking ethylene glycol after 40 min proteolysis.



Panel 3, Peak B) based on molecular weight. This small subunit preparation did not contain a flavin cofactor nor possess enzymatic activity.

When proteolysis with chymotrypsin was carried out in buffer containing 20% ethylene glycol, degradation of the large subunit was initially limited to a single cleavage event producing a 50,000 molecular weight fragment (Figure 30, Panel 2, Peak C), presumably still bound to the small subunit. This species of enzyme contained the flavin cofactor and retained activity but was not stimulated by flavins.

The progress of the proteolytic degradation in 20% ethylene glycol is illustrated in Figure 31. It is evident that the flavin-independent activity, but not the flavin-stimulated activity, is protected by ethylene glycol. With a 7.5-fold increase in chymotrypsin, the loss of flavin-independent activity with time was essentially the same, whereas the capacity to be stimulated by exogenous flavins was lost much more rapidly.

The amount of intact large subunit and of the 50,000 molecular weight fragment present at various times was estimated by measuring the profiles from Coomassie Blue-stained SDS-PAGE gels. The amount of intact large subunit (Peak A) correlated well with the amount of exogenous flavin-dependent activity remaining (Figure 31). The flavin-independent activity resulted from the intact large subunit and the 50,000 molecular weight fragment. This

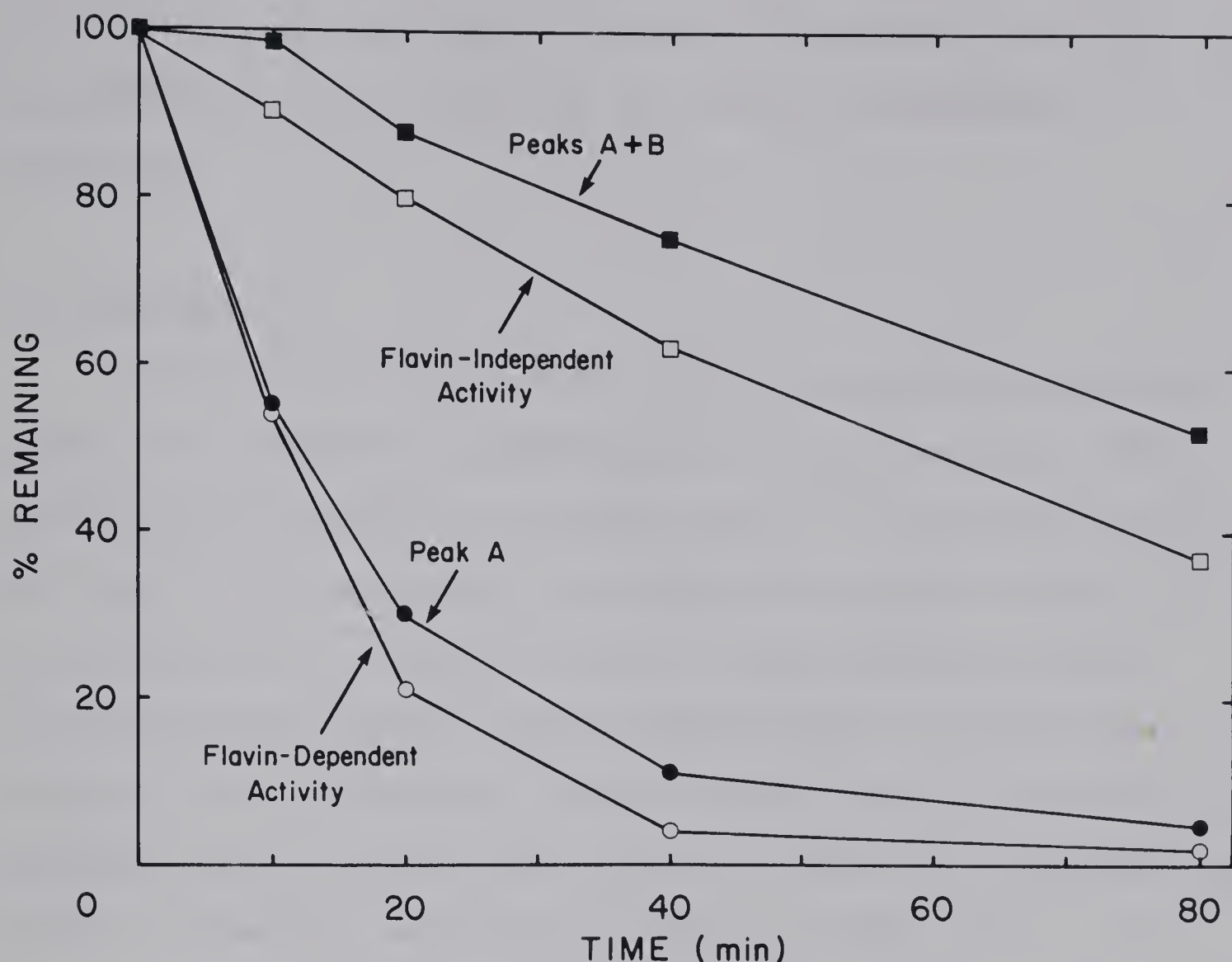


Figure 31. Effect of Proteolysis on Anaerobic Glycerol-3-phosphate Dehydrogenase. Proteolysis and enzymatic assays were performed as described in the methods chapter. Flavin-dependent activity (open circles) was determined by subtracting the flavin-independent activity (open squares) from the activity observed in the presence of 10 μM FAD and 1 mM FMN. The amount of the 62,000 and the 50,000 molecular weight polypeptides was estimated from measurements of the peaks in spectrophotometric scans of SDS-PAGE gels (Figure 30). The relationship: (height) \times (width at half-height) = 0.84 Area, was utilized in these calculations. Closed circles represent the amount of 62,000 molecular weight polypeptide remaining. Closed squares represent the amount of 62,000 plus 50,000 molecular weight species remaining. In these calculations it was assumed that the 50,000 molecular weight peak had 50/62 of the area of an equivalent peak of 62,000 molecular weight subunit.

is demonstrated in Figure 31 where the sum of these two polypeptides correlates with the flavin-independent activity.

C. Discussion

In an earlier study with partially purified anaerobic glycerol-3-phosphate dehydrogenase, Kistler and Lin (118) observed that addition of exogenous FAD and FMN stimulated the rate of the enzymatic reaction and suggested that the flavins acted at separate sites. I have shown that the stimulation by the two flavin nucleotides is independent (Figure 26). Furthermore, replacing the electron carrier phenazine methosulfate with methylene blue did not alter the effect of FAD but reversed the effect of FMN. The stimulatory and the inhibitory effect of FMN in the two assays was presumably due to the same FMN binding site since the concentration for half maximal stimulation was identical to the concentration for half maximal inhibition (Figure 25). It is interesting to note that limited proteolysis in the presence of ethylene glycol or treatment with sulfhydryl reagents can eliminate the effect of FMN yet not significantly alter flavin-independent activity. The fact that dideazaFMN inhibited the enzymatic reaction might be taken as evidence that exogenous FMN is involved in electron transfer reactions. However, the effect of dideazaFMN on the methylene blue-mediated assay and of 1-deazaFMN and 5-deazaFMN on both assays should be determined before any

conclusions can be drawn.

While the above results may be useful in ultimately determining the pathway of electron transfer in the anaerobic enzyme and the mechanism of FMN stimulation, they presently provide only clues on which to speculate.

Titration of enzymatic activity with substrate resulted in simple Michaelis-Menten kinetics whether or not exogenous FMN was present. This is in contrast to earlier results reported by Kistler and Lin (118) who observed two linear portions of a Lineweaver-Burk curve when FMN was present. The difference might be attributed to the fact their enzyme preparation was only partially purified. However, it should be noted that if one utilizes an assay mixture lacking enzyme as a blank rather than one lacking substrate, the activities at lower substrate concentration can be over-estimated and impart nonlinearity to Lineweaver-Burk plots.

When investigating the stabilizing effect of ethylene glycol on the anaerobic G3PDH we came to the conclusion that it was inhibiting subunit dissociation. In the sedimentation velocity experiments (Figure 20) the broadness and nonlinearity of the boundary in the sample lacking ethylene glycol was interpreted as dissociation of the dimer into subunits, thus generating heterogeneity in the sample. However, the relative sharpness of the boundary in the sample containing ethylene glycol may in part have been due to the effect of ethylene glycol on viscosity and diffusion

rates. This reservation was overcome by the fact that the curvature of the plots from the sedimentation equilibrium runs (Figure 21) was not a function of viscosity.

Estimations of molecular weight from the two linear portions of the curve from the sample lacking ethylene glycol yielded values of 59,000 and 107,000. This indicates that the curvature is probably due to dissociation and not aggregation.

It is interesting to speculate on the stabilizing effect of ethylene glycol during proteolysis. The initial cleavage event is probably due to a very susceptible region on the native enzyme (both trypsin and chymotrypsin are effective), and in the absence of ethylene glycol dissociation of the cleaved large subunit from the small subunit would allow it to be rapidly degraded. In the presence of ethylene glycol, the large subunit would remain associated with the small subunit and in this form be inert to further proteolysis. This interpretation is supported by the observation that increasing the protease concentration 7.5-fold does not increase the rate of loss of flavin-independent activity. Therefore, a protease-independent step is required to "sensitize" the enzyme to further proteolysis.

The results in this chapter indicate that the native enzyme contains 1 FAD and 2 non-heme irons per dimer. Furthermore, bleaching of the absorption spectrum by substrate indicated that the endogenous FAD was being

reduced by substrate. However, it will be difficult to unambiguously demonstrate the reduction of an iron-sulfur center by substrate using this approach. It will be necessary to perform electron spin resonance studies to determine the extent of involvement of the putative iron-sulfur center in the enzymatic reaction.

VI. Conclusions and Discussions

As an initial step towards the molecular characterization of the G3P-oxygen and G3P-fumarate electron transport pathways, the respective primary dehydrogenases were purified and characterized. The aerobic G3PDH is a dimer of two 58,000 molecular weight subunits, whereas the anaerobic enzyme is a dimer of polypeptides of 62,000 and 43,000 molecular weight. Both enzymes contain a non-covalently bound FAD cofactor that is reduced by addition of substrate, but the cofactor in the anaerobic enzyme is readily reoxidized by air while the cofactor in the aerobic enzyme is relatively inert to reoxidation. The anaerobic enzyme contains non-heme iron which may be in the form of an Fe_2S_2 center while no similar information on the aerobic enzyme is available. Interestingly, the aerobic enzyme was sensitive to incubation with the iron chelator, 1,10-phenanthroline, while the activity of the anaerobic enzyme was unaffected by this treatment. However, in the absence of information on the iron content of the aerobic enzyme, it is premature to speculate on the possible role of iron in enzymatic activity.

The aerobic G3PDH is an intrinsic membrane enzyme that requires detergents for solubilization (74,76,176). In contrast, the anaerobic dehydrogenase is an extrinsic membrane protein that is predominantly found in the cytoplasmic fraction from lysed cells (118,132). This feature may be largely responsible for the different effects

that amphipaths have on the enzymatic activity of these two enzymes. However, since amphipaths are not required for the ferricyanide reductase activity of the aerobic enzyme, the requirement for amphipaths in the PMS-MTT assay may be for generation of a PMS-binding site (182).

The aerobic glycerol-3-phosphate dehydrogenase can also be distinguished from the anaerobic enzyme by its insensitivity to exogenous flavins in the enzymatic assay. The anaerobic enzyme activity, in contrast, is stimulated 1.2-fold by exogenous FAD and 6-fold by exogenous FMN. The exogenous flavin stimulation is a much more labile property than basal enzyme activity as limited proteolysis or treatment with sulfhydryl reagents will eliminate it without affecting the flavin-independent enzyme activity. The physiological significance of the effect of FMN is questionable considering the non-physiological concentrations (100 μ M) at which it occurs. However, it may be a reflection of a physiological process involving a different effector molecule or the binding constants for FMN may be dramatically altered by other metabolites present *in vivo*.

During the course of my graduate studies I had the the additional objective of attempting to identify, purify, and characterize the cytoplasmic membrane carrier involved in active transport of glycerol-3-phosphate. However, although identification of the carrier was achieved, the purification and characterization of this component proved to be an

elusive goal. The success that Lo *et al.* (194) had achieved with the dicarboxylate transport system utilizing affinity chromatography convinced me to try a similar approach with the G3P system. A G3P analogue, 1-chloro-1--deoxyglycerol-3-phosphate, was synthesized according to the procedure of Fondy *et al.* (195) and, after demonstrating that it was an effective inhibitor of transport the ligand was coupled to Sepharose 4B with a 6 carbon linker (196,197,198). However, I was unable to obtain specific elution of the carrier from this column.

In an attempt to develop a reconstitution assay for the G3P carrier a variety of approaches were attempted. Crude membrane protein extracts were incorporated into synthetic phospholipid vesicles loaded with potassium (39,199,200) in an attempt to observe transient uptake of G3P upon addition of valinomycin. Alternatively, phospholipid vesicles were prepared with crude membrane protein extracts (201) and restoration of G3P transport in membrane vesicles prepared from a *glpT* mutant was attempted by fusing with the synthetic vesicles. Neither of these approaches was successful.

Despite the lack of success I obtained with the G3P carrier, I do not feel that its isolation, purification and characterization is an impossible goal. A recently developed reconstitution system for the lactose carrier based upon exchange diffusion (202) appears quite promising and has been successful with several other transport systems (203,

M.J. Newman, personal communication). Furthermore, the restriction analysis of the *glpT*-*glpA* region should facilitate the transfer of the *glpT* gene to vectors that could further amplify the levels of the *glpT* products (204). Since amplification of the intrinsic membrane enzyme, fumarate reductase, can result in it constituting greater than 50% of the total cytoplasmic membrane protein (205), it may be possible to achieve fairly extensive amplification of the levels of the G3P carrier. Taken together, the potential for greatly amplifying the levels of the carrier and the newly developed reconstitution system should considerably increase the chances of success.

Most of the primary dehydrogenases involved in electron transport reactions in *E. coli* are intrinsic membrane proteins that require detergents for solubilization. Their strong association with the membrane is logical when one considers that the components of the electron transport chain with which they interact are also tightly associated with the membrane. The anaerobic G3PDH is unusual in that it is found predominantly in the cytoplasmic fraction from lysed cells yet must interact with the membrane *in vivo*. This property is also observed with pyruvate dehydrogenase but the association with the inner aspect of the cytoplasmic membrane has been demonstrated in membrane vesicles by observing the effect of antibody and thiamin pyrophosphate analogues on enzyme activity (59,192).

It is interesting to compare the properties of pyruvate dehydrogenase and anaerobic G3PDH in light of the similarities mentioned above. Pyruvate dehydrogenase activity is dramatically stimulated by detergents (60) and has been shown to have lipid binding domains that are susceptible to proteolytic cleavage in the absence of lipids (63). The anaerobic dehydrogenase activity, on the other hand, is only slightly stimulated by detergents (Table 18) but probably has hydrophobic regions since it binds more tightly to hydrophobic resins than the bulk of the cytoplasmic proteins (Figure 16).

The presence of pyruvate dehydrogenase and anaerobic G3PDH in the cytoplasmic fraction from lysed cells could be due to the conditions of preparation of the crude lysates. It is possible that the conditions of lysis result in a decreased level of some metabolite or ion that facilitates binding of the enzyme to the membrane. Alternatively, lysis may result in activation of a protease that releases the enzymes from the membrane as has been demonstrated in other systems (193), although no variations in the molecular weight of either subunit is observed. Another interesting possibility is that binding of enzyme to the membrane is dependent upon the redox state of the enzyme. In this respect it is interesting to note that proteolysis of pyruvate dehydrogenase is drastically affected by the redox state of the flavin cofactor (62). The above considerations suggest that studies involving changes in conditions of

preparation of membrane vesicles or during reconstitution studies with the purified anaerobic G3PDH may prove to be quite informative. Thus by varying ionic conditions, metabolites present, electron transport inhibitors or other parameters one could determine whether any conditions result in an increased association with the membrane.

Our ability to reconstitute the detergent-depleted aerobic G3PDH with membrane vesicles prepared from a *glpD* mutant is an interesting result. The aerobic dehydrogenase was added to the external surface of the membrane while it interacts with the cytoplasmic surface *in vivo* (133). Thus, either it is interacting with a different electron acceptor than *in vivo* or the physiological electron acceptor (ubiquinone-8) can act at either surface of the membrane. This type of reconstitution has also been observed with lactate dehydrogenase (181,206).

Reconstitution studies with the purified aerobic dehydrogenase and anaerobic dehydrogenase may be a useful approach to study the specificity of interactions required to achieve electron transport reactions which generate a protonmotive force. The availability of mutants in *glpA*, *glpD* or in both loci would facilitate reconstitution studies with native membrane vesicles or with inverted vesicle preparations. A systematic study assaying for the redox activities (207), for uptake of transportable substrates dependent upon the redox activities (109), for ATP synthesis dependant upon the redox activities (111), and for

generation of a pH-gradient (208) in the reconstituted systems could be used as a measure of the capability of the two enzymes to interact with the electron transport complexes present. This work could be extended in the glycerol-fumarate system to attempted reconstitution from the purified components, since presently both the primary dehydrogenase and the terminal reductase are available in reasonable quantity in a homogeneous preparation.

References

1. Slater, E.C. 1953. *Nature* 172:975-978.
2. Lipmann, F. 1946. *Currents in Biochemical Research* (D.E. Green, ed.) pp 137-148. New York; Interscience.
3. Boyer, P.D. 1965 in *Oxidases and Related Redox Systems*. (T.E. King, H.S. Mason, M. Morrison, ed.) 2:994-1008, Wiley, New York.
4. Mitchell, P. 1961. *Nature* 191:144-148
5. Mitchell, P. 1977. *Ann. Rev. Biochem.* 46:996-1005.
6. Mitchell, P. 1966. *Biol. Rev.* 41:445-502
7. Mitchell, P. and Moyle, J. 1965. *Nature* 208:1205-1206
8. Neumann, J. and Jagendorf, J.T. 1964. *Arch. Biochem. Biophys.* 107:109-119
9. Mitchell, P. 1967. *Fed. Proc.* 26:1370-1379.
10. Mitchell, P. and Moyle, J. 1967. *Biochem. J.* 105:1147-1162.
11. Mitchell, P. and Moyle, J. 1965. *Nature* 208:147-151
12. Leung, K.H. and Hinkle, P.C. 1975. *J. Biol. Chem.* 250:8467-8471.
13. Ernster, L. 1977. *Ann. Rev. Biochem.* 46:981-995.
14. Harold, F.M. 1977. *Curr. Top. Bioenerg.* 6 : 83-149
15. Kanner, B.I. and Racker, E. 1975. *Biochem. Biophys. Res. Comm.* 64:1054-1061.
16. Jagendorf, A.T. and Uribe, E. 1966. *Proc. Natl. Acad. Sci. USA* 55:170-177.
17. Reid, R.A., Moyle, J. and Mitchell, P. 1966. *Nature* 212:257-258.
18. Maloney, P.C. and Wilson, T.H. 1975. *J. Membr. Biol.* 25:285-310.
19. Thayer, W.S. and Hinkle, P.C. 1975. *J. Biol. Chem.* 250:5336-5342.
20. Amann, H., Motojima, K., Yamaguchi, A. and Anraku, Y. 1977. *Biochem. Biophys. Res. Comm.* 74:366-373.
21. Hirata, H., Sone, N., Yoshida, M. and Kagawa, Y. 1976. *Biochem. Biophys. Res. Comm.* 69:665-671.
22. Harold, F.M. 1972. *Bact. Rev.* 36:172-230
23. Hamilton, W.A. 1975. *Adv. Microb. Physiology* 12:1-53
24. Hopfer, U., Lehninger, A.L. and Lenauz, W.J. 1970. *J. Membr. Biol.* 3:142-155.
25. Liberman, E.A. and Topaly, V.P. 1968. *Biochim. Biophys. Acta* 163:125-136.
26. Racker, E. and Stoeckenius, W. 1974. *J. Biol. Chem.* 249:662-663.
27. Chance, B. 1977. *Ann. Rev. Bioch.* 46:967-980.
28. Racker, E. 1977. *Ann. Rev. Biochem.* 46:1006-1014.
29. Slater, E.C. 1977. *Ann. Rev. Bioch.* 46:1015-1026.
30. Brand, M.D., Reynafarje, B. and Lehninger, A.L. 1976. *Proc. Natl. Acad. Sci. USA* 73:437-441.
31. Alexandre, A., Reynafarje, B. and Lehninger, A.L. 1978. *Proc. Natl. Acad. Sci. USA* 75:5296-5300.
32. Alexandre, A., Galianzo, F. and Lehninger, A.L. 1980 *J. Biol. Chem.* 255:10721-10730.
33. Garland, P.B. and Jones, R.W. 1977. In *Structure and*

- Function of Energy-Transducing Membranes* (Van Dam, K. and Van Gelder, B.F., ed.) pp 117-126. Elsevier, Amsterdam.
34. Boyer, P.D. 1975. *FEBS Letters* 58:1-6.
 35. Papa, S. 1976. *Biochim. Biophys. Acta* 456:39-84.
 36. Lehninger, A.L., Reynafarje, B. and Alexandre, A. 1977. In *Structure and Function of Energy-Transducing Membranes* (Van Dam, K. and Van Gelder, B.F., ed.) pp 95-116. Elsevier, Amsterdam.
 37. Bragg, P.D. 1979. In *Membrane Proteins in Energy Transduction Vol. 2* pp 341-449. Marcel Dekker Inc. New York.
 38. Gutman, M. Schejter, A. and Avi-Dor, Y. 1968. *Biochim. Biophys. Acta* 162:506-517
 39. Bragg, P.D. and Hou, C. 1967. *Arch. Biochem. Biophys.* 119:202-208
 40. Kashket, E.R. and Brodie, A.F. 1963. *J. Biol. Chem.* 238:2564-2570
 41. Dancey, G. F., Levine, A.E. and Shapiro, B.M. 1976. *J. Biol. Chem.* 251:5911-5920.
 42. Thomson, J.W. and Shapiro, B.M. 1981. *J. Biol. Chem.* 256:3077-3084.
 43. Dancey, G.F., and Shapiro, B.M. 1976. *J. Biol. Chem.* 251:5921-5928.
 44. Silhavy, T.J., Hartig-Beeckman, I. and Boos, W. 1976. *J. Bacteriol.* 126:951-958.
 45. Young, I.G., Jaworowski, A. and Poulis, M.I. 1978. *Gene* 4:25-36.
 46. Young, I.G., Rogers, B.L., Campbell, H.D., Jaworowski, A. and Shaw, D.C. 1981. *Eur. J. Biochem.* 116:165-170.
 47. Kohn, L.D. and Kaback, H.R. 1973. *J. Biol. Chem.* 248:7012-7017.
 48. Futai, M. 1973. *Biochemistry* 12:2468-2474.
 49. Pratt, E.A., Fung, L.W.-M., Flowers, J.A. and Ho, C. 1979. *Biochemistry* 18:312-316.
 50. Tanaka, Y., Anraku, Y. and Futai, M. 1976. *J. Biochem.* 80:821-830.
 51. Fung, L.W.-M., Pratt, E.A. and Ho, C. 1979. *Biochemistry* 18:317-324.
 52. Futai, M. and Kimura, H. 1977. *J. Biol. Chem.* 252:5820-5827.
 53. Kimura, H. and Futai, M. 1978. *J. Biol. Chem.* 253:1095-1100.
 54. Williams, F.R. and Hager, L.M. 1961. *J. Biol. Chem.* 236:PC36-PC37.
 55. Williams, F.R. and Hager, L.P. 1966. *Arch. Bioch. Biophys.* 116:168-176.
 56. Raj, T., Russel, P., Flygare, W.H. and Gennis, R.B. 1977. *Biochim. Biophys. Acta* 481:42-49.
 57. O'Brien, T.A., Blake, R., II, and Gennis, R.B. 1977. *Biochemistry* 16:3105-3109.
 58. O'Brien, T.A. and Gennis, R.B. 1980. *J. Biol. Chem.* 255:3302-3307.
 59. Shaw-Goldstein, L.A., Gennis, R.B. and Walsh, C. 1978.

- Biochemistry* 17:5605-5613.
60. Blake, R., II, Hager, L.P. and Gennis, R.B. 1978. *J. Biol. Chem.* 253:1963-1971.
 61. Stevens, D.J. and Gennis, R.B. 1980. *J. Biol. Chem.* 255:379-383.
 62. Russel, P., Hager, L.P. and Gennis, R.B. 1977. *J. Biol. Chem.* :252:7877-7882.
 63. Russel, P., Schrock, H.L. and Gennis, R.B. 1977. *J. Biol. Chem.* 252:7883-7887.
 64. Kim, I.C. and Bragg, P.D. 1971. *Can. J. Biochem.* 49:1098-1104.
 65. Kasahara, M. and Anraku, Y. 1974. *J. Biochem.* 76:959-966.
 66. Spencer, M.E. and Guest, J.R. *J. Bacteriol.* 117:947-953.
 67. Davis, K.A. and Hatefi, Y. 1971. *Biochemistry* 10:2509-2516.
 68. Davis, K.A., Hatefi, Y., Crawford, I.P. and Baltscheffsky, H. 1977. *Arch. Bioch. Biophys.* 180:459-469.
 69. Weiss, H. and Kolb, H.J. 1979. *Eur. J. Bioch.* 99:139-149.
 70. Hederstedt, L., Holmgren, E., and Rutberg, C. 1978. *J. Bacteriol.* 138:370-376.
 71. Kroger, A. 1978. *Biochim. Biophys. Acta* 505:129-145.
 72. Dickie, P. and Weiner, J.H. 1979. *Can. J. Biochem.* 57:813-821.
 73. Singer, T.P., Kearney, E.B. and Kenney, W.C. 1973. *Advances in Enzymol.* 37:189-272
 74. Kistler, W.S., Hirsch, C.A., Cozzarelli, N.R. and Lin, E.C.C. 1969. *J. Bacteriol.* 100:1133-1135.
 75. Kistler, W.S. and Lin, E.C.C. 1971. *J. Bacteriol.* 108:1223-1234.
 76. Weiner, J.H. and Heppel, L.A. 1972. *Biochem. Biophys. Res. Comm.* 47:1360-1365.
 77. Haddock, B.A., Downie, J.A. and Garland, P.G. 1976. *Biochem. J.* 154:285-294.
 78. Haddock, B.A. and Jones, C.W. 1977. *Bact. Rev.* 41:47-99.
 79. Bragg, P.D. 1974. In *Microbial Iron Metabolism*. (J.B. Neilands, ed.) p.303. Academic, New York.
 80. Downie, J.A. and Cox, G.B. 1978. *J. Bacteriol.* 133:477-484.
 81. Lawford, H.G. and Haddock, B.A. 1973. *Biochem. J.* 136:217-220.
 82. Gould, J.M. and Cramer, W.A. 1977. *J. Biol. Chem.* 252:5875-5882.
 83. Garland, P.B., Downie, J.A. and Haddock, B.A. 1975. *Biochem. J.* 152:547-559.
 84. Cox, J.C. and Haddock, B.A. 1978. *Biochem. Biophys. Res. Comm.* 82:46-52.
 85. Singh, A.P. and Bragg, P.D. 1976. *Biochem. Biophys. Res. Comm.* 72:195-201.
 86. Garland, P.B. 1977. In *Microbial Energetics* (Haddock,

- B.A. and Hamilton, W.A., eds.) pp.1-21. Cambridge Univ. Press, Cambridge.
87. Lawford, H.G. 1979. *Can. J. Biochem.* 57:172-177.
 88. Thauer, R.K., Jungermann, K. and Decker, K. 1977. *Bacteriol. Rev.* 41:100-180.
 89. Cole, J.A. and Wimpenny, J.W.T. 1968. *Biochim. Biophys. Acta* 162:39-48.
 90. Kistler, W.S. and Lin, E.C.C. 1971. *J. Bacteriol.* 108:1224-1234.
 91. Ruiz-Herrera, J., Showe, M.K. and DeMoss, J.A. 1969. *J. Bacteriol.* 97:1291-1297.
 92. Itagaki, E., Fujita, T. and Sato, R. 1962. *J. Biochem. (Tokyo)* 52:131-141.
 93. Enoch, H.G. and Lester, R.L. 1975. *J. Biol. Chem.* 250:6693-6705.
 94. MacGregor, C.H. 1976. *J. Bacteriol.* 126:122-131.
 95. Clegg, R.A. 1976. *Biochem. J.* 153:533-541.
 96. Forget, P. 1974. *Eur. J. Biochem.* 42:325-332.
 97. Lund, K. and DeMoss, J.A. 1976. *J. Biol. Chem.* 251:2207-2216.
 98. Ruiz-Herrera, J. and DeMoss, J.A. 1969. *J. Bacteriol.* 99:720-729.
 99. Enoch, H.G. and Lester, R.L. 1974. *Biochem. Biophys. Res. Comm.* 61:1234-1241.
 100. Dickie, P. and Weiner, J.H. 1979. *Can. J. Biochem.* 57:813-821.
 101. Singer, T.P., Kearney, E.B. and Kearney, W.C. 1973. *Adv. Enzymology* 37:189-272.
 102. Weiner, J.H. and Dickie, P. 1979. *J. Biol. Chem.* 254:8590-8593.
 103. Cole, S.T. 1981. Personal communication.
 104. Robinson, J.J. and Weiner, J.H. 1981. *Biochem. J.* In press.
 105. Newton, N.A., Cox, G.B. and Gibson, F. 1971. *Biochim. Biophys. Acta* 244:155-166.
 106. Singh, A.P. and Bragg, P.D. 1975. *Biochim. Biophys. Acta* 396:229-241.
 107. Singh, A.P. and Bragg, P.D. 1976. *Biochim. Biophys. Acta* 423:450-461.
 108. Konings, W.N. and Kaback, H.R. 1973. *Proc. Natl. Acad. Sci. USA* 70:3376-3381.
 109. Boonstra, J., Huttenen, M.T., Konings, W.N. and Kaback, H.R. 1975. *J. Biol. Chem.* 250:6792-6798.
 110. Boonstra, J., Sips, H.J. and Konings, W.N. 1976. *Eur. J. Biochem.* 69:35-44.
 111. Miki, K. and Lin, E.C.C. 1975. *J. Bacteriol.* 124:1282-1287.
 112. Lin, E.C.C. 1976. *Ann. Rev. Microb.* 30:535-578.
 113. Sanno, Y., Wilson, T.H. and Lin, E.C.C. 1968. *Biochem. Biophys. Res. Comm.* 32:344-349.
 114. Thorner, J.W. and Paulus, H. 1971. *J. Biol. Chem.* 246:3885-3894.
 115. Zwaig, N., Kistler, W.S. and Lin, E.C.C. 1970. *J. Bacteriol.* 102:753-759.

116. Hayashi, S., Koch, J.P. and Lin, E.C.C. 1964. *J. Biol. Chem.* 239:3098-3105.
117. Argast, M., Schumacher, G. and Boos, W. 1977. *J. Supra. Struct.* 6:135-153.
118. Kistler, W.S. and Lin, E.C.C. 1972. *J. Bacteriol.* 112:539-547.
119. St. Martin, E.J., Freedberg, W.B. and Lin, E.C.C. 1975. *J. Bacteriol.* 131:1026-1028.
120. Tang, C.-T., Ruch, Jr., F.E. and Lin, E.C.C. 1979. *J. Bacteriol.* 140:182-187.
121. Freedberg, W.B. and Lin, E.C.C. 1973. *J. Bacteriol.* 115:816-823.
122. Miki, K. Silhavy, T.J. and Andrews, K.J. 1979. *J. Bacteriol.* 138:268-269.
123. Miki, K. and Lin, E.C.C. 1980. *J. Bacteriol.* 143:1436-1443.
124. Cozzarelli, N.R., Freedberg, W.B. and Lin, E.C.C. 1968. *J. Mol. Biol.* 31:371-387.
125. Hayashi, S. and Lin, E.C.C. 1965. *J. Mol. Biol.* 14:515-521.
126. Silhavy, T.J., Hartig-Beecken, I. and Boos, W. 1976. *J. Bacteriol.* 126:951-958.
127. Boos, W., Hartig-Beecken, I. and Altendorf, K. 1977. *Eur. J. Biochem.* 72:571-581.
128. Schumacher, G. and Bussmann, K. 1978. *J. Bacteriol.* 135:239-250.
129. Argast, M. and Boos, W. 1979. *J. Biol. Chem.* 254:10931-10935.
130. Argast, M., Ludtke, D., Silhavy, T.J. and Boos, W. 1978. *J. Bacteriol.* 136:1070-1083.
131. Argast, M. and Boos, W. 1980. *J. Bacteriol.* 143:142-150.
132. Kistler, W.S., Hirsch, C.A., Cozzarelli, N.R. and Lin, E.C.C. 1969. *J. Bacteriol.* 100:1133-1135.
133. Weiner, J.H. 1974. *J. Memb. Biol.* 15:1-14.
134. Kaback, H.R. 1971. *Methods Enzymol.* 22:99-120
135. Ragan, C.I. 1976. *Biochem. J.* 156:367-374.
136. Capaldi, R.A., Bell, R.L. and Branchek, T. 1977. *Biochem. Biophys. Res. Comm.* 74:425-433.
137. Schwartz, S.A. and Helinski, D.R. 1971. *J. Biol. Chem.* 246:6318-6327.
138. Sancer, A., Hack, A.M. and Rupp, W.D. 1979. *J. Bacteriol.* 137:692-693.
139. Clarke, L. and Carbon, J. 1976. *Cell* 9: 91-99.
140. Weiner, J.H., Lohmeier, E. and Schryvers, A. 1978. *Can. J. Biochem.* 56:611-617.
141. Bachmann, B.J., Brooks-Low, K. and Taylor, A.L. 1976. *Bacteriol. Rev.* 40:116-167.
142. Miller, J.H. 1972. *Experiments in Molecular Genetics.* Cold Spring Harbour Laboratory. New York.
143. Tanaka, S., Lerner, S.A. and Lin, E.C.C. 1967. *J. Bacteriol.* 93:642-651.
144. Clewell, C.B. 1972. *J. Bacteriol.* 110:667-676.
145. Spencer, M.E. and Guest, J.R. 1973. *J. Bacteriol.* 114

- 563-570.
146. Inselburg, J. 1970. *J. Bacteriol.* 102:642-647.
 147. Weiner, J.H. and Heppel, L.A. 1971. *J. Biol. Chem.* 246:6933-6941.
 148. Clewell, D.B. 1972. *J. Bacteriol.* 110:667-676.
 149. Guerry, P., LeBlanc, D.J. and Falkow, S. 1973. *J. Bacteriol.* 116:1064-1066.
 150. Ziola, B.R. and Scraba, D.G. 1976. *Anal. Biochem.* 72:366-371.
 151. Griffith, I.P. 1972. *Anal. Biochem.* 46:402-412.
 152. Laemmli, U.K. 1970. *Nature* 227:680-685.
 153. Jovin, T.M., Englund, P.T. and Bertsch, L.L. 1969. *J. Biol. Chem.* 244:2996-3008.
 154. Mickel, S., Arena, V., Jr., and Bauer, W. 1977. *Nucleic Acids Res.* 4:1465-1482.
 155. Oikawa, K., Kay, C.M. and McCubbin, W.D. 1968. *Biochim. Biophys. Acta* 168:164-167.
 156. Lowry, O.H., Rosebrough, N.J., Farr, A.L. and Randall, R.J. 1951. *J. Biol. Chem.* 193:265-275.
 157. Moore, S., and Stein, W.H. 1954. *J. Biol. Chem.* 211:893-905.
 158. Moore, S. 1963. *J. Biol. Chem.* 238:235-237.
 159. Edelhoch, H. 1967. *Biochemistry* 6:1948-1954.
 160. Davies, G.E. and Stark, G.R. 1970. *Proc. Natl. Acad. Sci. USA* 66:651-656.
 161. Brumby, P.E. and Massey, V. 1967. *Meth. Enzymol.* 10:463-471.
 162. King, T.E. and Morris, R.O. 1967. *Meth. Enzymol.* 10:634-641.
 163. Ellman, G.L. 1959. *Arch. Bioch. Biophys.* 82:70-77.
 164. Spencer, R., Fisher, J. and Walsh, C.. 1976. *Biochemistry* 15:1043-1053.
 165. Ashton, W., Brown, D., Brown, J., Graham, D. and Rogers, E. 1977. *Tetrahedron Letters* 30:2551-2554.
 166. Matsumura, P., Silverman, M. and Simon, M. 1977. *J. Bacteriol.* 132:996-1002.
 167. Wilkinson, G.N. 1961. *Biochem. J.* 80:324-332.
 168. Adler, H.I., Fisher, W.D., Cohen, A. and Hardigree, A.A. 1967. *Proc. Natl. Acad. Sci. USA* 57:321-326.
 169. Roozen, K.J., Fenwick, Jr., R.G. and Curtiss, R. III. 1971. *J. Biol. Chem.* 246:6318-6327.
 170. Inselburg, J. and Appelbaum, B. 1978. *J. Bacteriol.* 133:1444-1451.
 171. Matsumura, P., Silverman, M. and Simon, M. 1977. *J. Bacteriol.* 132:996-1002.
 172. Kennedy, N., Bentin, L., Achtman, M., Skuvray, R., Rahmsdassdorf, U. and Herrlich, P. 1977. *Nature (London)* 270:580-585.
 173. Clewell, D.B. and Helinski, D.R. 1972. *J. Bacteriol.* 110:1135-1146.
 174. Dougan, G., Saul, M., Warren, G., and Sherratt, D. 1978. *Mol. Gen. Gen.* 158:325-327.
 175. Argast, M., Schumacher, G. and Boos, W. 1977. *J. Supra. Struct.* 6:135-153.

176. Schryvers, A., Lohmeier, E., and Weiner, J.H. 1978. *J. Biol. Chem.* 253:783-788.
177. Branzoli, U., and Massey, V. 1974. *J. Biol. Chem.* 249:4339-4345.
178. Mahler, H.R. and Cordes, E.H. 1966. *Biological Chemistry* pp.554-561. Harper and Row, New York.
179. Dawson, A.P., and Thorne, C.J.R. 1969. *Biochem. J.* 114:4339-4345.
180. Donnellan, J.F., Barker, M.D., Wood, J. and Beechy, R.B. 1970. *Biochem. J.* 120:467-478.
181. Futai, M. 1974. *Biochemistry* 13:2327-2333.
182. Robinson, J.J. and Weiner, J.H. 1980. *Can. J. Biochem.* 58:1172-1180.
183. Marshall, A.G. 1978. *Biophysical Chemistry: Principles, Techniques and Applications*. John Wiley and Sons. Toronto.
184. Holmes, A.M. and Johnstone, I.R. 1973. *FEBS Letters* 29:1-6.
185. Weiner, J.H., Bertsch, L.L. and Kornberg, A. 1975. *J. Biol. Chem.* 250:1972-1980.
186. Freifelder, D. 1976. *Physical Biochemistry* p.452. W.H. Freeman and Co., San Francisco.
187. Chen, Y.H., Yang, J.T., and Martinez, H. 1972. *Biochemistry* 11:4120-4131
188. Chen, Y.-H., Yang, J.T. and Chan, K.H. 1974. *Biochemistry* 13:3350-3359.
189. Udenfriend, S. 1962. *Fluorescence Assay in Biology and Medicine* Academic Press, New York.
190. Malkin, R. 1973. in *Iron-Sulfur Proteins* (Lovenberg W., ed.) Vol. 2, pp 1-23, Academic Press, New York.
191. Spencer, R., Fisher, J. and Walsh, C. 1976. *Biochemistry* 15:1043-1053.
192. Cunningham, C.C. and Hager, L.P. 1975. *J. Biol. Chem.* 250:7139-7146.
193. MacGregor, C.H., Bishop, C.W. and Blech, J.E. 1979. *J. Bacteriol.* 137:574-583.
194. Lo, T.C.Y. and Bewick, M.A. 1978. *J. Biol. Chem.* 253:7826-7831.
195. Fondy, T.P., Ghangas, G.S. and Reza, M.J. 1970. *Biochemistry* 9:3272-3280.
196. March, S.C., Parkh, I. and Cuatrecasas, P. 1974. *Anal. Biochem.* 60:149-152.
197. Cuatrecasas, P. 1970. *J. Biol. Chem.* 245:3059-3065.
198. Kornbluth, R.A., Ostro, M.J., Rittmann, L.S. and Fondy, T.P. 1974. *FEBS Letters* 39:190-194.
199. Hayakawa, K., Ueda, T., Kusaka, I. and Fukui, S. 1976. *Biochem. Biophys. Res. Comm.* 72:1548-1553.
200. Hirata, H., Sone, N., Yoshida, M. and Kogawa, Y. 1977. *J. Supramol. Struct.* 6:77-84.
201. Chiesi, M., Peterson, S.W. and O. Acuto. 1978. *Arch. Biochem. and Biophys.* 189:132-136.
202. Newman, M.J. and Wilson, T.H. 1980. *J. Biol. Chem.* 255:10583-10586.
203. Newman, M.J. and Wilson, T.H. 1981. *Abst. Ann. Meet.*

- A.S.M. p.158, K 125.
204. Uhlin, B.E., Molin, S., Gustafsson, T. and Novdstrom, K. 1979. *Gene* 6:91-106.
205. Lohmeier, E., Hagen, D.S., Dickie, P. and Weiner, J.H. 1981. *Can. J. Biochem.* 59:158-164.
206. Short, S.A., Kaback, H.R. and Kohn, L.D. 1975. *J. Biol. Chem.* 250:4291-4296.
207. Miki, K. and Lin, E.C.C. 1973. *J. Bacteriol.* 114:767-771.
208. Haddock, B.A. and Kendall-Tobias, M.W. 1975. *Biochem. J.* 152:655-659.

B30329